

**Communications, Signal Processing,
and Telemetry Research
Program Review**

1N-32
028576

February 23, 1999

NMSU-ECE-99-001

**NMSU Program Review
February 23, 1999**

Time	Topic
8:30 - 8:45	Welcome & Introductions
8:45 - 9:00	Program Overview - Stephen Horan
9:00 - 10:00	Bandwidth Efficient Modulation and Equalization Techniques - James LeBlanc
10:00 - 10:30	Parallel Signal Processing - Phillip DeLeón
10:30 - 10:45	Break
10:45 - 11:45	Turbo Codes and Low SNR Carrier Recovery Techniques - William Ryan
12:00 - 1:30	Lunch
1:30 - 3:30	Small Satellite Communications Techniques: Flight Experiments - Stephen Horan Real-Time Doppler Tracking - Phillip DeLeón Protocol Testing - Stephen Horan Optical Communications Techniques - Tom Shay
3:30 - 4:00	Laboratory Demonstrations
4:00 - 5:00	Faculty & NASA review
5:00	Adjourn

1

2

3

4

5

6

7

8

9

10

11

12

13



1999 NASA Review Participants

February 23, 1999

<u>Name</u>	<u>Affiliation/Address</u>	<u>Phone/Fax/Email</u>
Scott Allen	ATSC/WSC P.O. Drawer 9000 Las Cruces, NM 88004	(505) 527-7022 (505) 527-7302 sallen@mail.wsc.nasa
Phillip De Leon	Telemetry and Telecommunications Research Center Klipsch Dept. of Elec. & Comp. Engr. Box 30001, MSC 3-0 Las Cruces, NM 88003	(505) 646-1008 (505) 646-6417 FAX pdeleon@nmsu.edu
Charlene Gilbert	NASA/JSC 2101 NASA Rd. 1 Houston, TX 77058	(281) 483-7049 Charlene.E.Gilbert1@jsc.nasa.gov
Brian Gioannini	NASA, White Sands Complex P.O. Drawer GSC Las Cruces, NM 88004	(505) 527-7002 (505) 527-7302 bryan.gioannini@gsfc.nasa.gov
Garth Henning	NASA/GSFC SGT-INC 7701 Greenbelt Road Greenbelt, MD 20771	(301) 614-8600 ext. 367 ghenning@sgt-inc.com
Stephen Horan	Telemetry and Telecommunications Research Center Klipsch Dept. of Elec. & Comp. Engr. Box 30001, MSC 3-0 Las Cruces, NM 88003	(505) 646-5870 (505) 646-6417 FAX shoran@nmsu.edu
James LeBlanc	Telemetry and Telecommunications Research Center Klipsch Dept. of Elec. & Comp. Engr. Box 30001, MSC 3-0 Las Cruces, NM 88003	(505) 646-3919 (505) 646-6417 FAX leblanc@nmsu.edu
Warner Miller	Goddard Space Flight Center Code 564 Greenbelt, MD 20771	(301) 286-8183 (301) 286-0220 FAX warnerh.miller@gsfc.nasa.gov
William Ryan	Electrical and Computer Engr. University of Arizona P.O. Box 210104 Tucson, AZ 85721-0104	(520) 621-8690 (520) 621-8076 FAX Ryan@ece.arizona.edu

Tom Shay	<i>Telemetry and Telecommunications Research Center</i> Klipsch Dept. of Elec. & Comp. Engr. Box 30001, MSC 3-0 Las Cruces, NM 88003	(505) 646-4817 (505) 646-6417 FAX ishay@nmsu.edu
Robert Stone	<i>NASA/GSFC</i> Code 561 Greenbelt, MD 20771	(301) 286-5659 Robert.W.Stone@gsfc.nasa.gov
Virgil True	<i>NASA (Retired)</i> 701 Frank Maes Ave. Las Cruces, NM 88005	505) 523-1497
Don Wilson	<i>NASA/GSFC</i> 7701 Greenbelt Road Greenbelt, MD 20771	(301) 614-8600 ext. 341 Don.Wilson@SGT-INC.com
Roger Wye	<i>NASA/GSFC</i> SGT-INC 7701 Greenbelt Rd. Greenbelt, MD 20771	(843) 342-3633
Pen-Shu Yeh	<i>Goddard Space Flight Center</i> Code 564 Greenbelt, MD 20771	(301) 286-4477 psyeh@psy.gsfc.nasa.gov

PROGRAM OVERVIEW

Communications, Signal Processing and Telemetry Research: Program Review

**Lujan Space Tele-Engineering
Program
Klipsch School of Electrical and
Computer Engineering**

Topics

- **NMSU Background**
- **Communications, Signal Processing, and Telemetry Program**
- **Facilities**
- **Faculty & Staff**
- **Review Program**

NMSU Background

- NMSU is the Land Grant University and NASA Space Grant University for New Mexico
- NMSU is a federally-designated minority-serving university
- NMSU is a Carnegie-I Research University

Communications, Signal Processing, and Telemetry Program

- Leverage and Spin-offs
 - ACTS
 - Air Force Nanosatellite Program
 - Wireless Communications Lab
 - Sandia National Laboratory
 - Magnetic Recording Research
 - Digital Signal Processing Laboratory

Communications, Signal Processing, and Telemetry Program

- ACTS Propagation
 - Completed 5 years of data collection at STGT
 - Results being used in revised NASA RP 1082
 - Results used in revised Crane rain models
 - Weather results used by WSTF



- Developed antenna wetting model

Facilities

- Thomas & Brown Hall
 - Hardware development Laboratory
 - Software simulation Laboratory
 - Digital Signal Processing Laboratory
- Jett Hall
 - Optical Communications Laboratory

Faculty & Staff

- NMSU Faculty
 - Dr. Stephen Horan - Director
 - Dr. Phillip DeLeon - Associate Director
 - Dr. James LeBlanc - Associate Director
 - Dr. Thomas Shay
- NMSU Staff
 - Mr. Lawrence Alvarez
 - Ms. Janice Apodaca

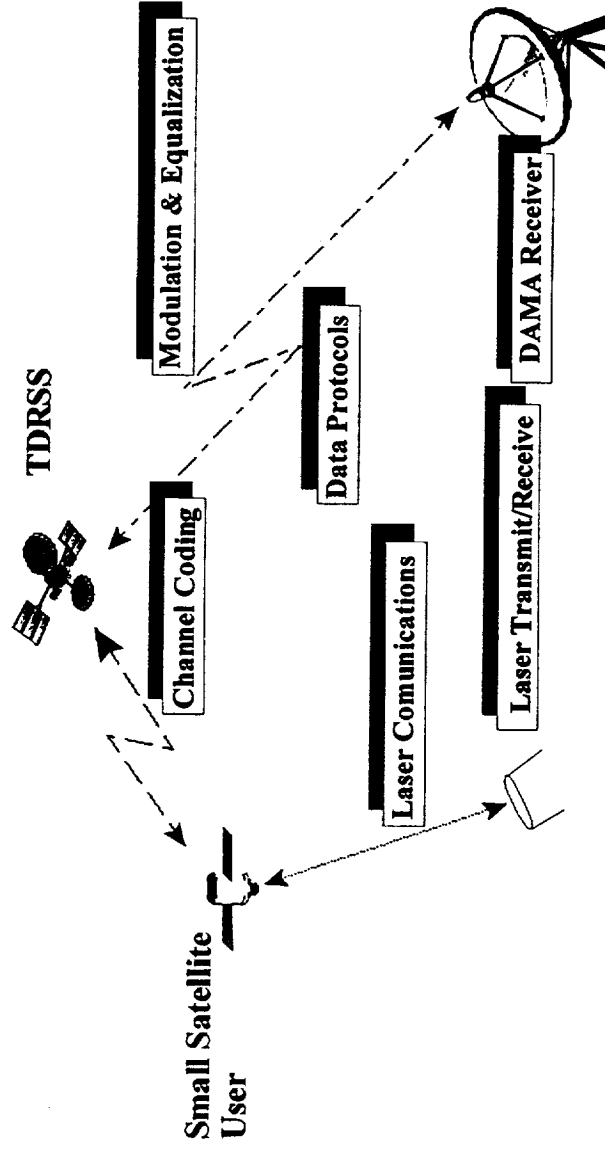
Faculty & Staff

- University of Arizona
– Dr. William Ryan

February 23, 1999

Program Overview

Review Program



- Improve access by
- new techniques for antenna configuration
 - improved access requests
 - improved transmission throughput by using more efficient modulation and equalization techniques
 - improved performance by using improved channel coding techniques
 - improved data throughput by using data packaging protocols
 - efficient telemetry transmission through low-power laser communications

Review Program

- 8:30 - 8:45 Welcome & Introductions
- 8:45 - 9:00 Overview
- 9:00 - 10:00 - Bandwidth-Efficient Modulation & Equalization
- 10:00 - 10:30 - Parallel Signal Processing
- 10:30 - 10:45 Break
- 10:45 - 11:45 Turbo Codes & Low SNR Carrier Recovery
- 12:00 - 1:30 Lunch
- 1:30 - 3:45 - Small Satellite Communications:
 - Flight Experiments
 - Real-Time Doppler Tracking
 - Space Protocol Testing
 - Optical Communications
- 3:45 - 4:00 Tour
- 4:00 - 5:00 Wrap-up Review

BANDWIDTH EFFICIENT MODULATION

Bandwidth Efficient Modulation & Nonlinear Equalization

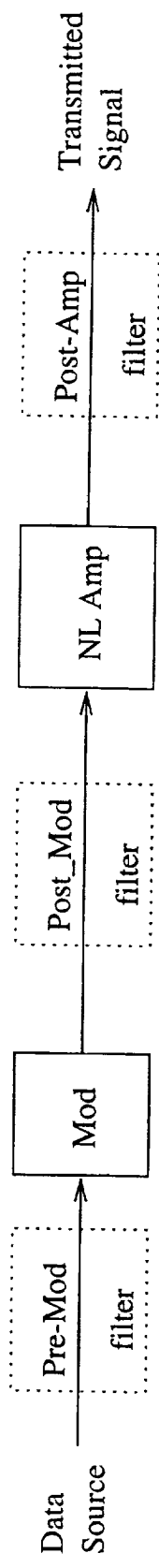
James P. LeBlanc
Klipsch School of ECE
New Mexico State University
Las Cruces, NM
leblanc@nmsu.edu

Bandwidth Efficient Modulation

Motivation

- High-rate communication thru nonlinear ISI channels is of interest as available spectrum becomes scarce.
- Within this bandlimited nonlinear environment, typical methods:
 - increase symbol rates
 - use a higher order modulation schemes (next talk)
- To offset increased symbol rates, use Spectral Shaping via filtering to increase frequency utilization.

Problem Setting



Possible Filter Placement:

- post-amplifier \Leftrightarrow Heavy, expensive, not compatible
- post-modulator \Leftrightarrow Nonconstant modulus signal (requires nonlinear equalization) can cause spreading through NL amp.
- pre-modulator \Rightarrow Continuous Phase Modulation (CPM)
- variety of options available
- effects of data imbalance, $p_{\text{one}} \neq p_{\text{zero}}$

Related Issues

- Transmitter Complexity
- Robustness to Data Imbalance
- Spectral Occupancy
- Error Rates
- Receiver Complexity

General Phase Modulation

- Constant Modulus
- Written as

$$\begin{aligned}s(t) &= \operatorname{Re} \left(v(t) e^{j2\pi f_c t} \right) \\ &= \operatorname{Re} \left(p(t) e^{j2\pi \theta(t; I)} e^{j2\pi f_c t} \right) \\ &= p(t) \cos (2\pi f_c t + \theta(t; I))\end{aligned}$$

- ◊ $p(t)$ is the pulse amplitude shaping
- ◊ $\theta(t; I)$ is a function of time t and information sequence I .
- baseband waveform is $v(t)$.
- for constant modulus signals, $p(t) = 1$.

Phase Modulation (cont.)

- simple M -ary digital phase modulation
 - ◊ choose $\theta(t : I)$ constant over T_s
 - ◊ $\theta(t : I) = \pi \frac{\alpha_k}{M}$ for $kT_s < t < (k+1)T_s$
- note discontinuous phase
- no ISI

Continuous Phase Modulation (CPM)

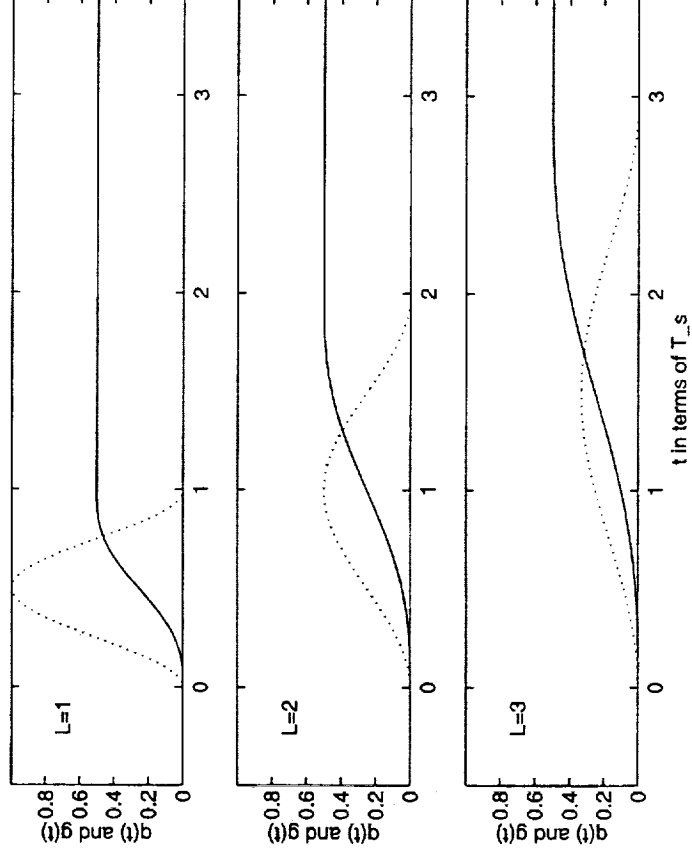
- θ may be written as

$$\theta(t; I) = 2\pi h \sum_{k=-\infty}^{\infty} I_k q(t - kT_s) \quad nT_s \leq t \leq (n+1)T_s$$

- I_k is the sequence of M -ary alphabet members,
- h is the modulation index, and ...
- $q(t)$ is the phase pulse shaping.

Phase Shaping (cont.)

- common phase shaping derived from a raised cosine
- other forms: MSK, Gaussian MSK, etc.
- the # of symbol periods for which $g(t)$ is nonzero denoted L .
- L also denotes the number of terms in ISI sum.

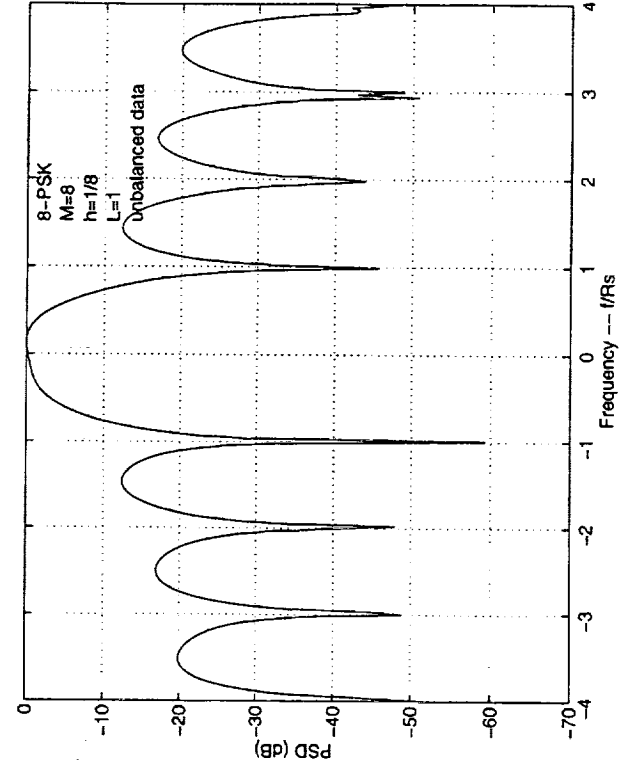
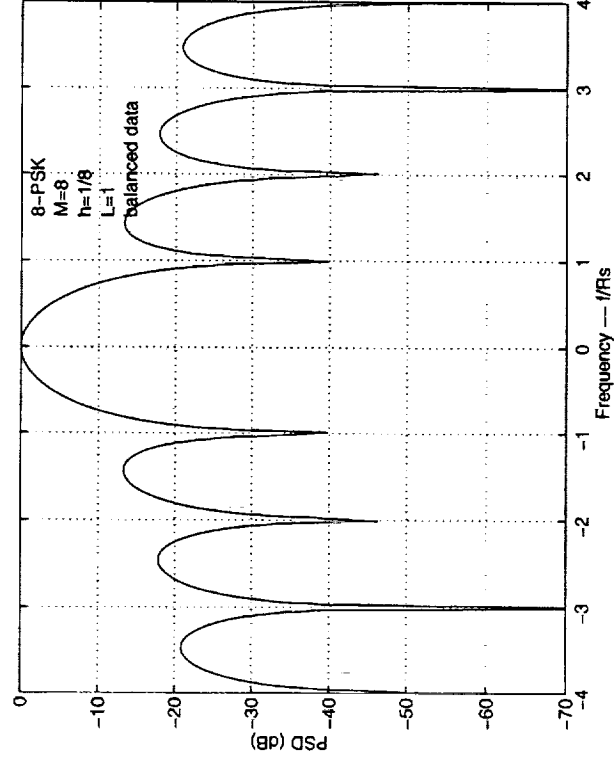


PSD Calculation

- PSD of CPM may be computed
 - ◇ closed-form solution exists
 - ◇ may require numerical integration
- Conditions for Spectral spikes are known (and may be avoided).

PSD Results

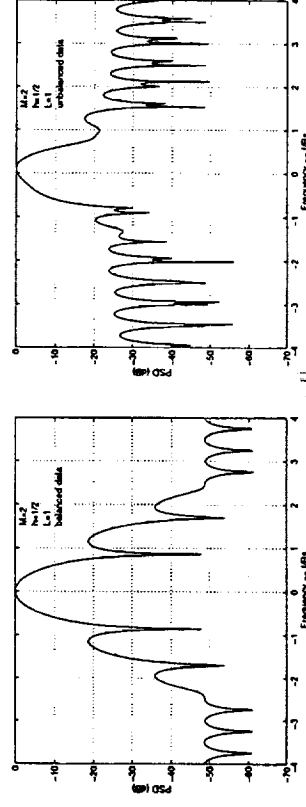
8-PSK (No phase shaping)



BALANCED DATA

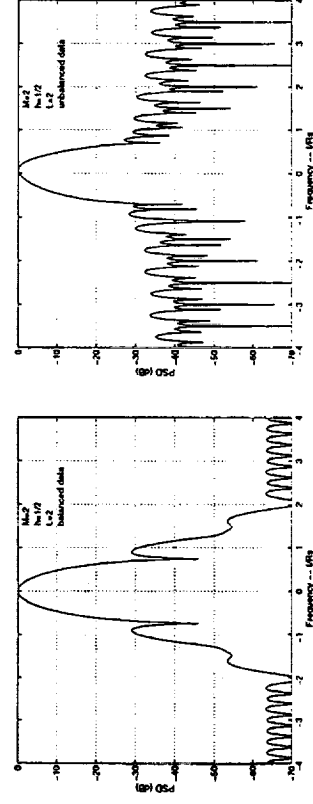
UNBALANCED DATA

Binary CPM – Raised Cosine $L = 1$



BALANCED DATA UNBALANCED DATA

Binary CPM – Raised Cosine $L = 2$ (Partial Resp.)



BALANCED DATA UNBALANCED DATA

Generalizations

- Better spectral properties may be achieved by allowing for more ISI ...
- ...this has cost of impacting receiver complexity.

Conclusion

- Infinite options for selecting phase smoothed modulation parameters.
- Choice can greatly affect:
 - ◇ Spectral Efficiency
 - ◇ Receiver Complexity
 - ◇ Sensitivity to Data Imbalance
- Proper Modulation Design will depend on
 - ◇ Spectral Mask
 - ◇ Tolerable Receiver Complexity (i.e. cost)
 - ◇ Amount of Data Imbalance

Nonlinear Equalization for BW Efficiency

Motivation – High Data Rate Missions

- Higher-rate communication through existing infrastructure over presently available spectrum.
- Power efficiency issues requires use of saturating amplifiers.
- Typical methods to increase data rate:
 - Faster symbol rates \Rightarrow Hardware difficulties
 - higher order modulation schemes \Rightarrow Nonlinear ISI

Earlier Proposed Solutions

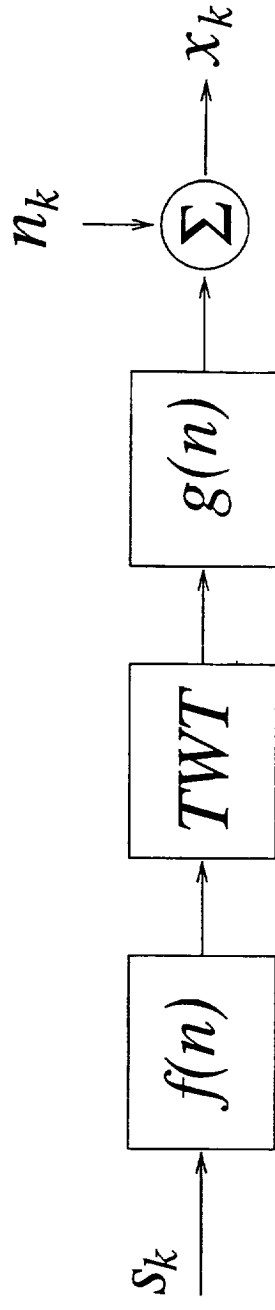
- Predistortion techniques.
 - requires additional transmitter (& feedback) hardware.
- Nonlinear Volterra equalizers
 - large parameter space, noise sensitivity
- Neural Networks
 - large parameter space, noise sensitivity, training issues

Our proposed technique

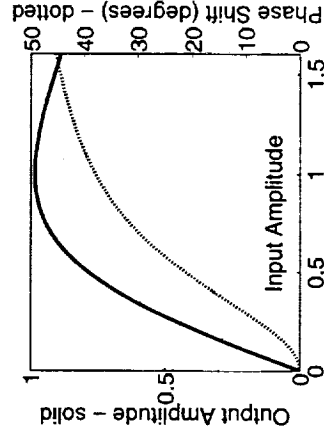
Enhanced RAM-based Equalization

- appears robust to channel noise
- requires no additional transmit hardware,
- has rather modest receiver hardware needs.
- borrows from recent work in the magnetic storage channel and digital communications communities.

Problem Setting: TDRSS Channel Model

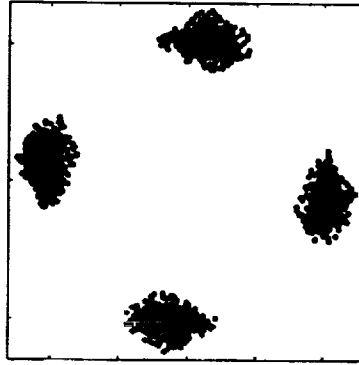


- Bandlimited, nonlinear channel
 - pre-filtering, $f(n)$
 - saturating amplifier TWT
 - post-filtering, $g(n)$
 - additive Gaussian noise



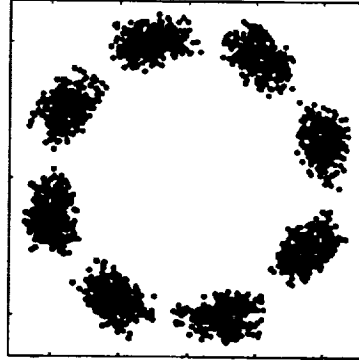
Example Distortion - No Noise, ISI only

QPSK



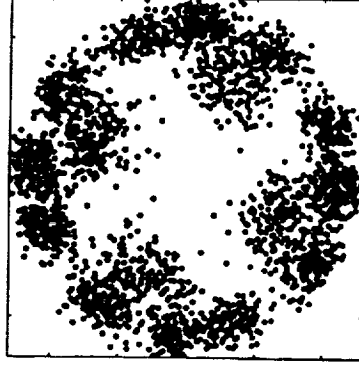
2 bits/symbol

8-PSK



3 bits/symbol

16-QAM

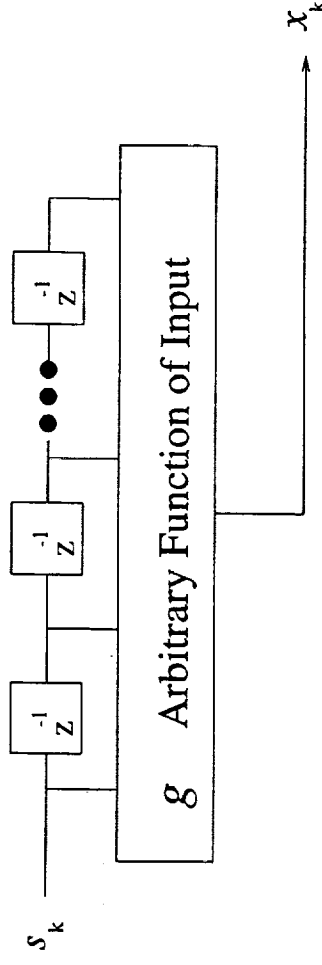


4 bits/symbol

RAM-Based Compensation Techniques

Basic idea:

- regard the nonlinear channel with memory as an state-machine

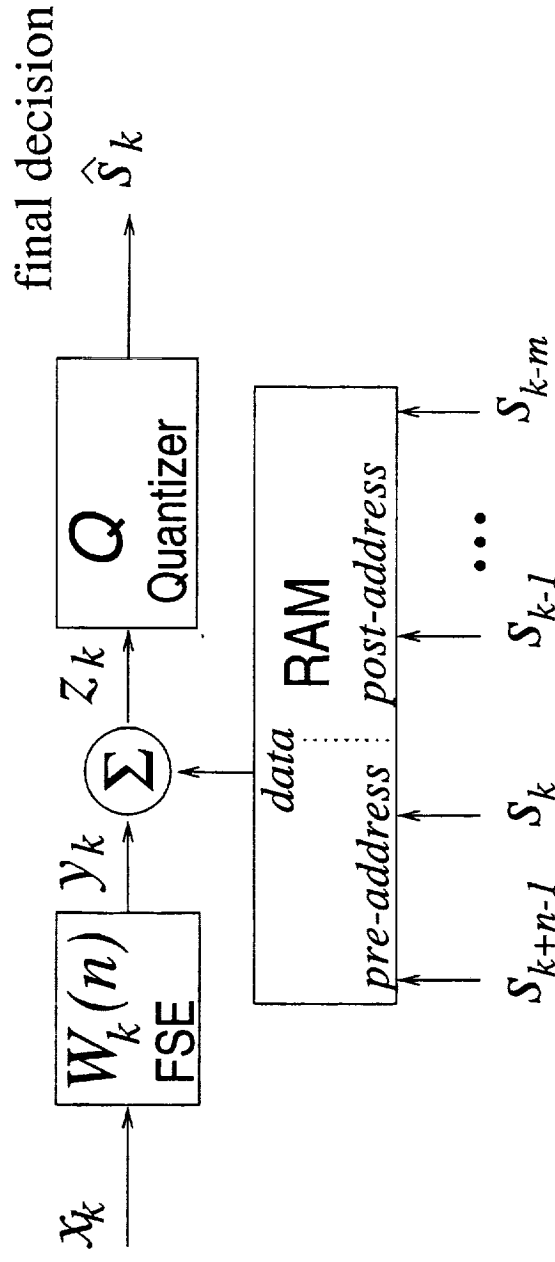


- noiseless channel output considered to be an arbitrary function of the channel inputs

... then ...

- receiver implements a version of this function to subtract nonlinear ISI from received signal.
- arbitrary function is encoded as RAM lookup table.

RAM-Based Equalizer



The equalizer which embodies this idea is depicted above

- $\hat{g}(\cdot)$ is represented by a RAM table.
- but is *not* implementable, it requires:
 - $\{s_{k+n-1}, \dots, s_k, \dots, s_{k-m}\}$ which is not known.
- uses a feedforward equalizer W_k in concert with RAM

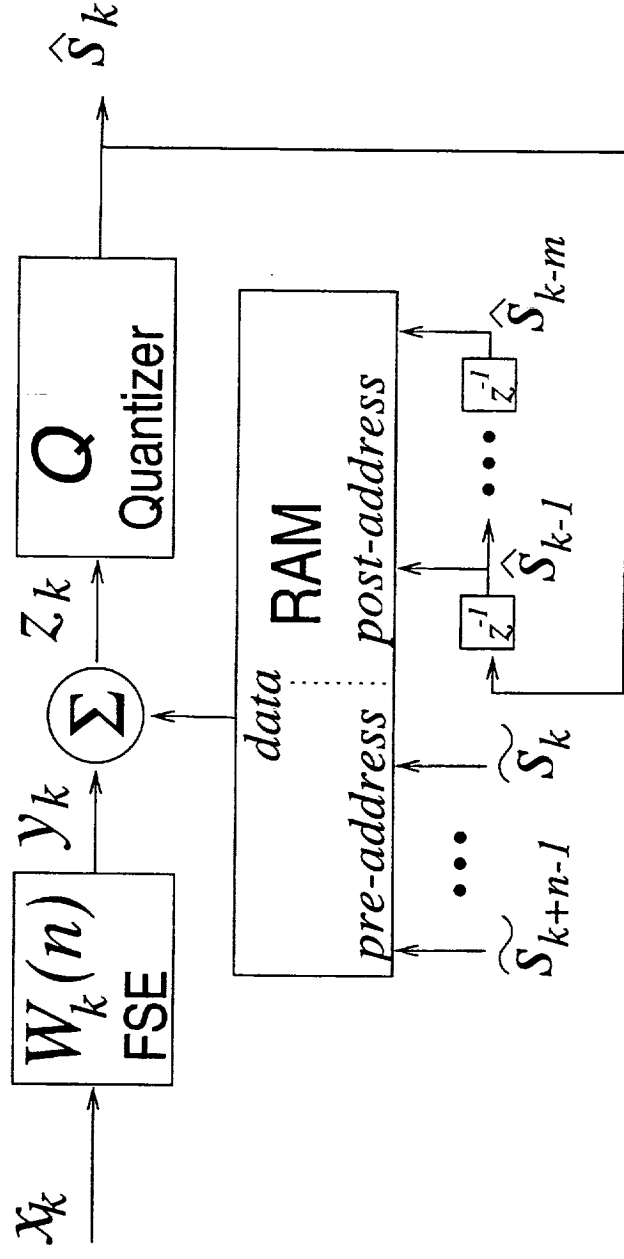
Family of RAM-based equalizers...

- Use various *local* decisions on values of present and past inputs are used: RAM-DFE, RAM-canceler, PERC (Pre-Cursor Enhance RAM-DFE/Canceler).
- Such equalizers **traditionally** work in cooperation with a feedforward equalizer to
 - act as pseudo-matched filter (to maximize SNR)
 - aid symbol synchronization
 - set delay for training
 - **a non-traditional use can improve RAM equalizer performance** (to be discussed).

The PERC(n, m):

Pre-Cursor Enhanced RAM-DFE/Canceler

- RAM has address lines consisting of
 - m past decisions \hat{s}_{k-1} to \hat{s}_{k-m} (denoted post-address)
 - n present/future potential decisions \tilde{s}_k to \tilde{s}_{k+n-1} .



PERC Training

- PERC must be trained first to learn the channel:
 - all “post” and all “pre” source symbols are known.
- Feedforward Eq uses *LMS-like* update relation for MMSE-channel shortening.

$$W_{k+1} = W_k + \mu_{ff}(\text{error term}) + \text{correction term}$$

- Feedforward Eq. is fixed, then RAM component is updated using *LMS-like* updates.

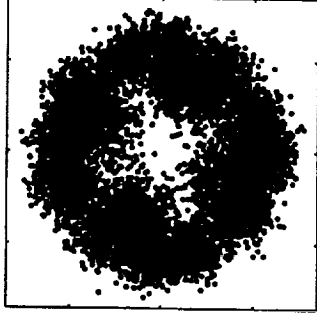
$$RAM_{k+1}(A_k) = RAM_k(A_k) + \mu_{fb}(\text{error term})$$

PERC Operation

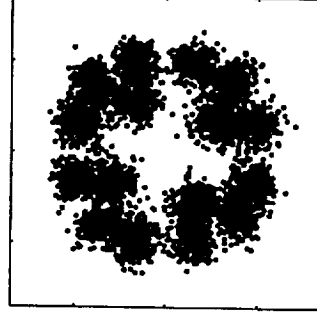
- After training, the PERC may be run in:
 - “fixed mode” with no adaptation or...
 - “decision-directed” mode.
- Only difficulty becomes what is the proper “pre-cursor” address component A_{pre} ?
 - idea is to test over all possible symbols of A_{pre}
 - choose address that places z_k closest to a valid symbol value (address that minimizes $|e_k|^2 = |z_k - Q(z_k)|^2$).
 - error propagation is possible and MSE in non-training mode is worse.

Simulation Examples: 16-QAM at SNR=15dB

Received Signal

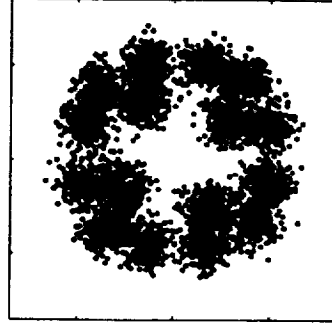


Linear Eq. Output



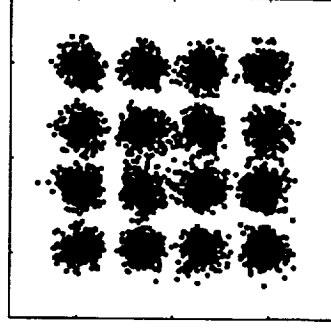
MSE = -11.65

PERC(0,3)



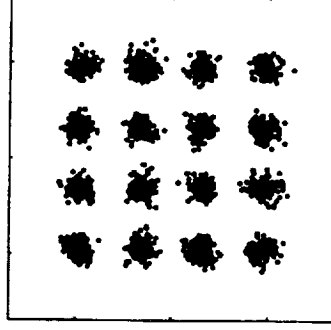
MSE = -11.4

PERC(1,3)



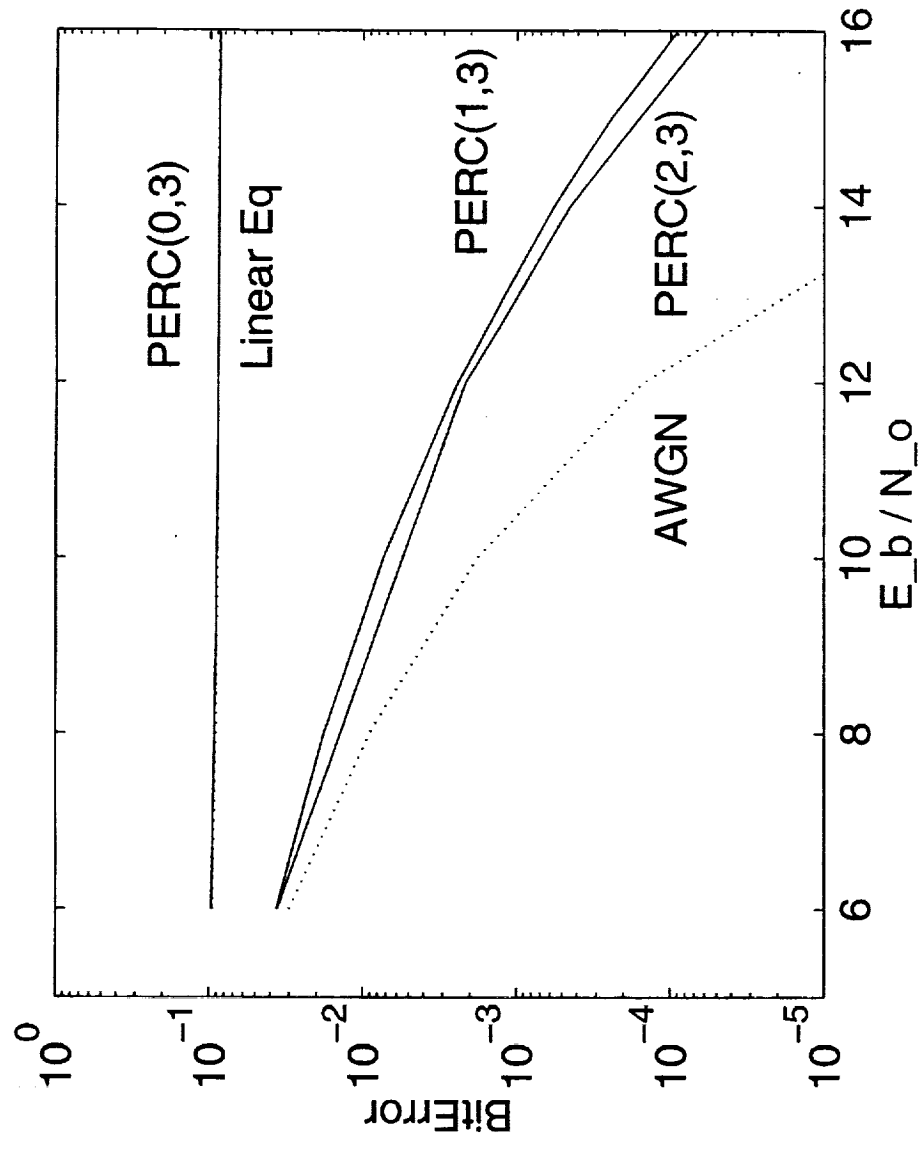
MSE = -13.96

PERC(2,3)



MSE = -15.63

Simulation Examples: 16-QAM Bit Error Rates



Feedforward Eq. Design Criteria

- With high order constellations, even channels of moderate length can lead to unfeasibly large RAM tables for PERC.
- Standard FF Eq design criterion minimizes mean-square error (due to all source terms (s_k)).
- New FF Eq design criterion minimizes mean-square error due only to source terms (s_k) “outside” of PERC’s timespan of compensation.

Design Criteria – MMSE-CS

Minimum Mean Square Error - Channel Shortening

In cases with sequence detector following the equalizer

- choose criterion with no cost associated with ISI within the sequence detector's window.
- $J_{CS} = \mathcal{E} \left\{ \left| y_k - \left(s_{k-\Delta} + \sum_{\ell=1}^L h_{\ell} s_{k-\Delta-\ell} \right) \right|^2 \right\}$
- L values of chan-eq may take any value, without penalty nor constraint.
- MMSE-CS equalizer can be solved in closed form for linear channels.

Nonlinear Channels?

- For nonlinear channels, one can not design using this method...
- ... but an adaptive version (w/o knowledge of C) has been developed.
- Use in the LMS fashion

$$\Phi_{k+1} = \alpha \Phi_k + (1 - \alpha) X_k^* S_k^{LH}$$

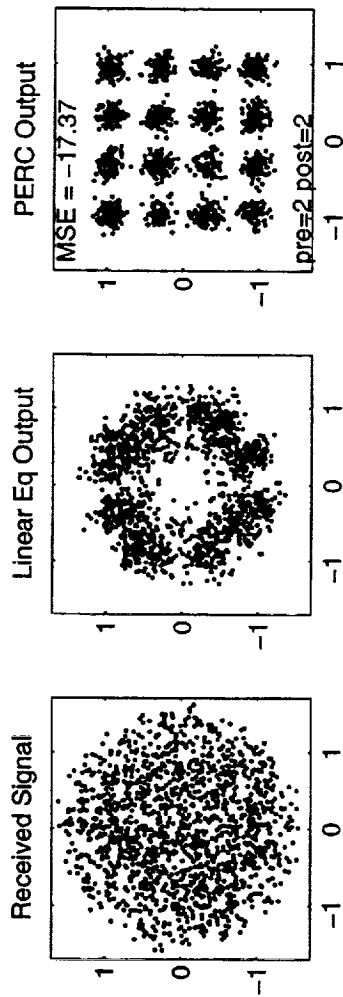
$$y_k = X_k^T D_k$$

$$D_{k+1} = D_k - \mu_{ff} X_k^* (y_k - s_{k-\Delta}) - \Phi^* \Phi^T D_k$$

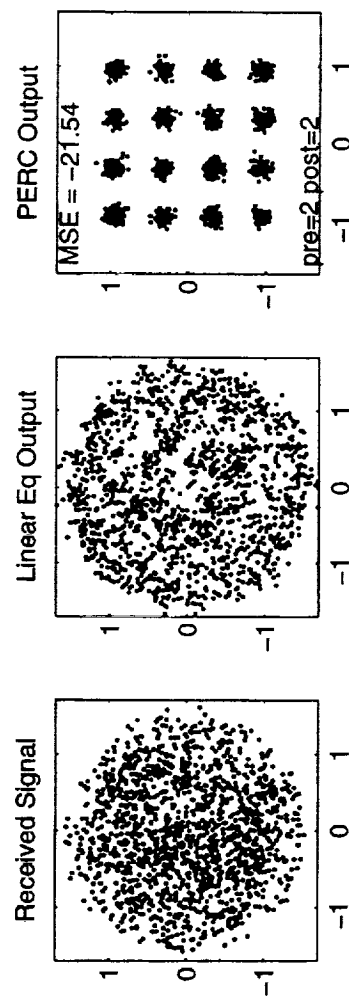
- Where $S_k^L = \begin{bmatrix} s_{k-\Delta-1} \\ \vdots \\ s_{k-\Delta-L} \end{bmatrix}$, $X_k = \begin{bmatrix} x_{k-\Delta-1} \\ \vdots \\ x_{k-\Delta-L} \end{bmatrix}$, and α, μ_{ff} are stepsize parameters.

Nonlinear Channel, MMSE-CS FF Eq and PERC(2,2)

Traditional MMSE FF Eq. Design



New MMSE-CS FF Eq. Design



MMSE-CS Results

- Designed FF Equalizer with non-traditional design criterion
- Implemented adaptive version for nonlinear channels.
- Enhances performance of nonlinear PERC equalizer.

Status, Open Issues and Continued Research

- Research implies successful use of higher-order modulation through nonlinear channels (such as the TDRSS channel).
- Simulation results have been verified on data collected through lab bench hardware:
 - Used actual TWT in saturation mode.
 - Butterworth Pre-filtering/Post-filtering.
 - Data collected in real-time.
 - Data post-processed in a high level language.

Continuing/Further work

- Phase II hardware verification experiment using actual TDRSS data.
- Implement algorithm in real-time using programmable DSP and field programmable gate arrays (FPGA's).
- Assess methods for proper pre/post address parameterization for PERC(m,n).
- Enhanced training convergence algorithms.

Technical Spinoffs From Nonlinear Eq. Research

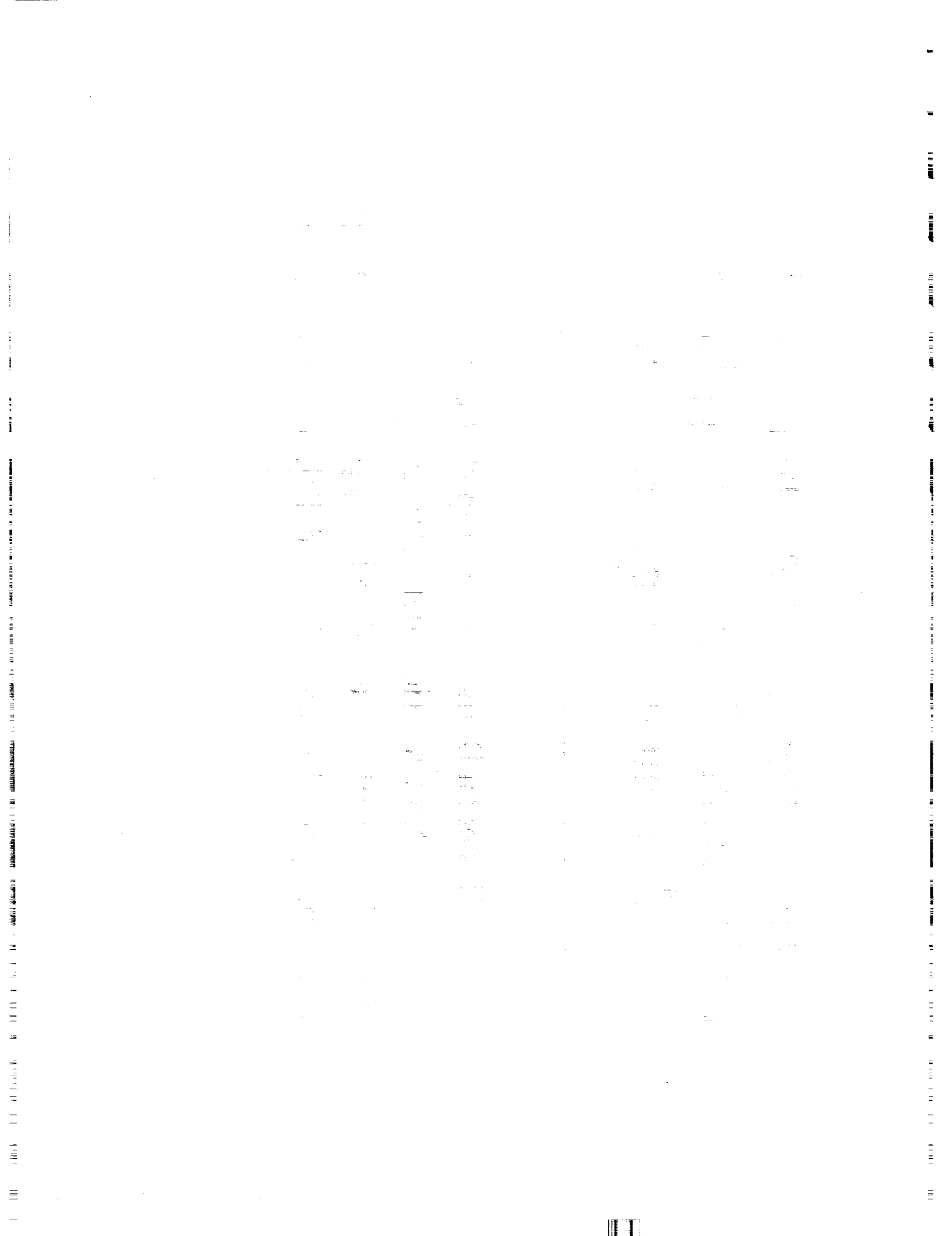
- Sandia Nat'l laboratories is interested in PERC technology and implementing PERC hardware for space telemetry and ranging applications.
- The MMSE-CS technology will be presented at the IEEE international magnetics conference in May 1999, for possible application in commercial data recording.

PARALLEL SIGNAL PROCESSING

Investigation of an Architecture for Parallel Signal Processing Applicable to Communications Problems

Stephan Berner and Phillip De Leon
New Mexico State University

Klipsch School of Electrical and Computer Engineering
Center for Space Telemetry and Telecommunications



Fundamental Problems

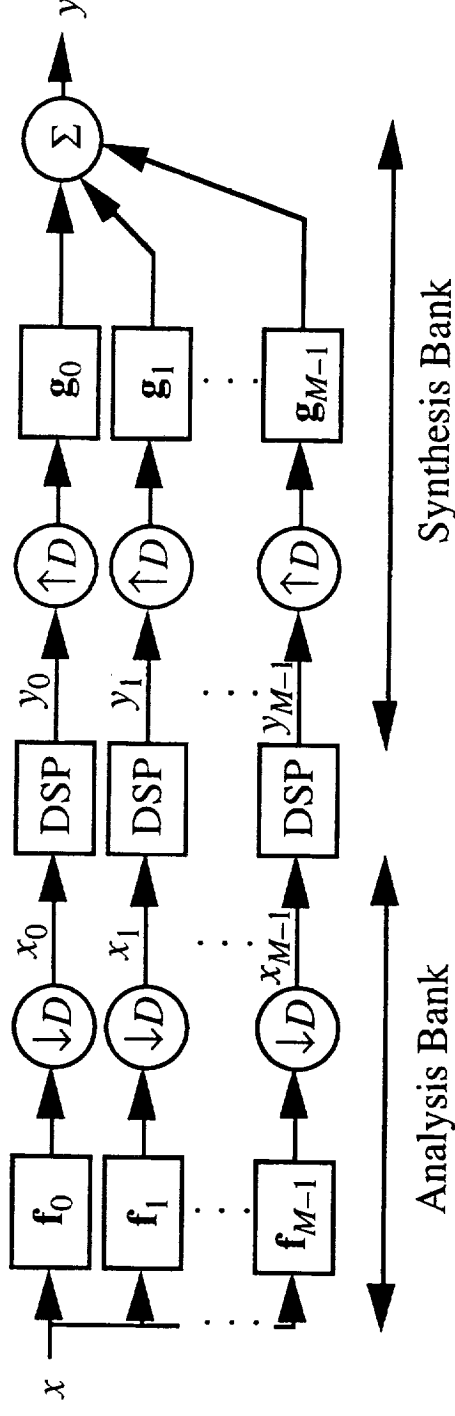
- Sequential nature of data (signal) combined with high-bandwidth, complex processing, i.e. high data rate, DSP-based receiver, yields a formidable challenge
- Algorithm partitioning is often difficult and/or ineffective with the above problem
- An alternate approach is to partition (decompose) the signal itself and assign a processor to each data partition
 - Data partitioning approach has been applied successfully in a number of problems such as search problems
 - Not all problems have data which can be partitioned

Preliminary Objectives

- Investigate low-order, oversampled, linear-phase filterbanks for use in signal decompositions
 - Require very good reconstruction properties with minimal subband aliasing
 - Filterbank should be linear phase for all-digital receiver applications (essential for tracking the phase and determining Doppler effects)
 - Require efficient filterbank architecture for high-bandwidth applications
- Investigate a FPGA implementation of a filterbank for use in a parallel processing architecture
 - Configurations of 4, 8, and 16 subbands and scalable
 - Serial distributed arithmetic in filtering
 - 2x oversampled subbands
 - Area efficient as well as high-speed implementation versions

Parallel Signal Processing in Subbands

- Sampled signal is decomposed through the analysis bank
- Subbands are independently processed on multiple DSPs
- Subband outputs are synthesized to form fullband output



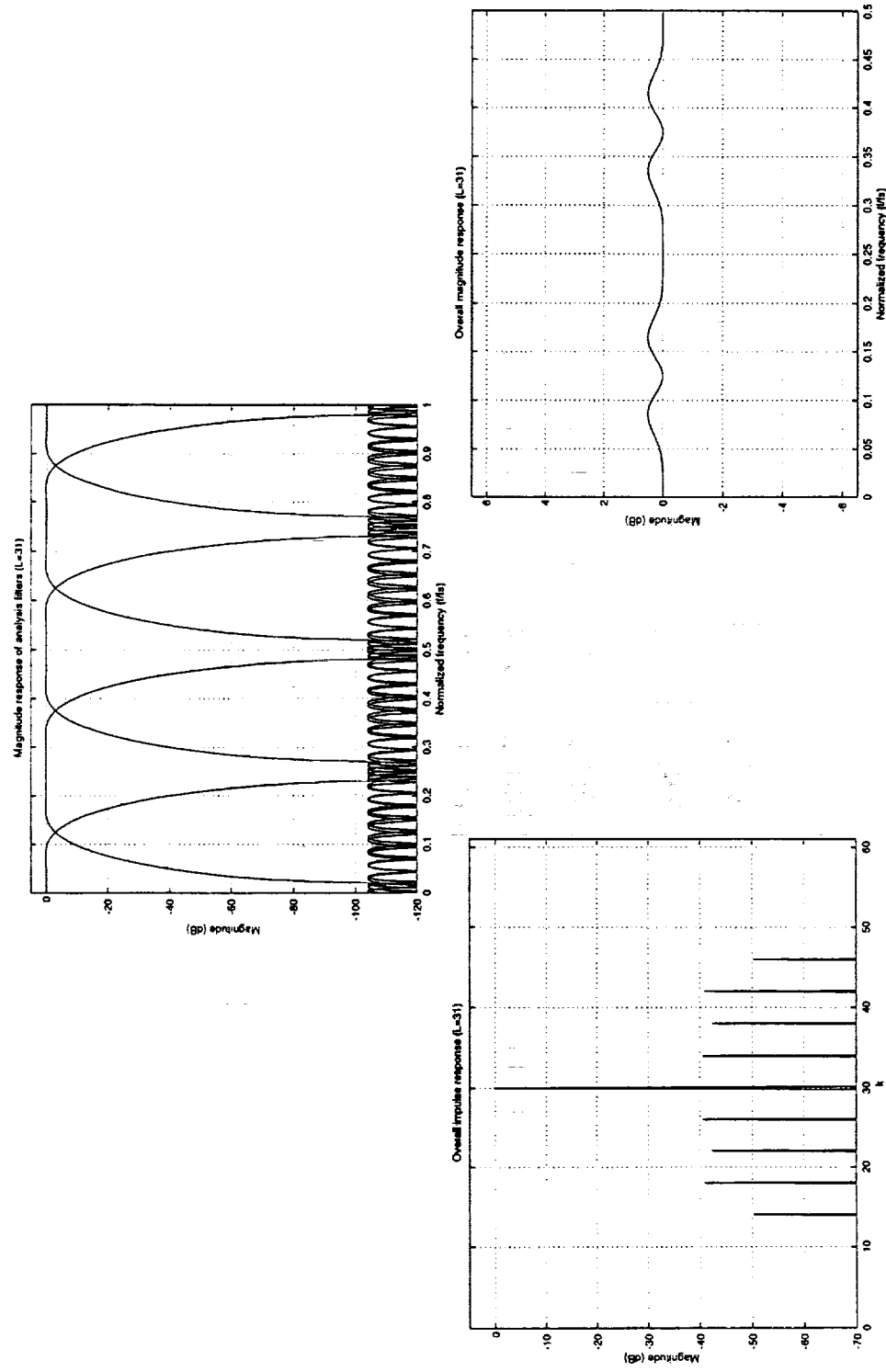
Potential Applications

- Many communication applications lend themselves to subband processing
- All-digital modem using filter banks
 - JPL Publication 94-20 (R. Sadr, P.P. Vaidyanathan, D. Raphaeli, S. Hinedi)
 - Lower processing rate in DSP hardware than input sample rate
 - Expansion to higher rates is easily accommodated due to parallel structure
 - Detected symbol stream is directly output from subbands with no increase in error rate
 - Suited for high data rate applications such as gigabit satellite channels
- Discrete Multitone Transceivers (DMT)
 - Employs a *set* of modulation functions (filters) which utilize unevenness of channel response in order to maximize total achievable bit rate
- Spread-spectrum codes based in subband transform bases

Filterbanks

- Filterbank decomposes or analyzes signal into M subbands using a bank of bandpass filters
- After filtering, signals are downsampled by a factor of D
 - Choose oversampled subbands ($D < M$) to avoid subband aliasing which will interfere with subband processing
- After subband processing, signals are upsampled to original rate and synthesis filtered to remove spectral images
- Fullband signal is constructed from the sum of synthesis filtered signals
- If analysis/synthesis filters are designed properly and no modifications are made to subbands, overall impulse response of filterbank will be equal to a pure delay

Example of Low-Order, Oversampled, Linear-Phase Filterbank Response



New Filterbank Design Result

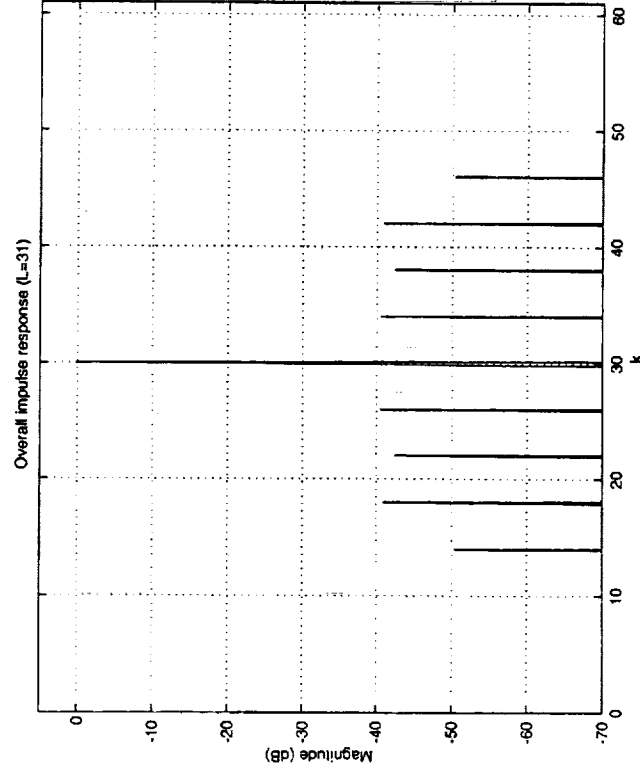
- Numerical methods are often employed for perfect or near-perfect reconstruction filterbanks (critical and oversampled) under linear-phase, uniform-DFT constraints
- We have shown that assuming a linear-phase prototype, i.e. window or Parks-McClellan design, with -3dB crossover magnitudes, virtually all phase distortion (primarily at crossover) can be eliminated by a simple filter length rule:

$$2(L - 1) / M \text{ is odd}$$

- Numerical methods can then be applied (if desired) to further enhance filterbank (even though above rule is usually “good enough”)

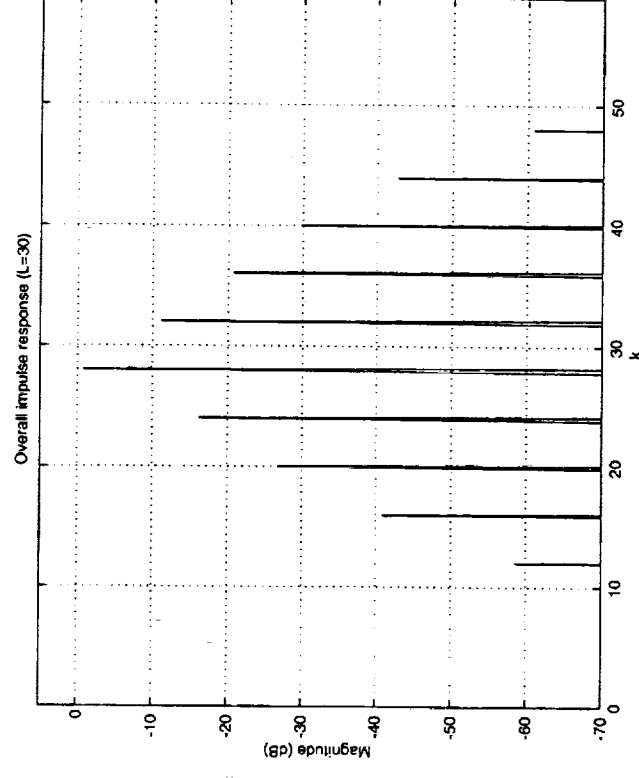
Filterbank Design Example

- Filterbank parameters $M = 4$, $D = 2$
- Parks-McClellan designs Case I: $L = 31$, Case II: $L = 30$



Simple rule satisfied

New Mexico State University

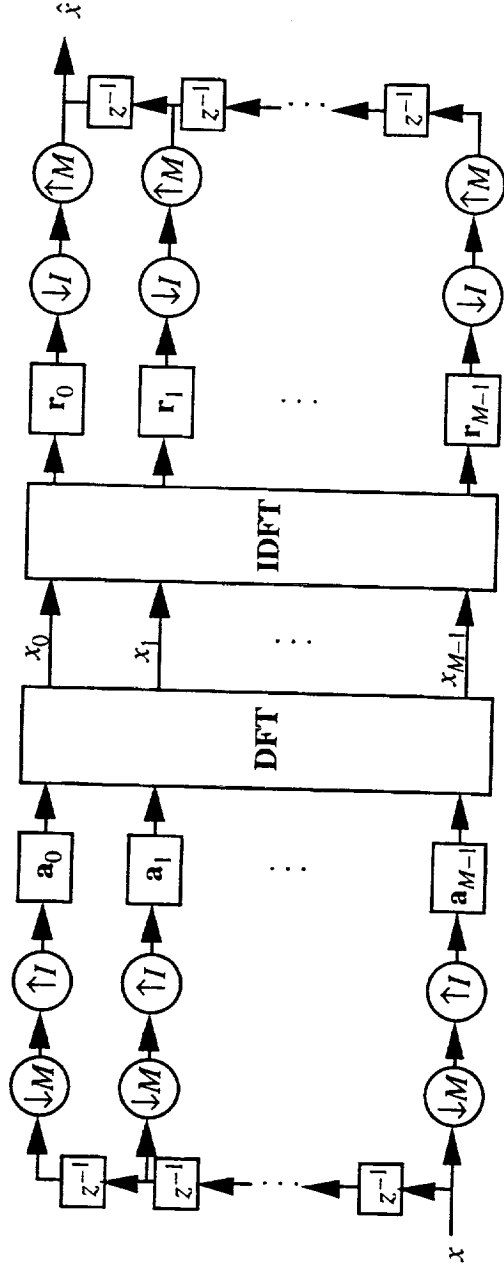


Simple rule not satisfied

Center for Space Telemetry and Telecommunications

Polyphase, Uniform-DFT Filter Bank

- Polyphase representation of filterbank (standard form) greatly reduces computations.
- Filterbank constraints
 - equal bandwidth subbands (uniform)
 - analysis/synthesis filters derived from prototype via frequency shifting



High-Speed Filterbank Implementation

- High-speed filter bank implementation completed
 - Filterbank described in VHDL and scalable in subbands and wordlengths
 - COTS FPGA selected for reprogrammability and efficient implementation compared with with PALs or TTL-ICs
 - Analysis/synthesis filters realized with serial distributed arithmetic and lookup tables
 - 8MHz input/output sample rate, $8(2) / M$ MHz subband rate

	# Subbands, M		
	4	8	16
Analyzer ($L = 31$)	701 CLBs 18K Gates	1544 42K	3237 88K
Synthesizer ($L = 31$)	680 17K	1407 39K	2861 78K

Work in Progress

- Further investigation of low-order, linear-phase, uniform-DFT filterbanks with good reconstruction properties
- Refine VHDL codes for more area-efficient filterbank implementations especially at higher subbands levels
 - Use of arithmetic Fourier transform to reduce area
- Prototype end-to-end unit

Conclusions

- Subband decompositions appear to be a useful method for data (signal) decomposition in parallel signal processing
- Several communications applications have been simulated in subbands and results indicate better performance than the fullband counterpart and/or reduced processing rates
- Designs for low order, linear-phase, uniform-DFT filterbanks have been studied and successfully applied
- Filterbank has been described in VHDL which leads to an easily scalable design on FPGA

TURBO CODES

CODED PARTIAL RESPONSE OVER SATELLITES

Ali Ghrayeb

Advisor

Dr. William Ryan

New Mexico State University
Center for Space Telemetry and Telecommunications

(Dr. Ryan and I are currently with the University of Arizona, Tucson, AZ)

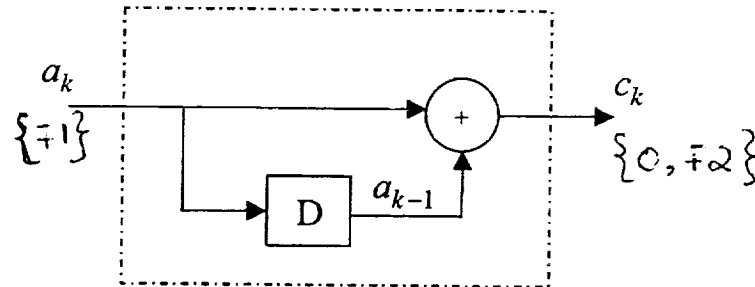
February 23, 1999

OUTLINE

- Introduction to Partial Response
 - Class I (PR1)
 - Class IV (PR4)
- Satellite Channel Model
- Signal Constellations for
 - QPSK
 - 8PSK
 - 2-dimensional PR1 and PR4
- Coded PR Simulation Diagram
- Performance of Coded PR1 and PR4 versus coded 8-PSK
- Future Work
- Conclusions

Introduction - Class I (PR1)

- Encoder



- $c_k = a_k + a_{k-1} \quad \Leftrightarrow \quad c(D) = a(D)(1+D) = a(D)h_1(D)$

- Frequency response:

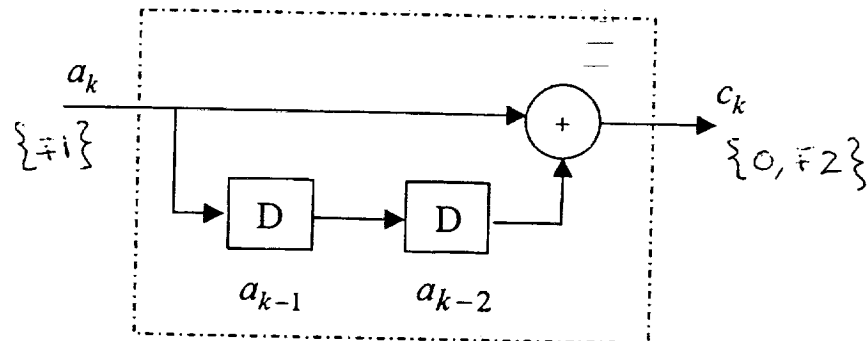
$$\begin{aligned} h_1(f) &= h_1(D) \Big|_{D=e^{-j2\pi f T_o}} \\ &= 1 + e^{-j2\pi f T_o} = (e^{j\pi f T_o} + e^{-j\pi f T_o}) \cdot e^{-j\pi f T_o} \\ &= 2 \cdot \cos(\pi f T_o) \cdot (e^{-j\pi f T_o}) \end{aligned}$$

- PSD:

$$G(f) = \frac{1}{T_o} |h_1(f)|^2 = \frac{4}{T_o} \cdot \cos^2(\pi f T_o)$$

Introduction (Cont'd) - Class IV (PR4)

- Encoder



- $c_k = a_k - a_{k-2} \quad \Leftrightarrow \quad c(D) = a(D)(1 - D^2) = a(D)h_2(D)$

- Frequency response:

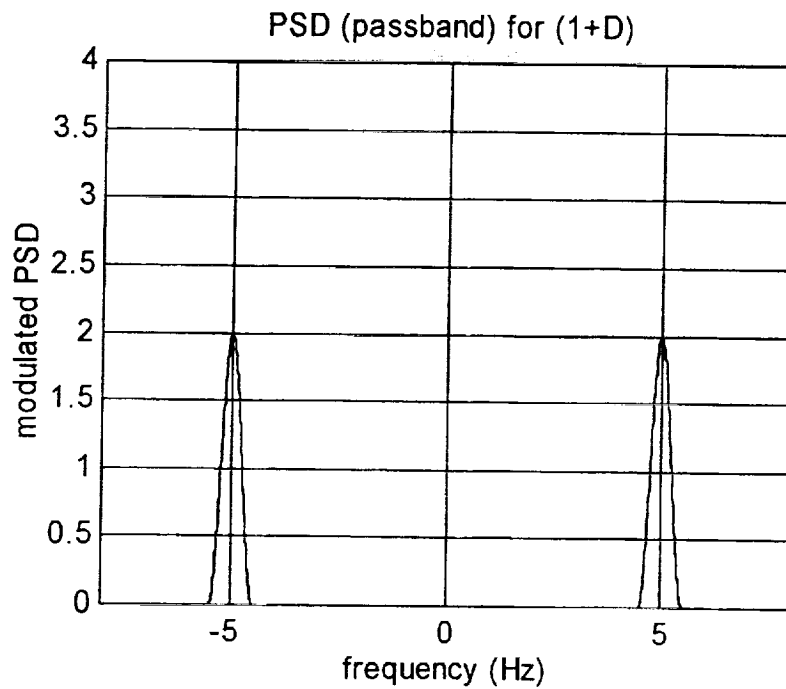
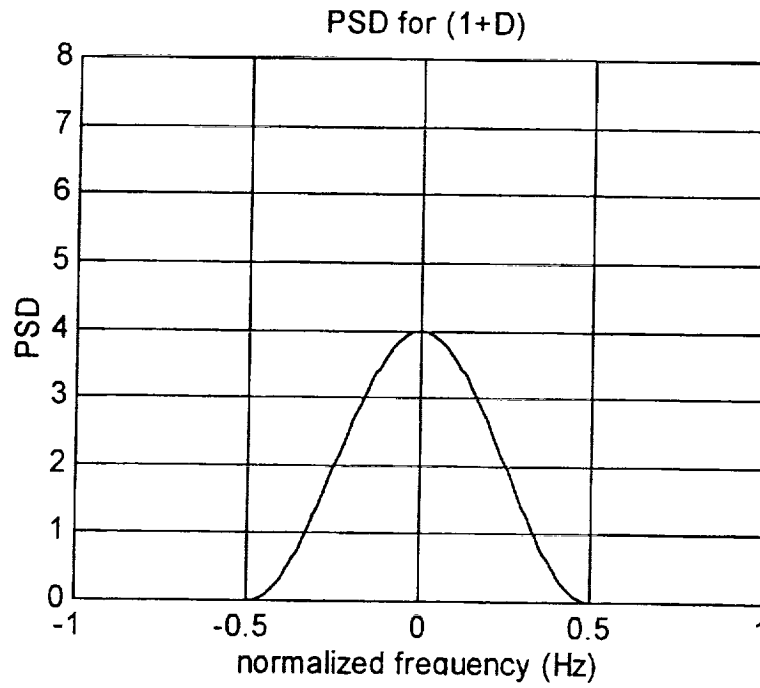
$$h_2(f) = h_2(D) \Big|_{D=e^{-j2\pi fT_o}}$$

$$= 2 \cdot T_o \cdot \sin(2\pi fT_o) \cdot \left(e^{-j2\pi fT_o} \right)$$

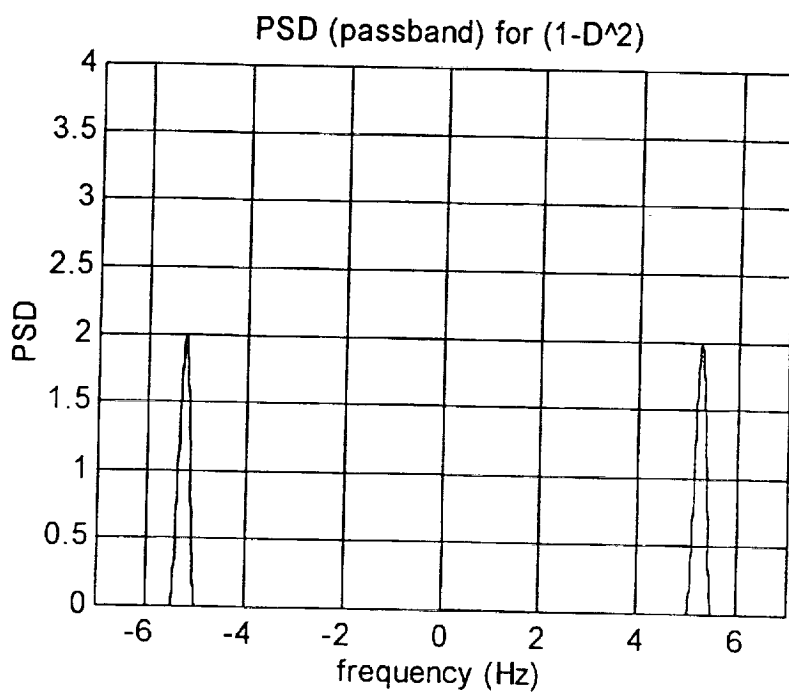
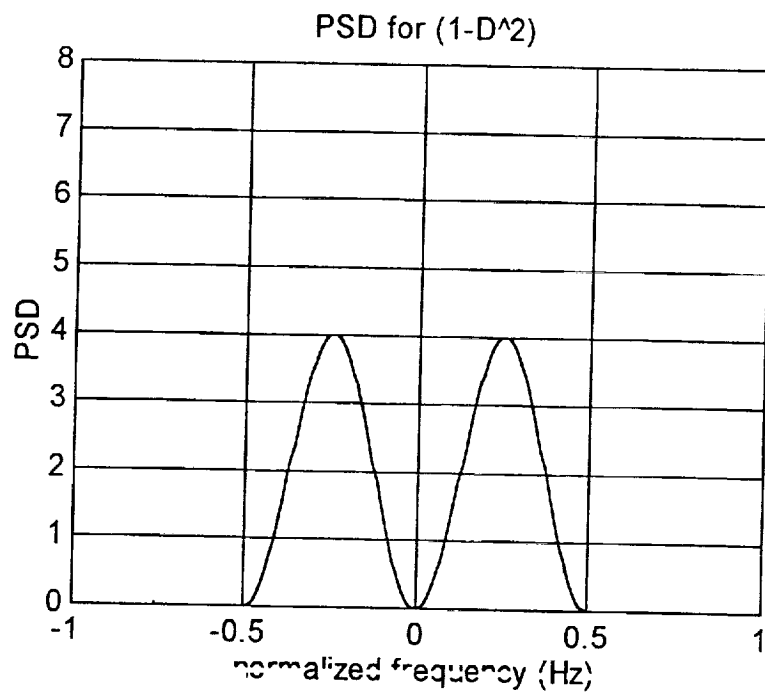
- PSD:

$$G(f) = \frac{1}{T_o} |h_2(f)|^2 = 4 \cdot T_o \cdot \sin^2(2\pi fT_o)$$

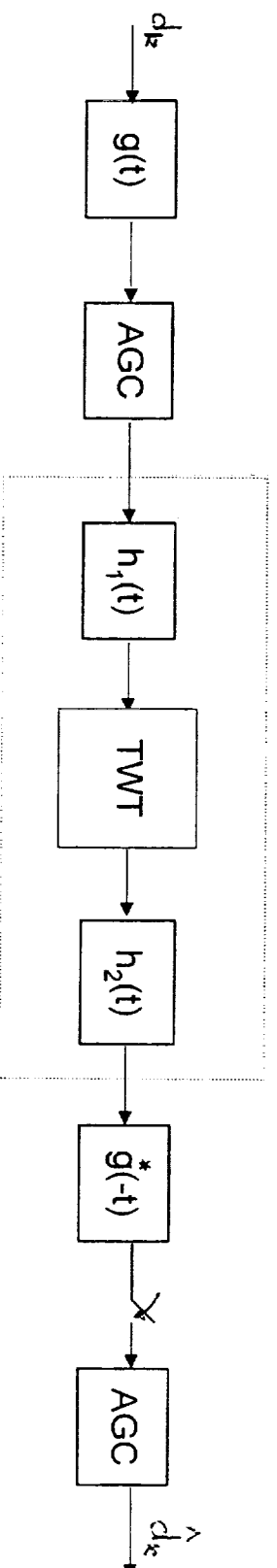
PSD - PR1



PSD (Cont'd) – PR4



Satellite Channel Model

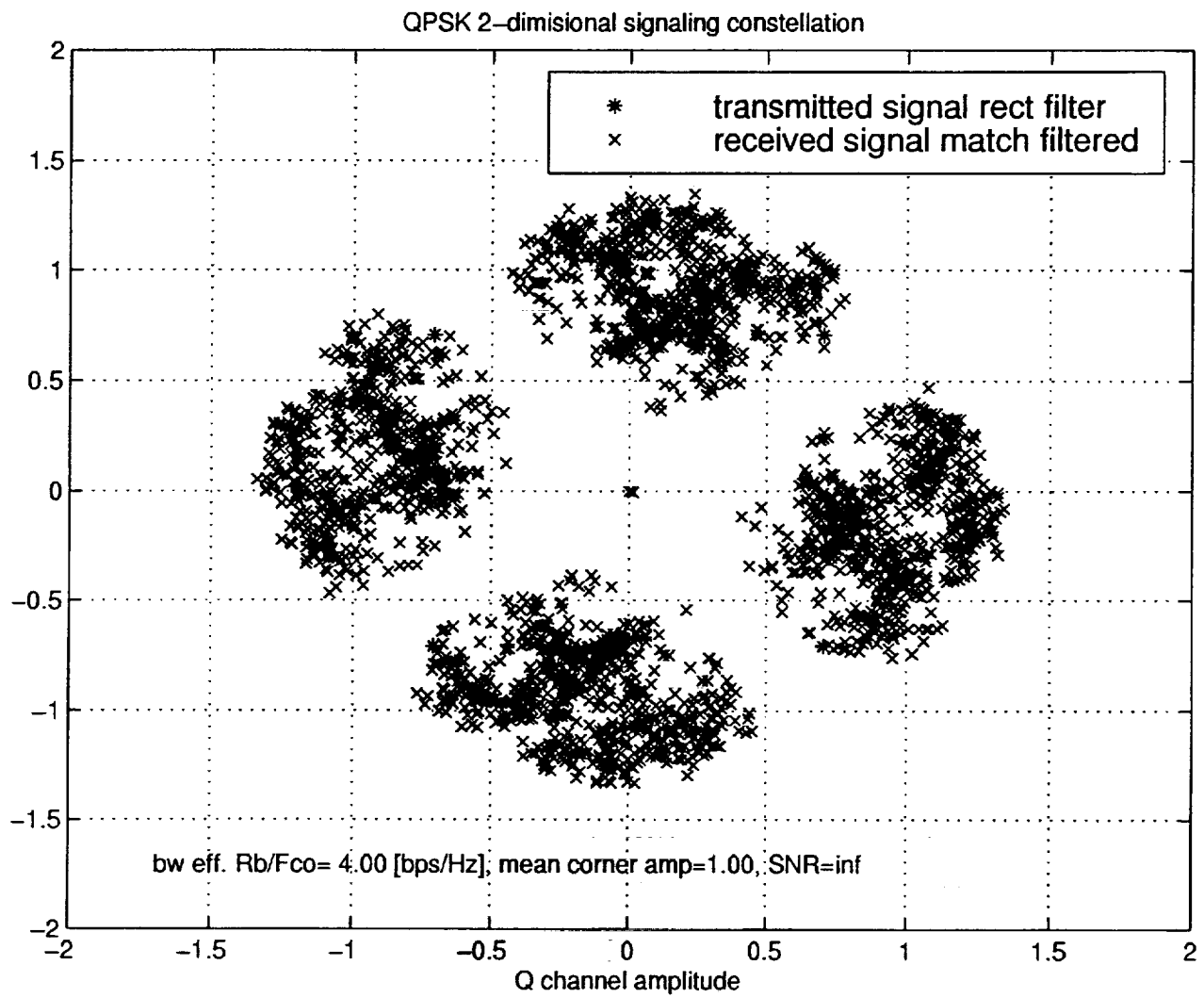


- For later convenience, define bandwidth-efficiency (BE) as

$$BE = \frac{R_b}{f_{cw}}, \text{ where } R_b = \text{bit rate, and } f_{cw} = \text{cut-off frequency}$$

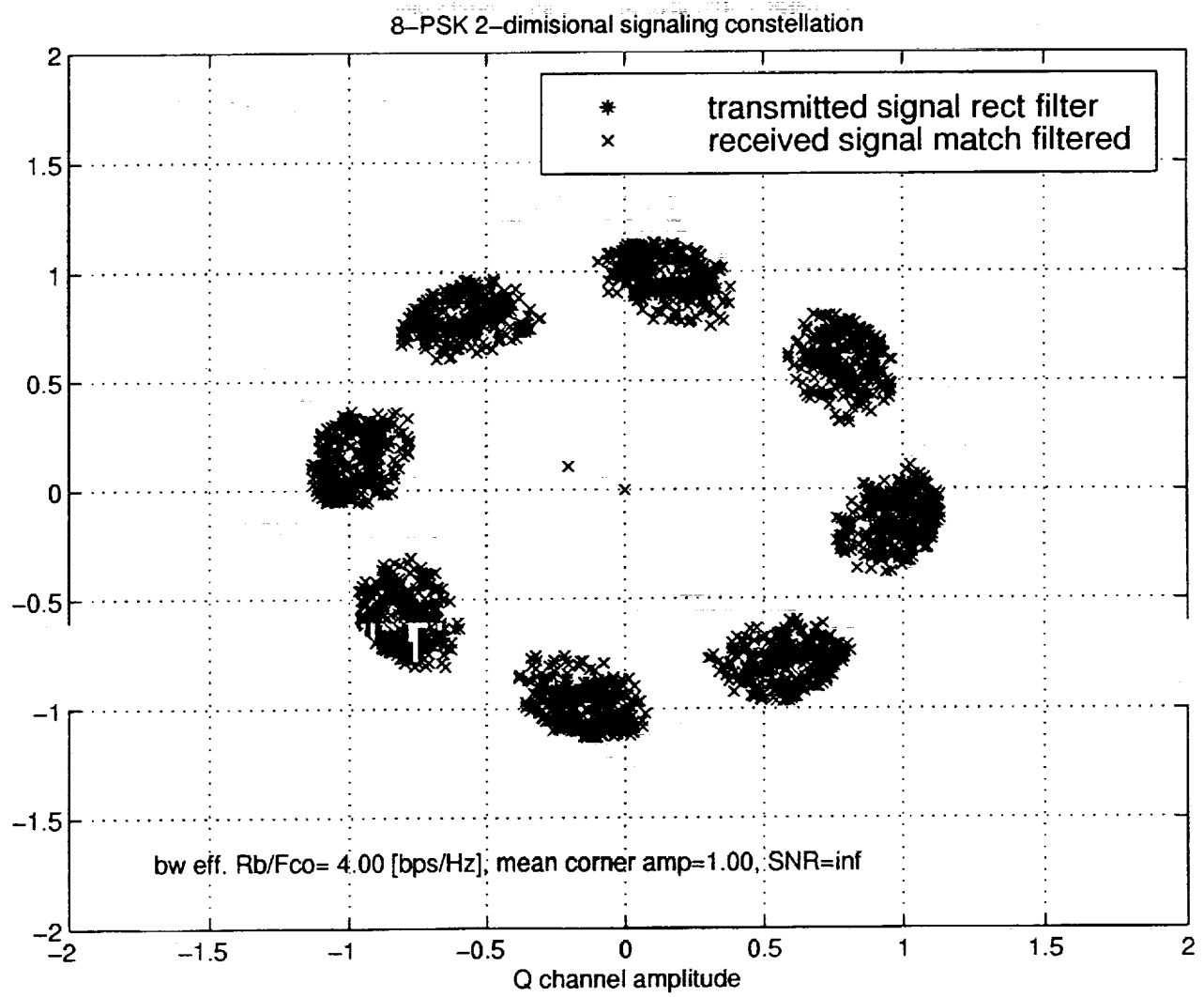
Signal Constellation

QPSK



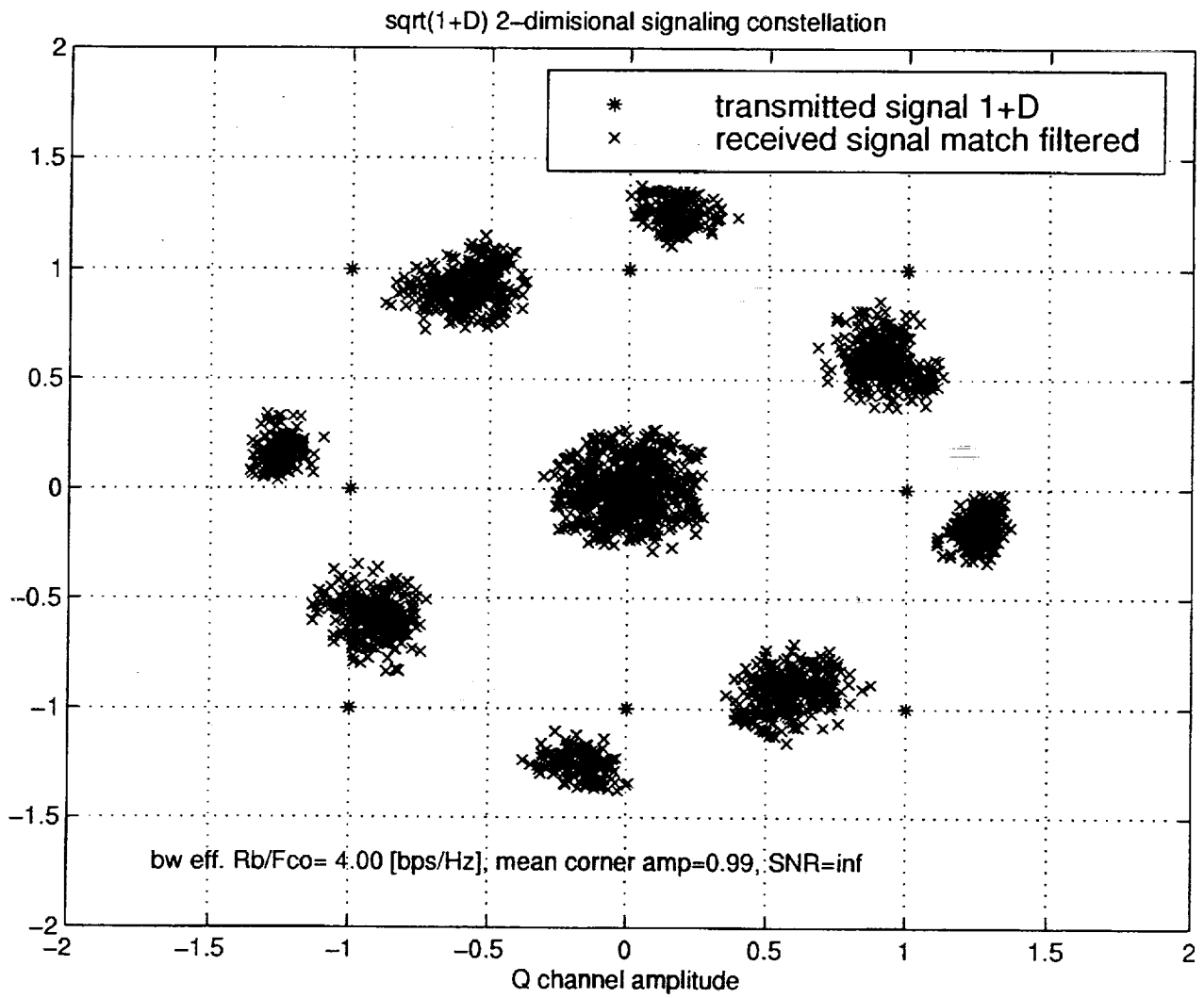
Signal Constellation

8PSK



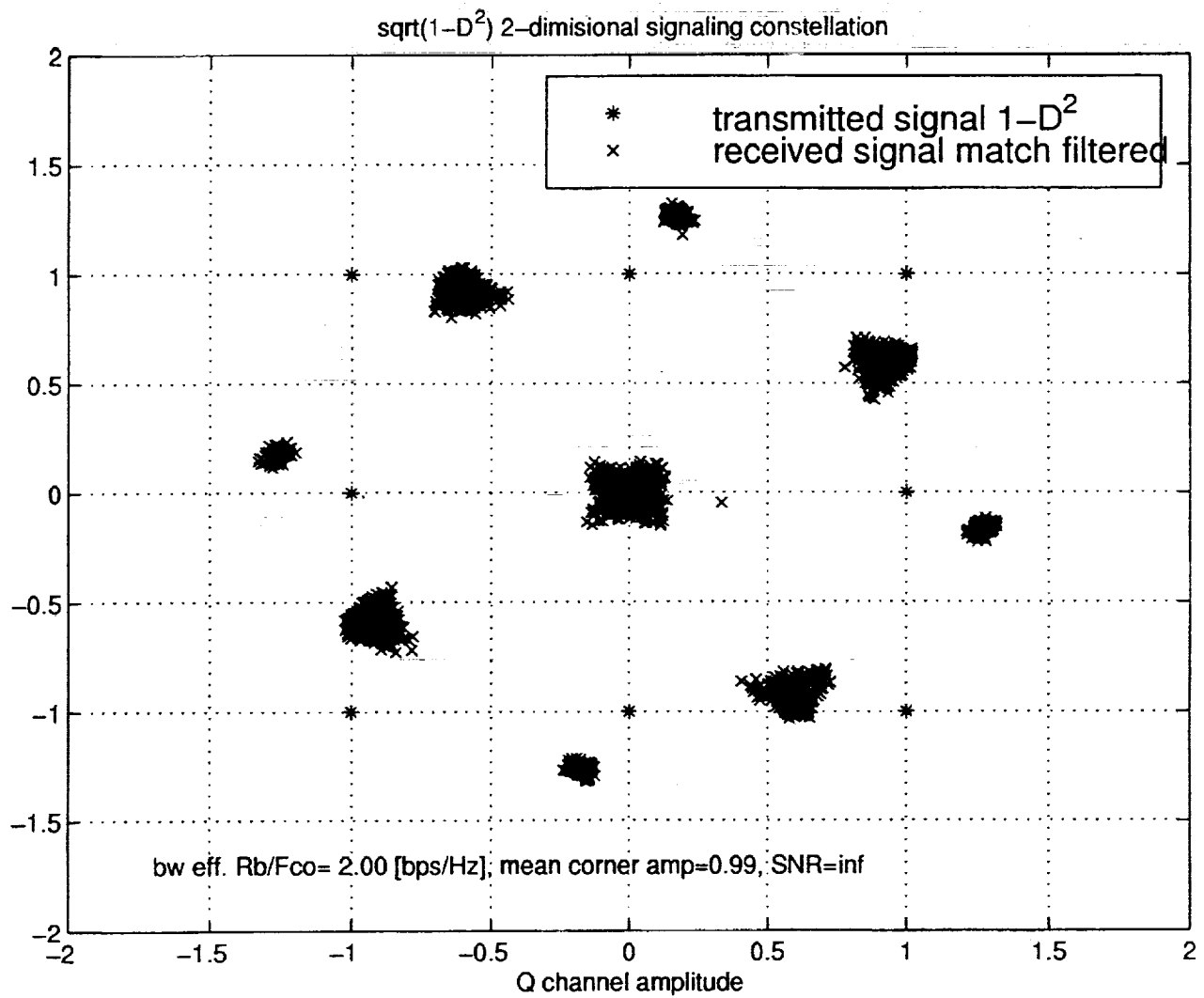
Signal Constellation

PR1

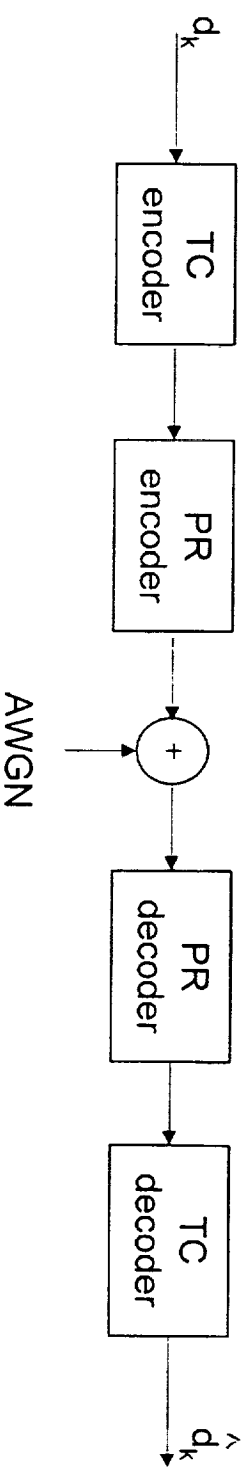


Signal Constellation

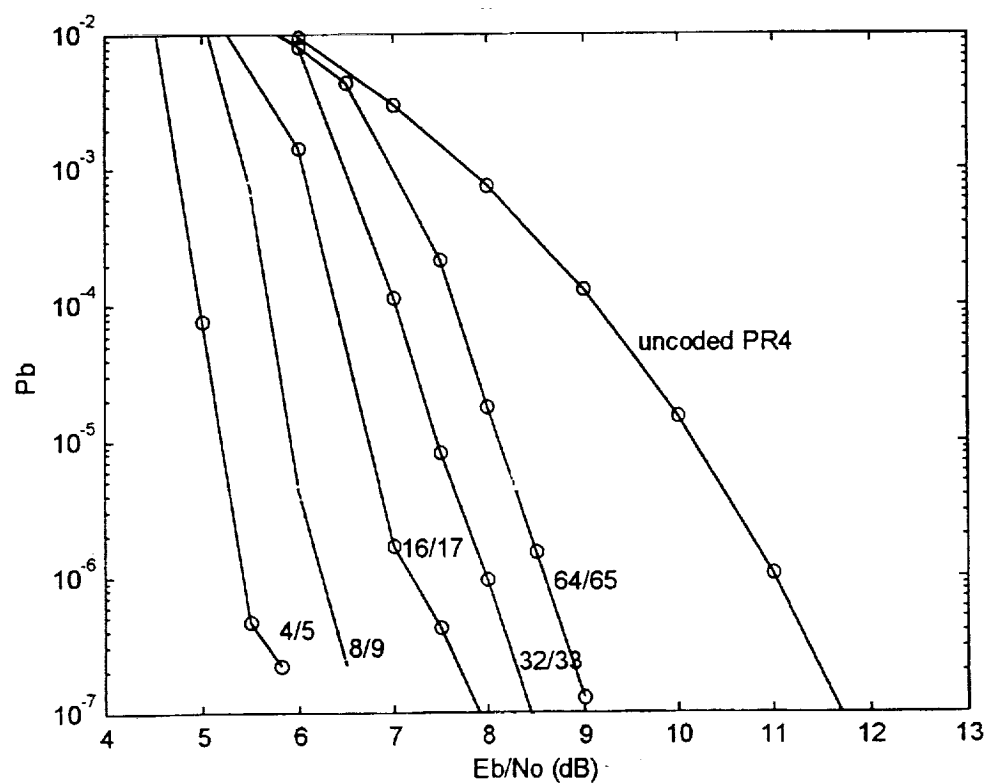
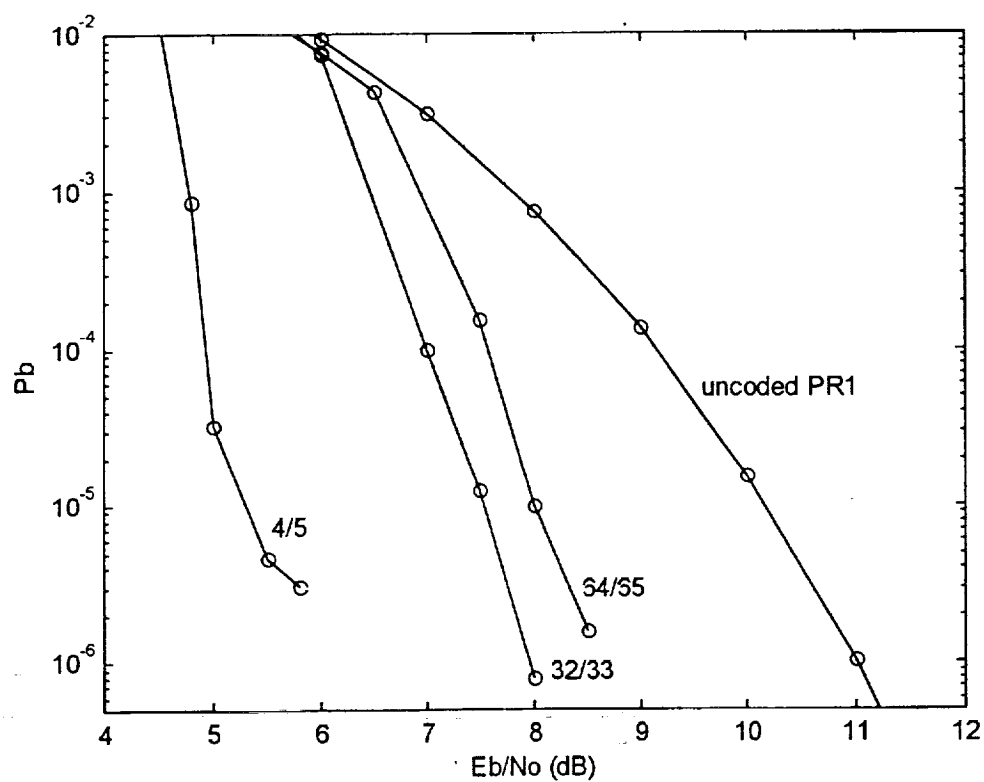
PR4



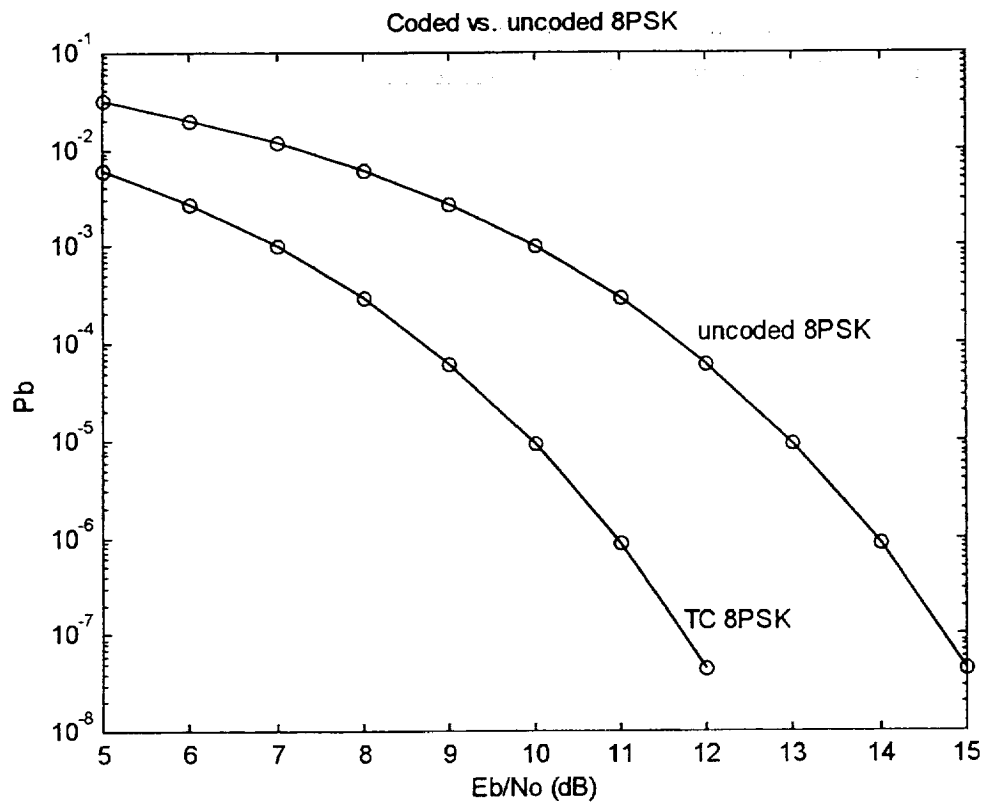
Coded Partial Response Simulation Diagram



Performance of coded PR



Performance of coded 8-PSK



Future Work

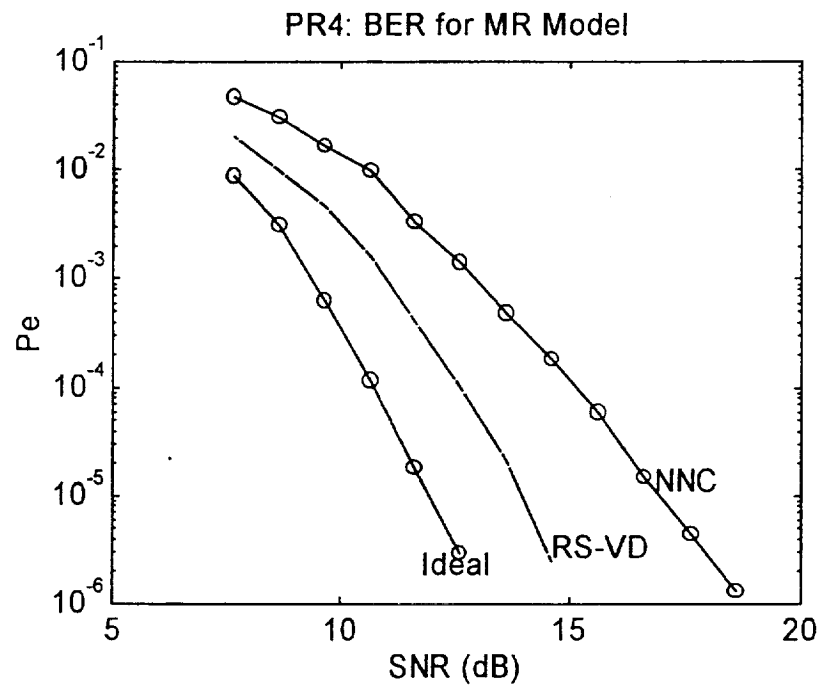
- Check the performance (bit error rate) of the actual system with more realistic assumptions, such as:

Assume non-perfect synchronization. Thus, carrier and timing recovery will be investigated.

Considering up-link and/or downlink additive noise.

- Design new high rate parallel as well as serial concatenated convolutional codes
- Try sub-optimal APP decoders, such as soft-output Viterbi algorithm (SOVA)
- Evaluate performance with nonlinear equalizers, such as RAM-based equalizers.

Performance of RAM-based equalizer

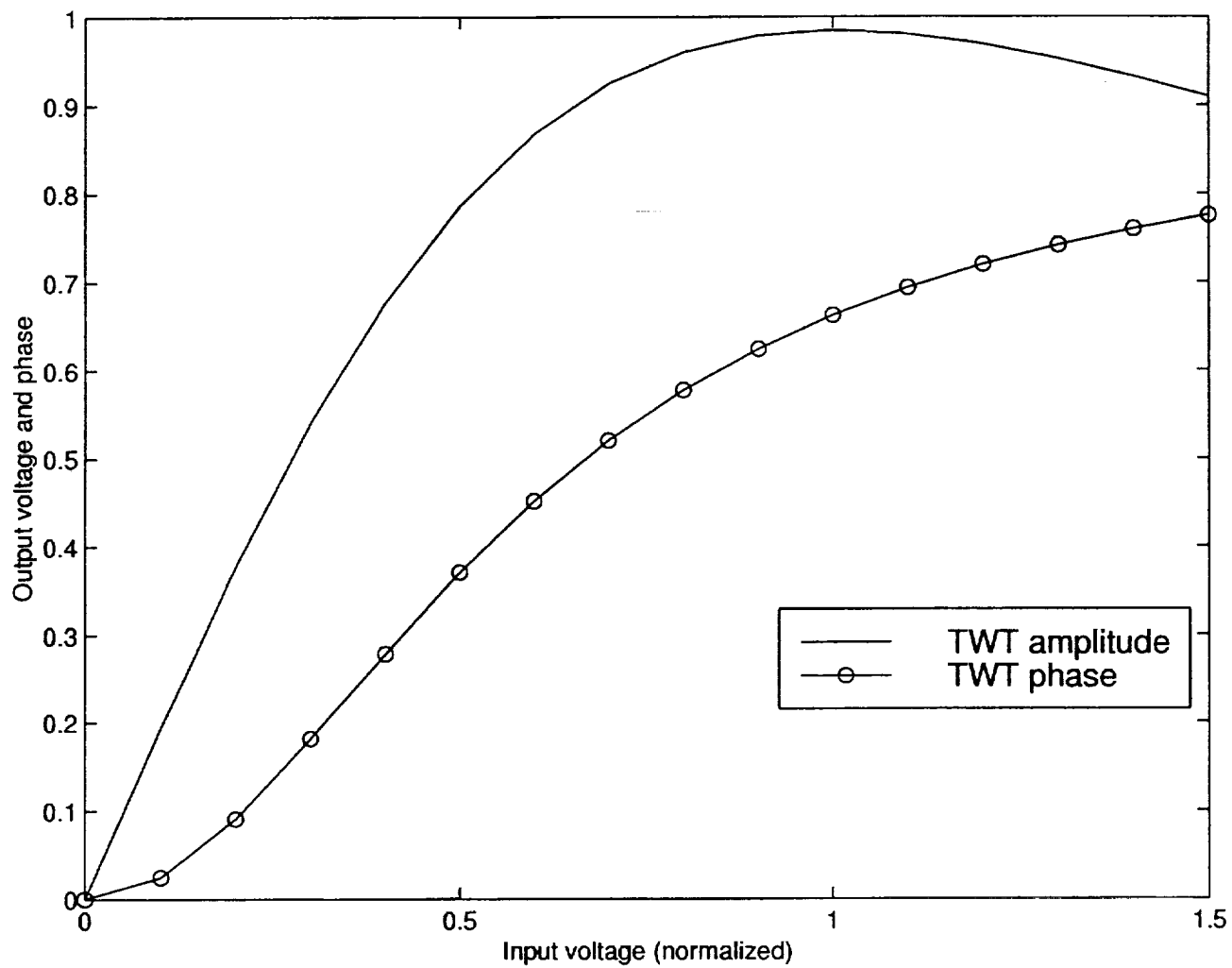


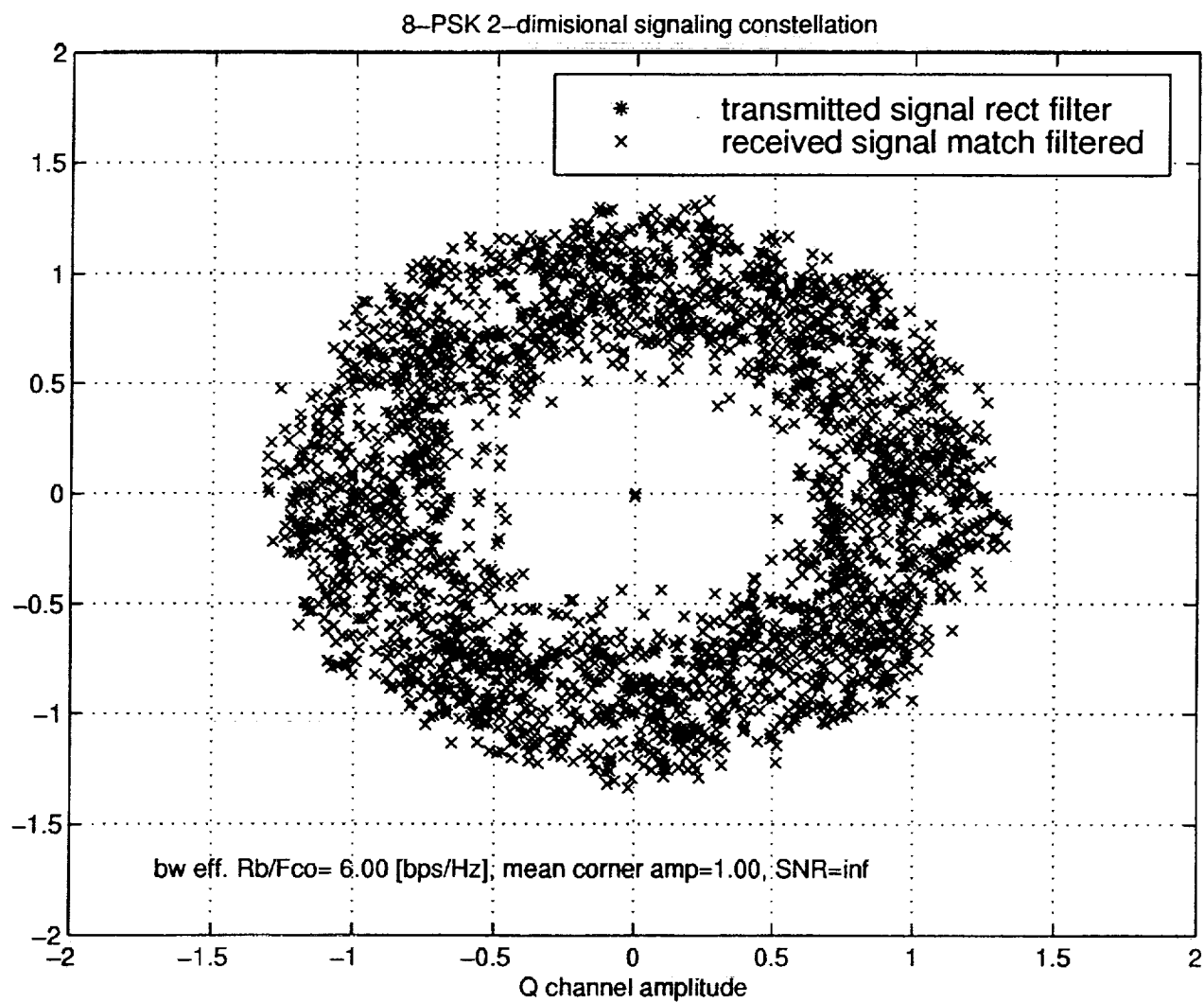
Conclusions

Why PR?

- BW efficient (no excess BW required)
- Constant envelope
- Easy to design binary TC.
- Operating at low SNR when combined with TC

TWT AMPLITUDE and PHASE MODEL





Synchronization at Low SNR

Jeffrey T. Drake

William E. Ryan - Thesis Advisor

New Mexico State University
Department of Electrical and Computer
Engineering

February 1999

OUTLINE

- Motivation
- Work performed since last review
- Partial Response Satellite Feasibility (Ali)
- Cramer-Rao Bounds (CRBs) for MPSK
 - Phase & symbol timing estimation simulations developed for CRB evaluation
 - Maximum a posteriori (MAP)
 - Decision Directed (DD) block no feedback
 - DD block w/ feedback
 - Soft DD block no feedback
 - Nonlinear block estimator
- Joint phase/timing estimation - FSE
- Conclusions and future work

MOTIVATION

- Operating SNR's moving lower e.g. $E_s/N_o < 0$ dB
 - higher data rates
 - major improvements in channel coding
 - Turbo codes
- Mandates new look at synchronization performance
 - Phase
 - Symbol

CRBs for MPSK

- What is the “best” estimate of the phase

- Quality measures

- a. Phase error

$$e = \hat{\phi} - \phi$$

- b. Mean Square Error (MSE - Jitter)

$$\overline{\phi_e^2} = E[(\hat{\phi} - \phi)^2]$$

- c. Cramer-Rao Bound (CRB)

- In general MSE difficult to compute
 - CRB provides lower bound on MSE for unbiased estimator of ϕ (non-random)

$$CRB(\phi) = [E\left\{\left(\frac{\partial \ln p(\bar{x}|\phi)}{\partial \phi}\right)^2\right\}]^{-1}$$

- Commonly compare MPSK synchronizer performance to CRB for unmodulated carrier.
- Very loose for low signal to noise ratios (SNR)
- Tighter bounds have been published for BPSK and QPSK (Cowley)

CRBs for MPSK

- Verified BPSK and QPSK CRBs
 - Derivation details were not available
- Extending work to 8-PSK CRB
 - I have intermediate result
 - Working on simplifying
 - QPSK had 4 equations with 3 terms each
 - 8-PSK has 8 equations with 10 terms each
 - Outline of derivation for 8-PSK

CRB for MPSK

Outline of 8PSK derivation

Received 8PSK signal with fixed phase offset set during the observation interval of N symbols

$$x_l = a_l e^{j\phi} + n_l, \text{ for } l = 1, \dots, N$$

Then we have for the AVERAGED 8-PSK log likelihood function

$$\Lambda_8(\theta, k) =$$

$$\sum_{l=k-N}^{k-1} \ln \left[\cosh \left(\frac{\operatorname{Re}(x_l e^{-j\phi})}{\sigma^2} \right) + \cosh \left(\frac{\operatorname{Im}(x_l e^{-j\phi})}{\sigma^2} \right) + \cosh \left(\frac{\operatorname{Re}(x_l e^{-j\frac{\pi}{4}} e^{-j\phi})}{\sigma^2} \right) + \cosh \left(\frac{\operatorname{Im}(x_l e^{-j\frac{\pi}{4}} e^{-j\phi})}{\sigma^2} \right) \right]$$

The CRB is a lower bound on the variance of any unbiased estimator of ϕ , and is given by Van Trees as

$$\operatorname{CRB}(\phi) = \left[E \left\{ \left(\frac{\partial \ln p(\mathbf{x} | \phi)}{\partial \phi} \right)^2 \right\} \right]^{-1}$$

$$\operatorname{CRB}^{-1}(\phi) =$$

$$E \left\{ \left(\sum_{l=k-N}^{k-1} \frac{\sinh \left(\frac{a_l^I + n_l^I}{\sigma^2} \right) \frac{1}{\sigma^2} (a_l^Q + n_l^Q) - \sinh \left(\frac{a_l^Q + n_l^Q}{\sigma^2} \right) \frac{1}{\sigma^2} (a_l^I + n_l^I)}{\cosh \left(\frac{a_l^I + n_l^I}{\sigma^2} \right) + \cosh \left(\frac{a_l^Q + n_l^Q}{\sigma^2} \right) + \cosh \left(\frac{\sqrt{2} (a_l^I + a_l^Q + n_l^I + n_l^Q)}{2\sigma^2} \right) + \cosh \left(\frac{\sqrt{2} (-a_l^I + a_l^Q - n_l^I + n_l^Q)}{2\sigma^2} \right)} \right. \right. \\ + \frac{\sinh \left(\frac{\sqrt{2} (a_l^I + a_l^Q + n_l^I + n_l^Q)}{2\sigma^2} \right) \frac{1}{\sigma^2} \frac{\sqrt{2}}{2} (-a_l^I + a_l^Q - n_l^I + n_l^Q)}{\cosh \left(\frac{a_l^I + n_l^I}{\sigma^2} \right) + \cosh \left(\frac{a_l^Q + n_l^Q}{\sigma^2} \right) + \cosh \left(\frac{\sqrt{2} (a_l^I + a_l^Q + n_l^I + n_l^Q)}{2\sigma^2} \right) + \cosh \left(\frac{\sqrt{2} (-a_l^I + a_l^Q - n_l^I + n_l^Q)}{2\sigma^2} \right)} \\ \left. \left. - \frac{\sinh \left(\frac{\sqrt{2} (-a_l^I + a_l^Q - n_l^I + n_l^Q)}{2\sigma^2} \right) \frac{1}{\sigma^2} \frac{\sqrt{2}}{2} (a_l^I + a_l^Q + n_l^I + n_l^Q)}{\cosh \left(\frac{a_l^I + n_l^I}{\sigma^2} \right) + \cosh \left(\frac{a_l^Q + n_l^Q}{\sigma^2} \right) + \cosh \left(\frac{\sqrt{2} (a_l^I + a_l^Q + n_l^I + n_l^Q)}{2\sigma^2} \right) + \cosh \left(\frac{\sqrt{2} (-a_l^I + a_l^Q - n_l^I + n_l^Q)}{2\sigma^2} \right)} \right) \right\}^2$$

Note: Through monte carlo integration using above eq. we can numerically calculate the 8-psk CRB! But of course we would like a more convenient and insightful form of the CRB, so we continue...

After much manipulation we can arrive at the simplified form of above eq.

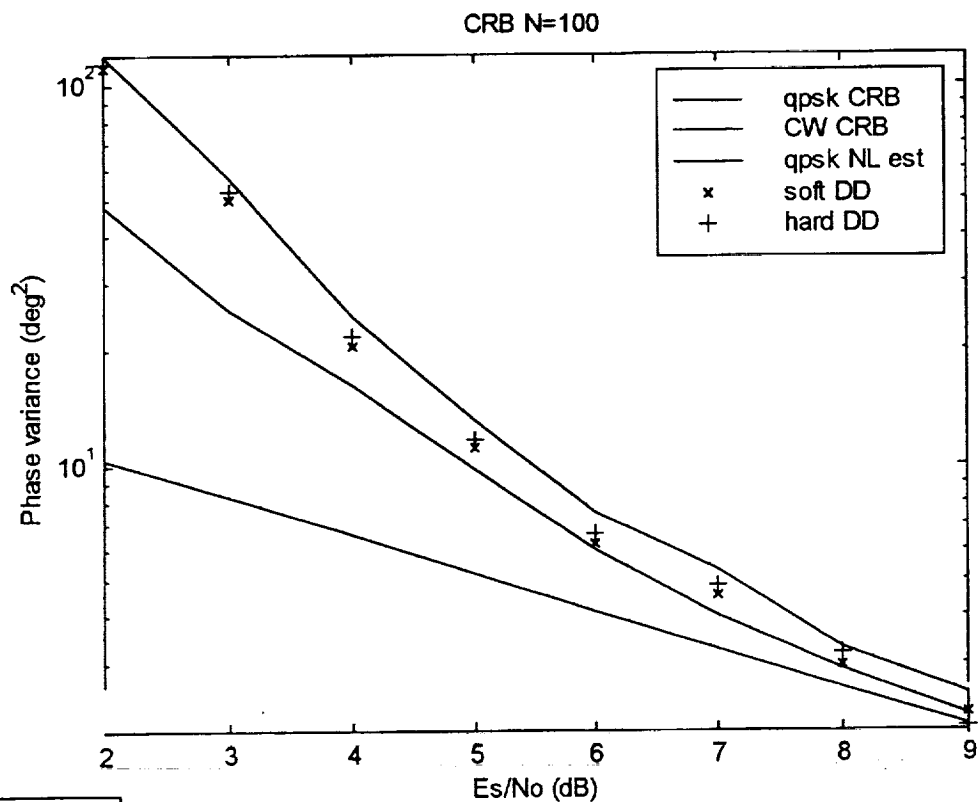
CRB⁻¹ (φ) =

$$\begin{aligned}
 & \frac{\left(\frac{a^0 \cdot \tilde{n}^0}{\sigma^2}\right)^2 \sinh^2\left(\frac{a^T \cdot \tilde{n}^T}{\sigma^2}\right)}{\left(\cosh\left(\frac{a^T \cdot \tilde{n}^T}{\sigma^2}\right) + \cosh\left(\frac{a^0 \cdot \tilde{n}^0}{\sigma^2}\right) + \cosh\left(\frac{\sqrt{2}(a^T \cdot a^0 + n^T + n^0)}{2\sigma^2}\right) + \cosh\left(\frac{\sqrt{2}(-a^T \cdot a^0 - n^T + n^0)}{2\sigma^2}\right)\right)^2} \\
 & + \frac{\left(\frac{a^T \cdot \tilde{n}^T}{\sigma^2}\right)^2 \sinh^2\left(\frac{a^0 \cdot \tilde{n}^0}{\sigma^2}\right)}{\left(\cosh\left(\frac{a^T \cdot \tilde{n}^T}{\sigma^2}\right) + \cosh\left(\frac{a^0 \cdot \tilde{n}^0}{\sigma^2}\right) + \cosh\left(\frac{\sqrt{2}(a^T \cdot a^0 + n^T + n^0)}{2\sigma^2}\right) + \cosh\left(\frac{\sqrt{2}(-a^T \cdot a^0 - n^T + n^0)}{2\sigma^2}\right)\right)^2} \\
 & + \frac{\left(\frac{\sqrt{2}(-a^T \cdot a^0 - n^T + n^0)}{2\sigma^2}\right)^2 \sinh^2\left(\frac{\sqrt{2}(a^T \cdot a^0 + n^T + n^0)}{2\sigma^2}\right)}{\left(\cosh\left(\frac{a^T \cdot \tilde{n}^T}{\sigma^2}\right) + \cosh\left(\frac{a^0 \cdot \tilde{n}^0}{\sigma^2}\right) + \cosh\left(\frac{\sqrt{2}(a^T \cdot a^0 + n^T + n^0)}{2\sigma^2}\right) + \cosh\left(\frac{\sqrt{2}(-a^T \cdot a^0 - n^T + n^0)}{2\sigma^2}\right)\right)^2} \\
 & + \frac{\left(\frac{\sqrt{2}(a^T \cdot a^0 + n^T + n^0)}{2\sigma^2}\right)^2 \sinh^2\left(\frac{\sqrt{2}(-a^T \cdot a^0 - n^T + n^0)}{2\sigma^2}\right)}{\left(\cosh\left(\frac{a^T \cdot \tilde{n}^T}{\sigma^2}\right) + \cosh\left(\frac{a^0 \cdot \tilde{n}^0}{\sigma^2}\right) + \cosh\left(\frac{\sqrt{2}(a^T \cdot a^0 + n^T + n^0)}{2\sigma^2}\right) + \cosh\left(\frac{\sqrt{2}(-a^T \cdot a^0 - n^T + n^0)}{2\sigma^2}\right)\right)^2} \\
 & - \frac{2\left(\frac{a^T \cdot \tilde{n}^T}{\sigma^2}\right)\left(\frac{a^0 \cdot \tilde{n}^0}{\sigma^2}\right) \sinh\left(\frac{a^T \cdot \tilde{n}^T}{\sigma^2}\right) \sinh\left(\frac{a^0 \cdot \tilde{n}^0}{\sigma^2}\right)}{\left(\cosh\left(\frac{a^T \cdot \tilde{n}^T}{\sigma^2}\right) + \cosh\left(\frac{a^0 \cdot \tilde{n}^0}{\sigma^2}\right) + \cosh\left(\frac{\sqrt{2}(a^T \cdot a^0 + n^T + n^0)}{2\sigma^2}\right) + \cosh\left(\frac{\sqrt{2}(-a^T \cdot a^0 - n^T + n^0)}{2\sigma^2}\right)\right)^2} \\
 & + \frac{2 \sinh\left(\frac{a^T \cdot \tilde{n}^T}{\sigma^2}\right) \sinh\left(\frac{\sqrt{2}(a^T \cdot a^0 + n^T + n^0)}{2\sigma^2}\right) \left(\frac{a^0 \cdot \tilde{n}^0}{\sigma^2}\right) \left(\frac{\sqrt{2}(-a^T \cdot a^0 - n^T + n^0)}{2\sigma^2}\right)}{\left(\cosh\left(\frac{a^T \cdot \tilde{n}^T}{\sigma^2}\right) + \cosh\left(\frac{a^0 \cdot \tilde{n}^0}{\sigma^2}\right) + \cosh\left(\frac{\sqrt{2}(a^T \cdot a^0 + n^T + n^0)}{2\sigma^2}\right) + \cosh\left(\frac{\sqrt{2}(-a^T \cdot a^0 - n^T + n^0)}{2\sigma^2}\right)\right)^2} \\
 & - \frac{2 \sinh\left(\frac{a^T \cdot \tilde{n}^T}{\sigma^2}\right) \sinh\left(\frac{\sqrt{2}(-a^T \cdot a^0 - n^T + n^0)}{2\sigma^2}\right) \left(\frac{a^0 \cdot \tilde{n}^0}{\sigma^2}\right) n_1^{I0} = \left(\frac{\sqrt{2}(a^T \cdot a^0 + n_1^T + n_1^0)}{2\sigma^2}\right)}{\left(\cosh\left(\frac{a^T \cdot \tilde{n}^T}{\sigma^2}\right) + \cosh\left(\frac{a^0 \cdot \tilde{n}^0}{\sigma^2}\right) + \cosh\left(\frac{\sqrt{2}(a^T \cdot a^0 + n^T + n^0)}{2\sigma^2}\right) + \cosh\left(\frac{\sqrt{2}(-a^T \cdot a^0 - n^T + n^0)}{2\sigma^2}\right)\right)^2} \\
 & - \frac{2 \sinh\left(\frac{a^0 \cdot \tilde{n}^0}{\sigma^2}\right) \sinh\left(\frac{\sqrt{2}(a^T \cdot a^0 + n^T + n^0)}{2\sigma^2}\right) \left(\frac{a^T \cdot \tilde{n}^T}{\sigma^2}\right) \left(\frac{\sqrt{2}(-a^T \cdot a^0 - n^T + n^0)}{2\sigma^2}\right)}{\left(\cosh\left(\frac{a^T \cdot \tilde{n}^T}{\sigma^2}\right) + \cosh\left(\frac{a^0 \cdot \tilde{n}^0}{\sigma^2}\right) + \cosh\left(\frac{\sqrt{2}(a^T \cdot a^0 + n^T + n^0)}{2\sigma^2}\right) + \cosh\left(\frac{\sqrt{2}(-a^T \cdot a^0 - n^T + n^0)}{2\sigma^2}\right)\right)^2} \\
 & + \frac{2 \sinh\left(\frac{a^0 \cdot \tilde{n}^0}{\sigma^2}\right) \sinh\left(\frac{\sqrt{2}(-a^T \cdot a^0 - n^T + n^0)}{2\sigma^2}\right) \left(\frac{a^T \cdot \tilde{n}^T}{\sigma^2}\right) \left(\frac{\sqrt{2}(a^T \cdot a^0 + n^T + n^0)}{2\sigma^2}\right)}{\left(\cosh\left(\frac{a^T \cdot \tilde{n}^T}{\sigma^2}\right) + \cosh\left(\frac{a^0 \cdot \tilde{n}^0}{\sigma^2}\right) + \cosh\left(\frac{\sqrt{2}(a^T \cdot a^0 + n^T + n^0)}{2\sigma^2}\right) + \cosh\left(\frac{\sqrt{2}(-a^T \cdot a^0 - n^T + n^0)}{2\sigma^2}\right)\right)^2} \\
 & - \frac{2 \sinh\left(\frac{\sqrt{2}(a^T \cdot a^0 + n^T + n^0)}{2\sigma^2}\right) \sinh\left(\frac{\sqrt{2}(-a^T \cdot a^0 - n^T + n^0)}{2\sigma^2}\right) \left(\frac{\sqrt{2}(-a^T \cdot a^0 - n^T + n^0)}{2\sigma^2}\right) \left(\frac{\sqrt{2}(a^T \cdot a^0 + n^T + n^0)}{2\sigma^2}\right)}{\left(\cosh\left(\frac{a^T \cdot \tilde{n}^T}{\sigma^2}\right) + \cosh\left(\frac{a^0 \cdot \tilde{n}^0}{\sigma^2}\right) + \cosh\left(\frac{\sqrt{2}(a^T \cdot a^0 + n^T + n^0)}{2\sigma^2}\right) + \cosh\left(\frac{\sqrt{2}(-a^T \cdot a^0 - n^T + n^0)}{2\sigma^2}\right)\right)^2}
 \end{aligned}$$

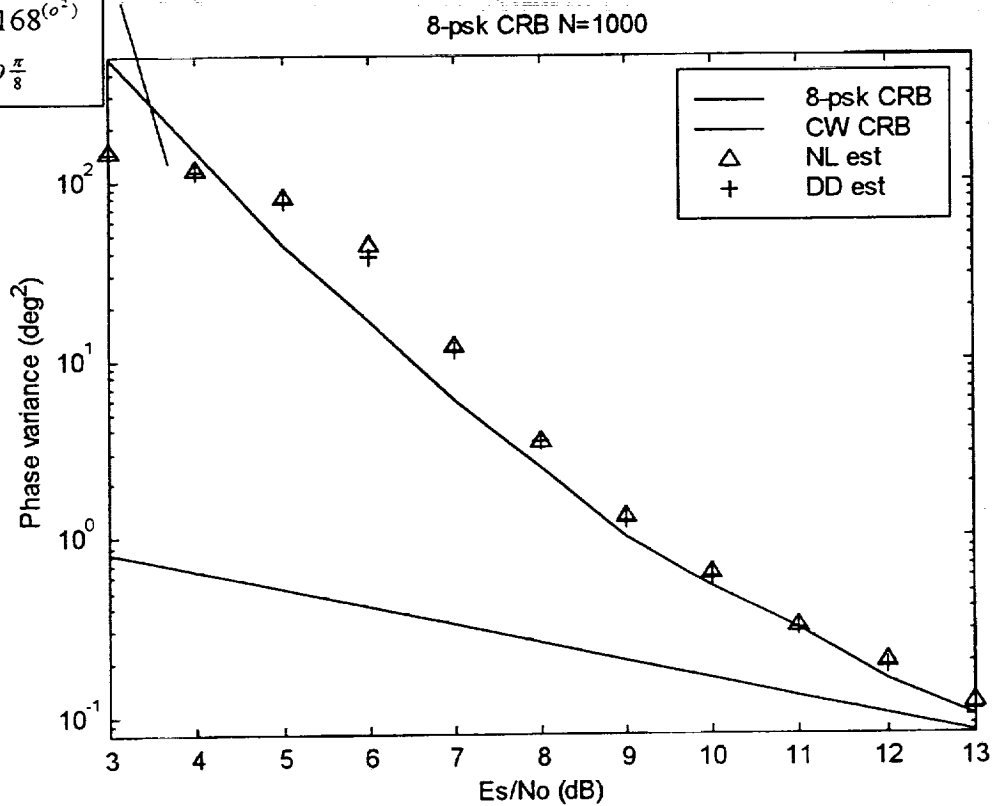
Next we must take the expectation of above over all three variables symbols a and noise \tilde{n}_I^I and \tilde{n}_I^Q .

This leads to an expansion by a factor of 8 in the number of terms.....

CRBs for MPSK



$\sigma^2(\text{uniform dist}) = 168^{(\sigma^2)}$
 uniform dist = $-\frac{\pi}{8}$ to $\frac{\pi}{8}$



Simulations Developed

- Implemented 4 phase estimation simulations for performance characterization w/ new CRBs
- Two widely applied criteria in estimation

1. MAP - Maximum a Posteriori Probability

$$\hat{\phi} = \arg_{\phi} \max P(\phi|\bar{r}) = \frac{P(\bar{r}|\phi)p(\phi)}{p(\bar{r})}$$

Where: - ϕ considered random
 - Characterized by a priori probability $p(\phi)$

2. ML - Maximum Likelihood

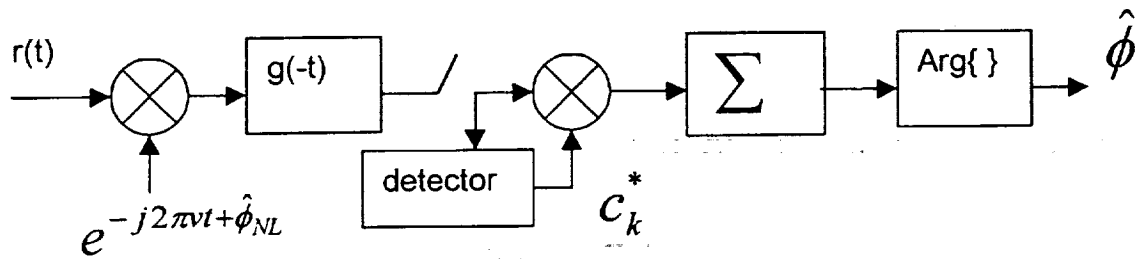
$$\hat{\phi} = \arg_{\phi} \max P(\phi|\bar{r}) = P(\bar{r}|\phi)$$

Where: - ϕ considered non-random but unknown

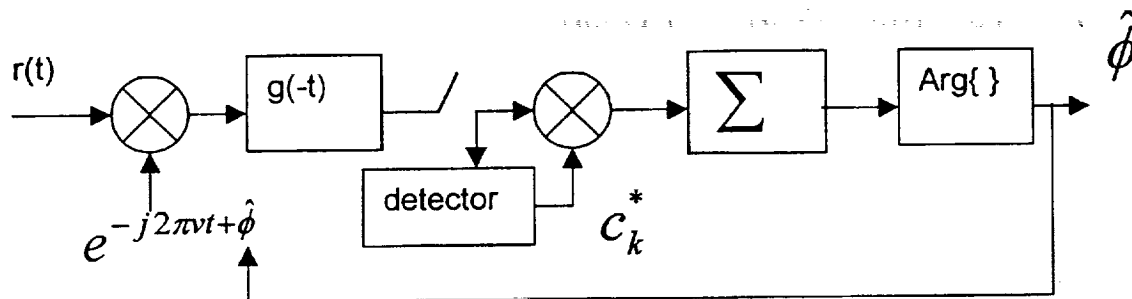
Note: if we have no a - priori knowledge of ϕ , if we assume $p(\phi)$ uniform we arrive at MAP = ML

3. Ad Hoc Techniques

1. Approximate ML Feed forward DD estimator

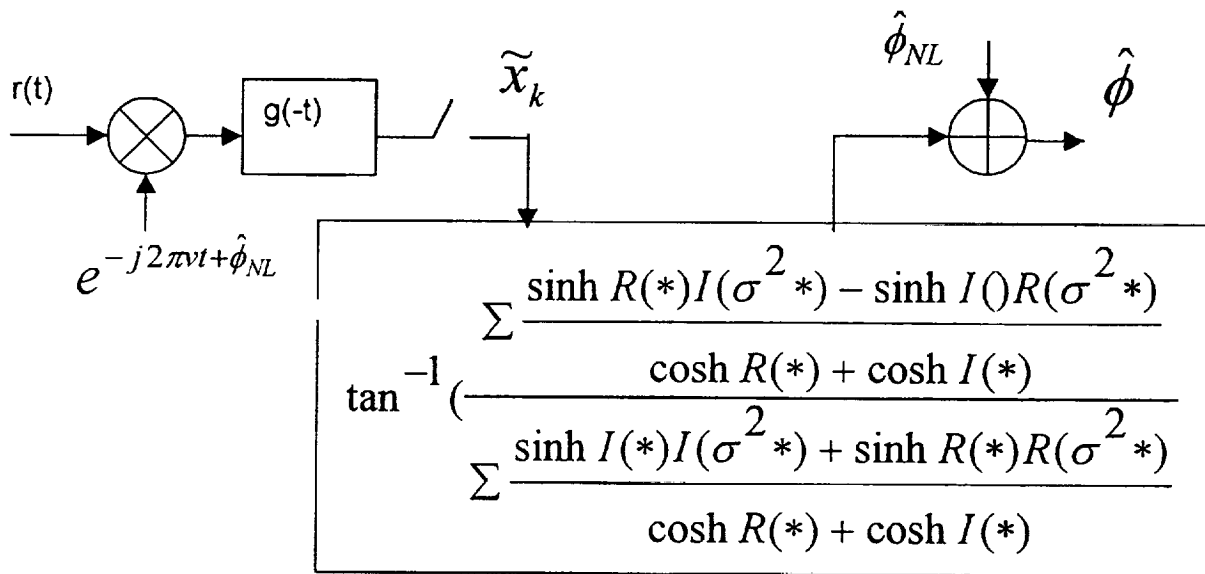


2. Approximate ML feed back DD estimator



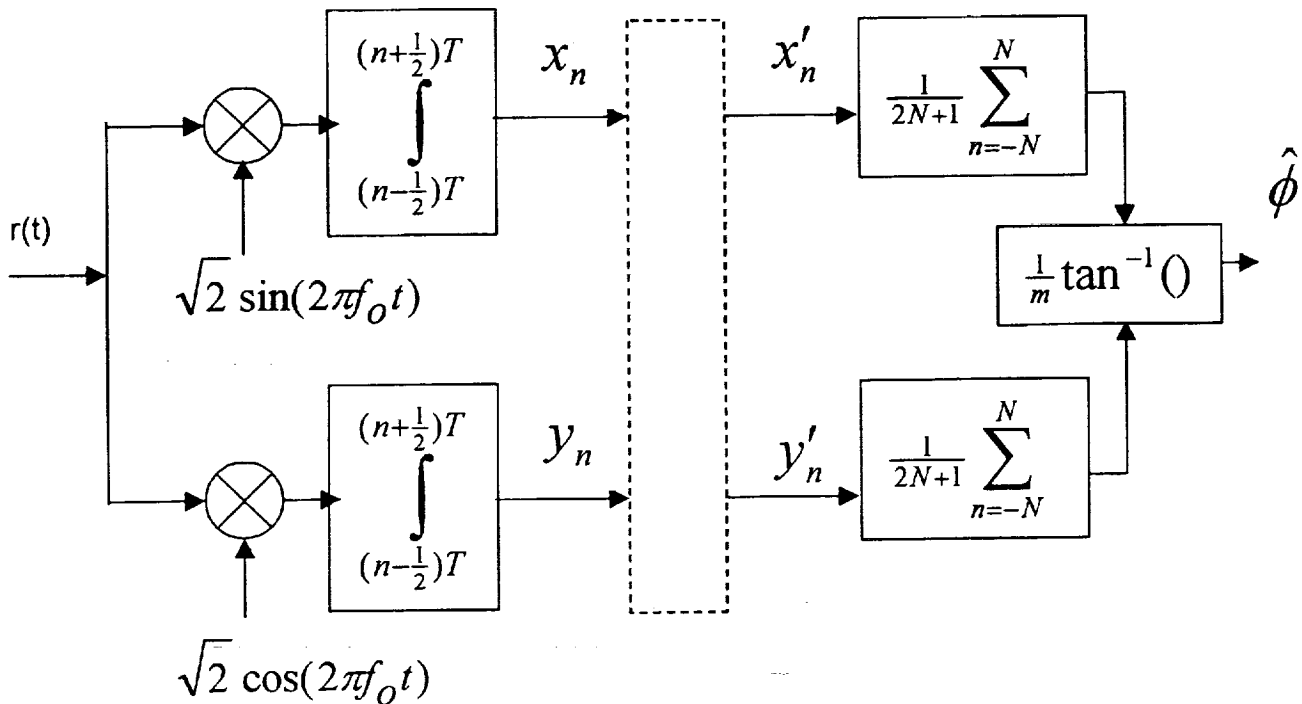
Simulations Developed

3. Approximate ML soft DD estimator (QPSK)



Simulations Developed

4. Ad-Hoc nonlinear phase estimator (Viterbi)



- ML unmodulated carrier phase estimate
 - with dotted box eliminated
- For PSK modulation replace dotted box with complex nonlinear function

$$x'_n + iy'_n = F(\rho_n) e^{im\phi_n}$$

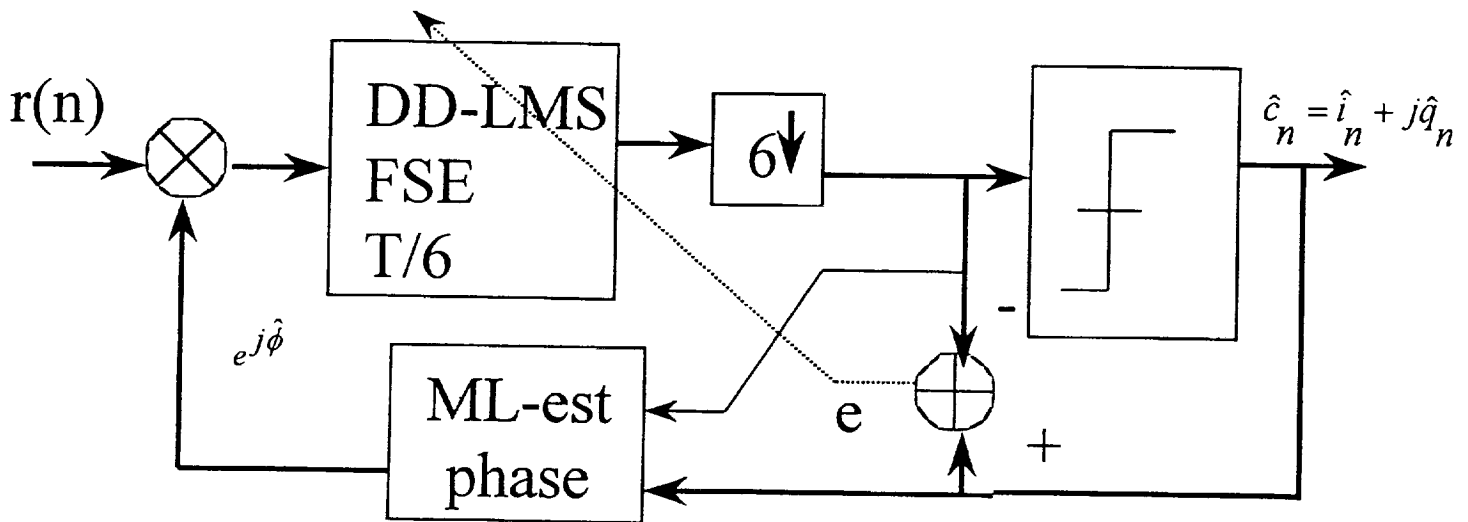
where

$$\rho_n = \sqrt{x_n^2 + y_n^2}, \phi_n = \tan^{-1}\left(\frac{y_n}{x_n}\right)$$

- This estimator performs nearly as well as ML

Joint estimation - With FSE

- Joint phase/timing estimation with FSE
 - Counters ISI effects
 - Symbol timing derived implicitly within FSE



- How does one characterize the symbol timing jitter performance of this estimator?
- To my knowledge no published results here
- I have developed a technique to measure FSE timing jitter
- Plan to prove analytically validity of approach

Future Work

- Complete 8-PSK CRB derivation
- Modify MPSK CRB for random parameter and constrained non-random
- Formalize FSE timing jitter algorithm

Serial Concatenated Convolutional Codes and Some Implementation Issues on High Rate Turbo Codes

Ömer Fatih Açikel

and

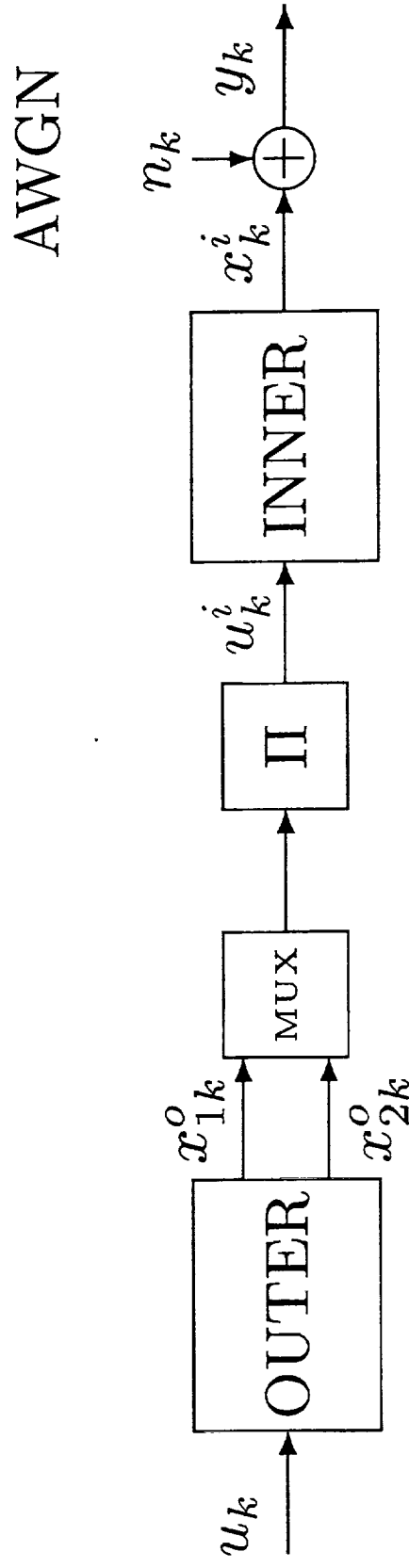
William E. Ryan, Thesis Advisor

February 23, 1999

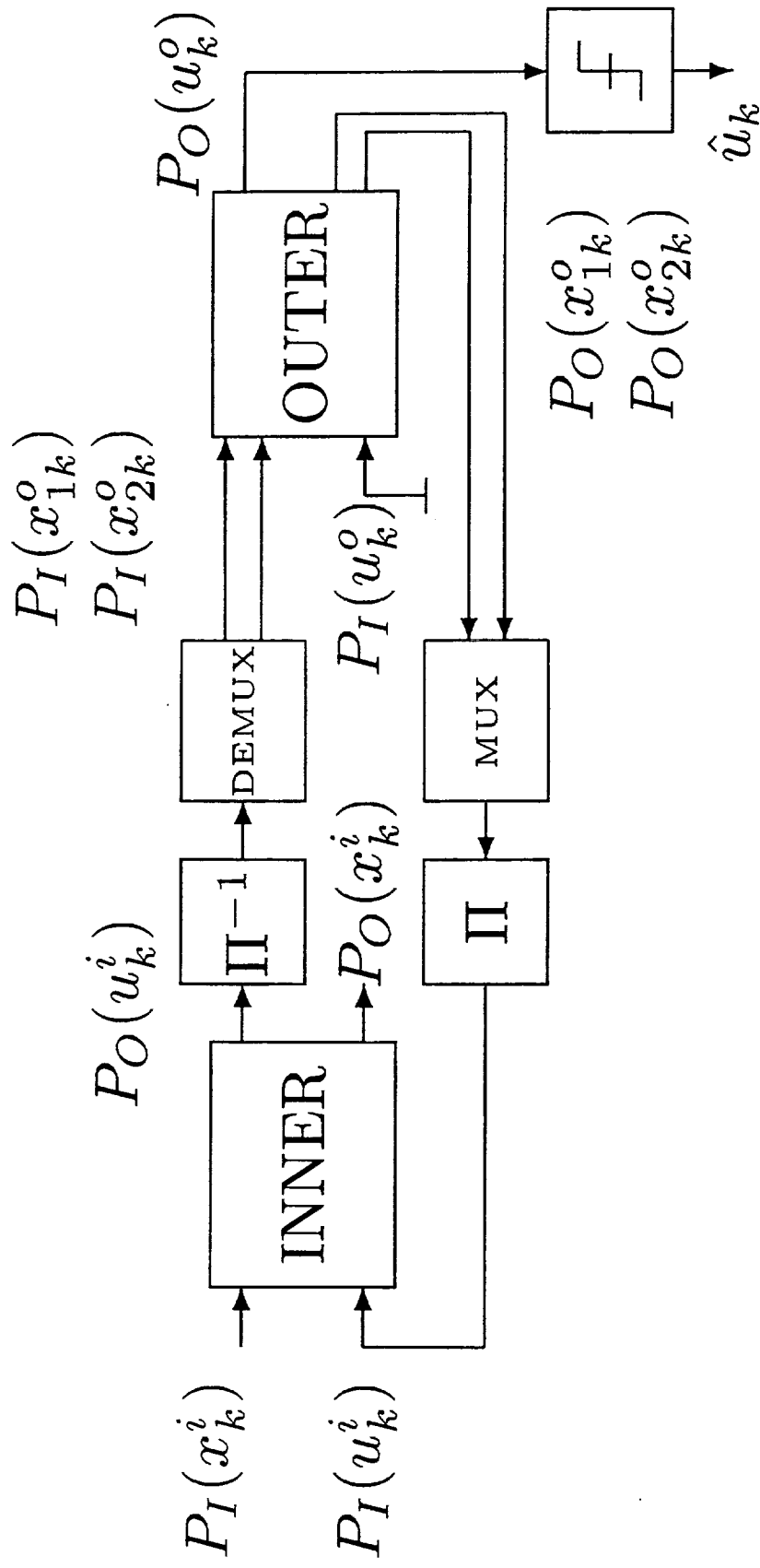
Outline

- Serial Concatenated Convolutional Codes (SCCC).
 - Encoder-decoder.
 - Simulation results for rates $1/2$ and $3/4$.
- Turbo code (TC) encoder-decoder.
- Implementation issues on TCs.
 - Quantization.
 - Effects of quantization, SNR offset, and decoding Delay (D) on BER performance.
 - Simulation results for rates $3/4$, $7/8$, and $15/16$.

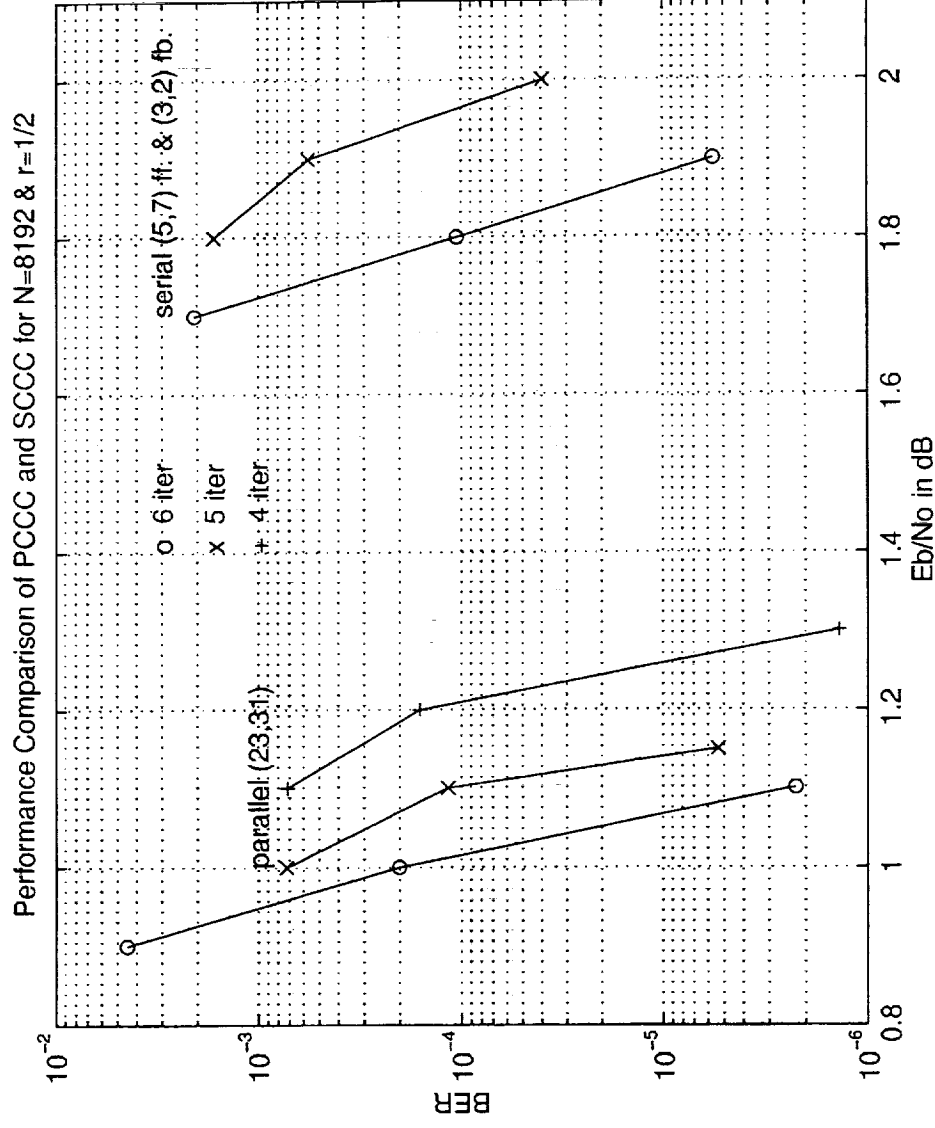
SCCC Encoder



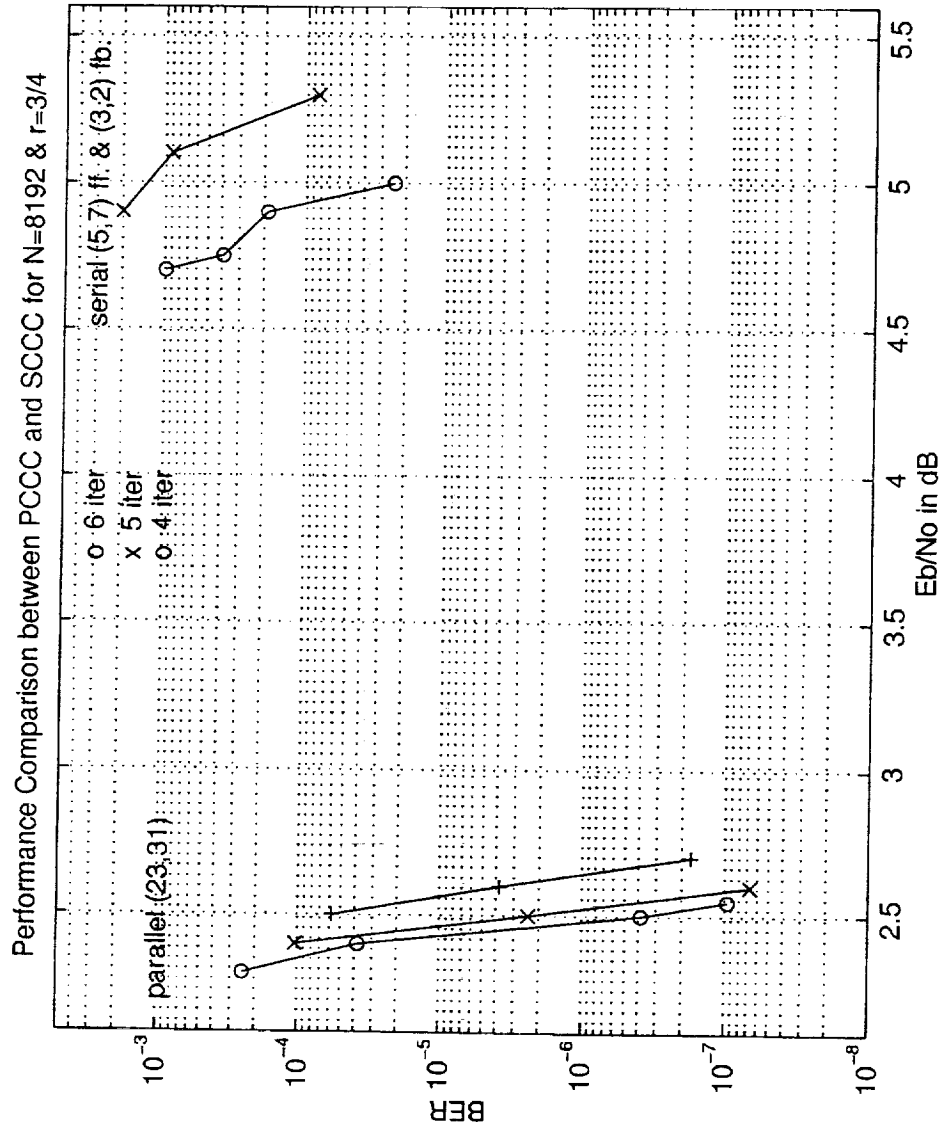
SCCC Decoder



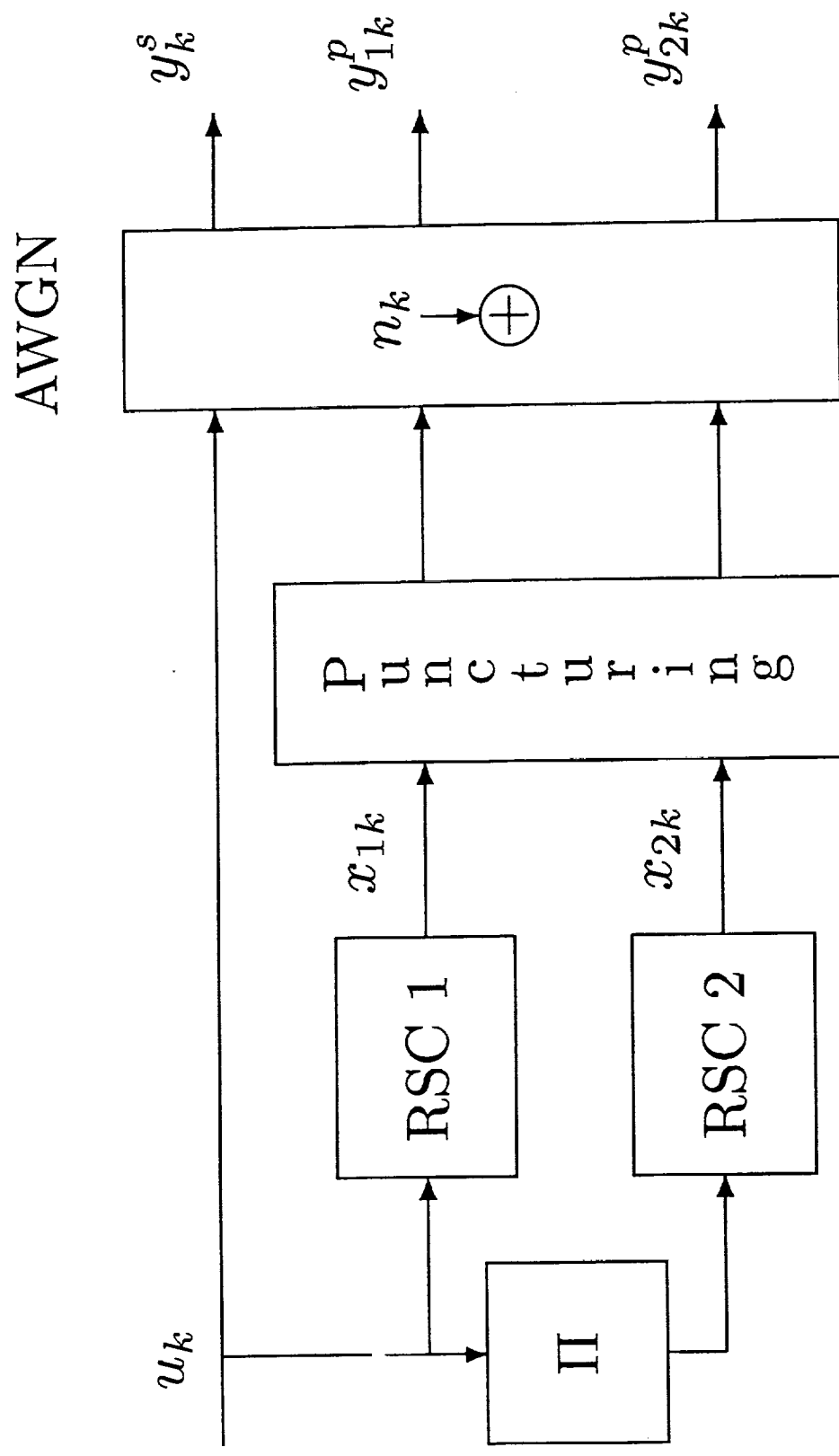
SCCC vs. TC Performance for $r=1/2$



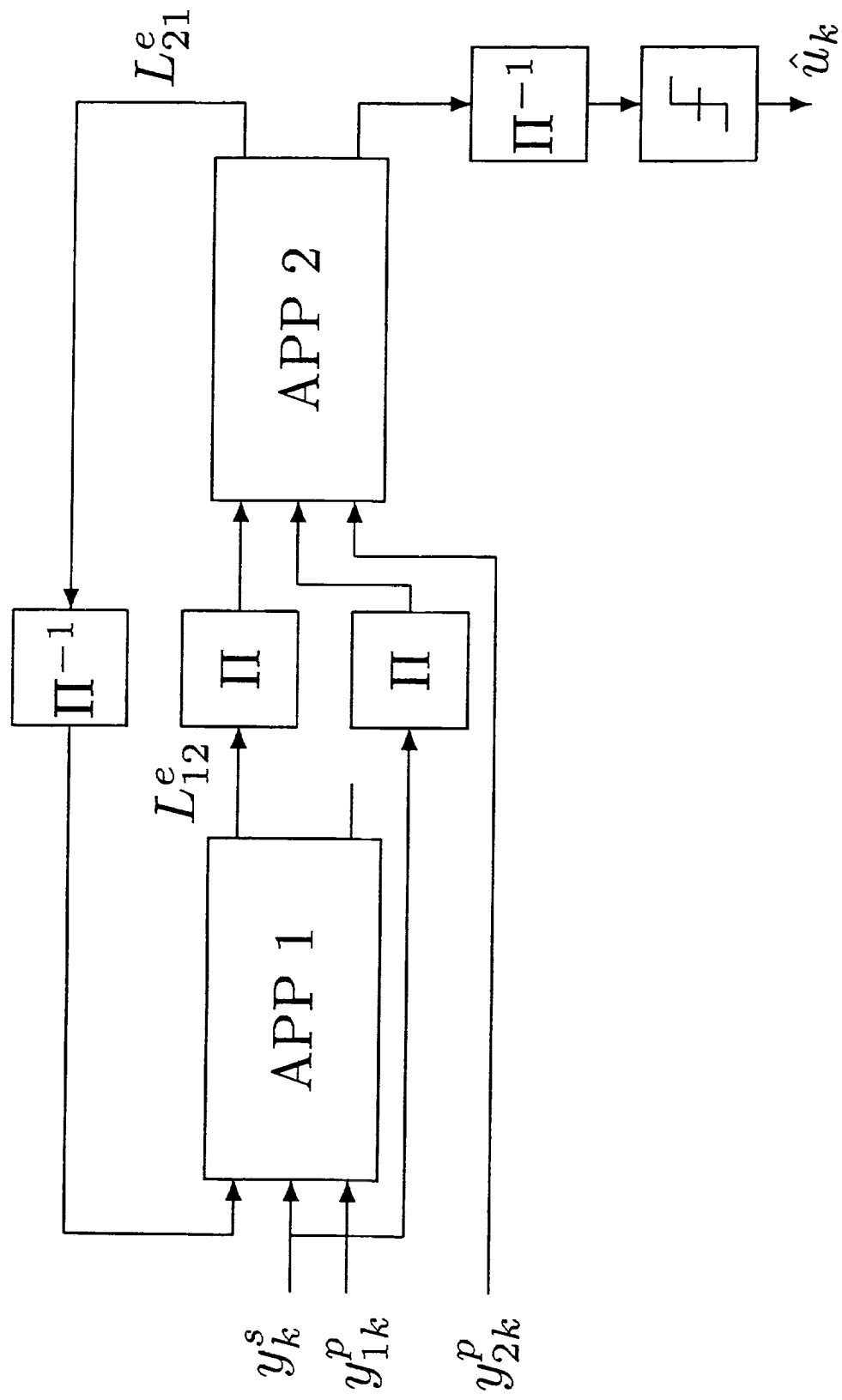
SCCC vs. TC Performance for $r=3/4$



TC Encoder



TC Decoder



Implementation Issues on TC: Quantization

Each *APP* decoder has the following parameters.

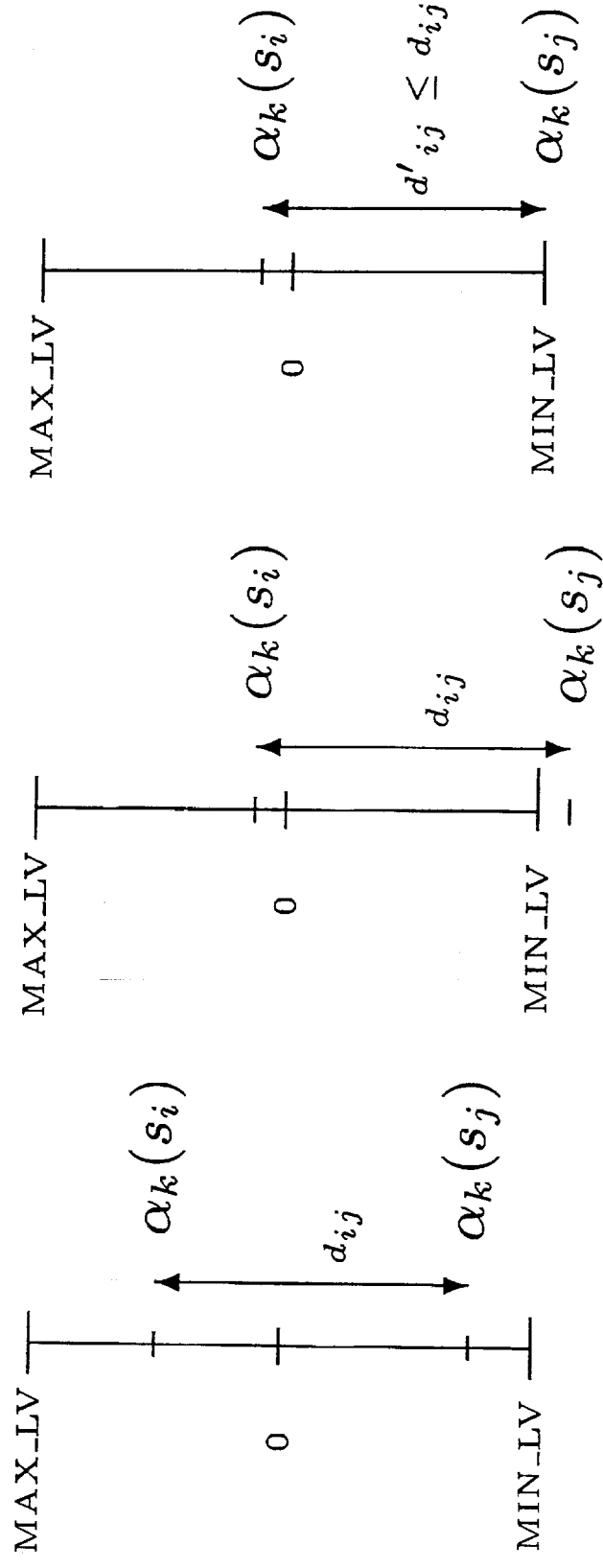
Due to their equal importance, all parameters assumed to have the same quantization level (4, 6, or 8-bit).

State Metric	$\gamma_k(L_c, y_k^s, y_{ik}^p)$	4, 6, 8-bit
Forward Recursion	$\alpha_k(\gamma_k, \alpha_{k-1})$	4, 6, 8-bit
Backward Recursion	$\beta_k(\gamma_{k+1}, \beta_{k+1})$	4, 6, 8-bit
Extrinsic Info.	$L_k^e(\gamma_k, \alpha_{k-1}, \beta_k)$	4, 6, 8-bit
Channel values	y_k^s, y_{ik}^p	up to 6-bit

Implementation Issues on TC:

Quantization (cntd')

$\alpha_k(s)$ increases as k increases and $\beta_k(s)$ increases as k decreases. Implementation is suboptimum when $d\{\alpha_k(s_i), \alpha_k(s_j)\} = d_{ij} \geq \frac{2^Q}{2} = 2^{Q-1}$.



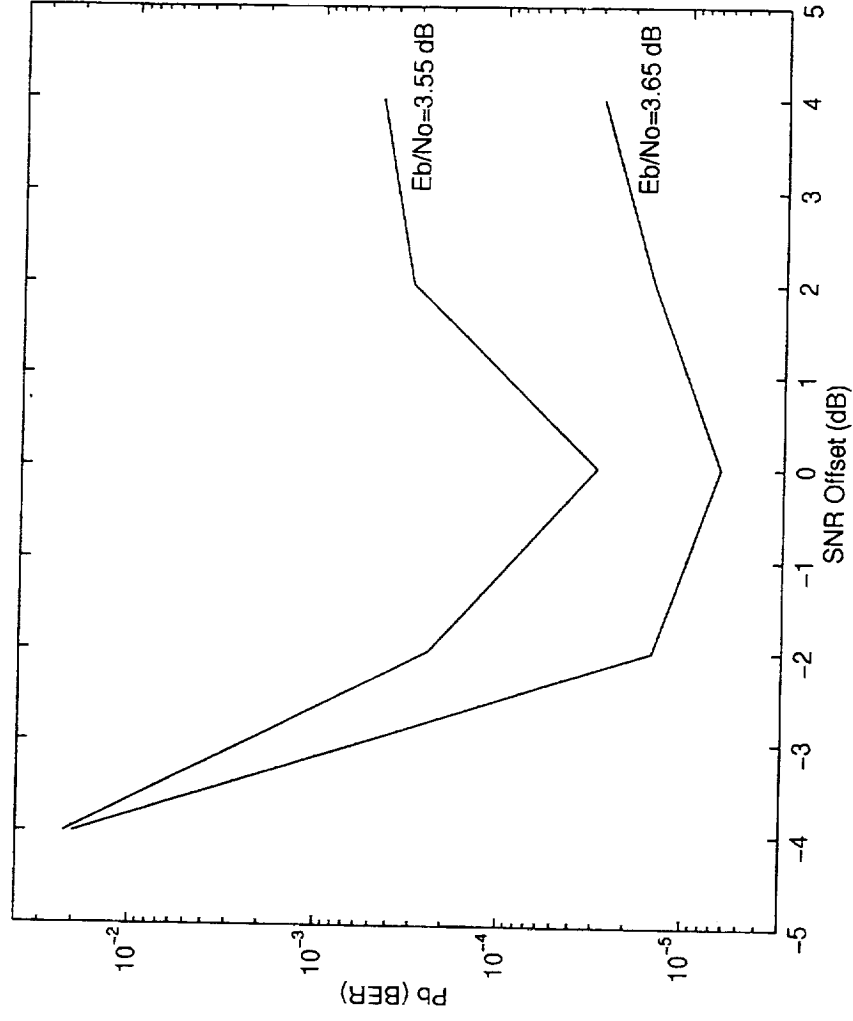
Implementation Issues on TC: SNR Estimation

TC decoder produces minimum number of errors when channel values are multiplied by $L_c = 2 * E_c/N_0$.
SNR offset, δ_E , defined as

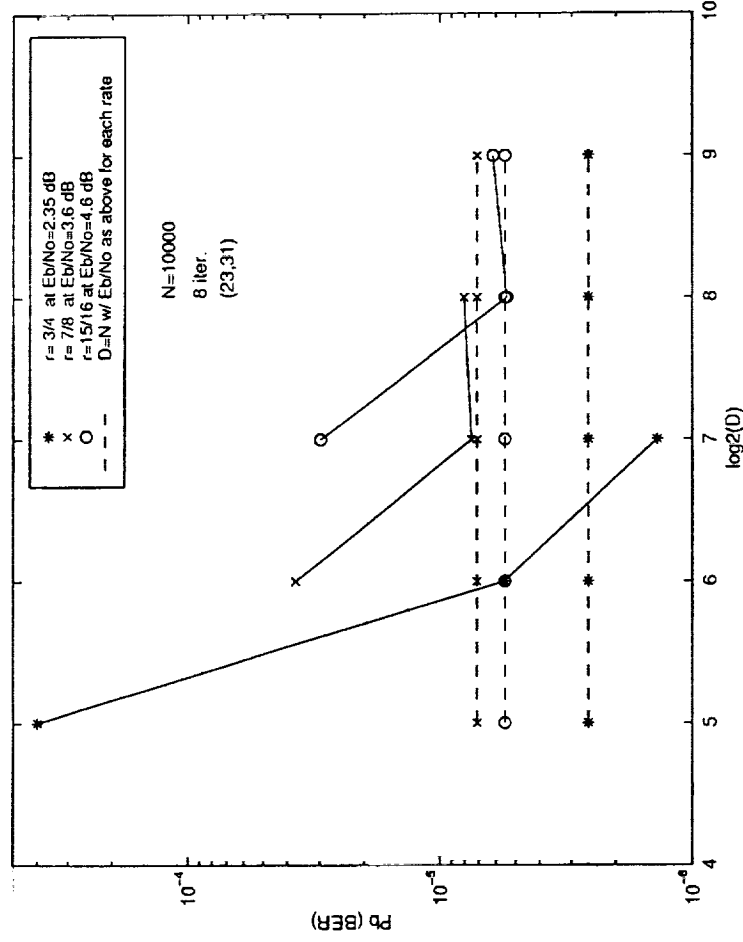
$$\delta_E(dB) = 10 * \log_{10} \left\{ \frac{(\frac{\hat{E}_c}{N_0})}{(\frac{E_c}{N_0})} \right\}$$

The Effect of SNR Offset on the BER

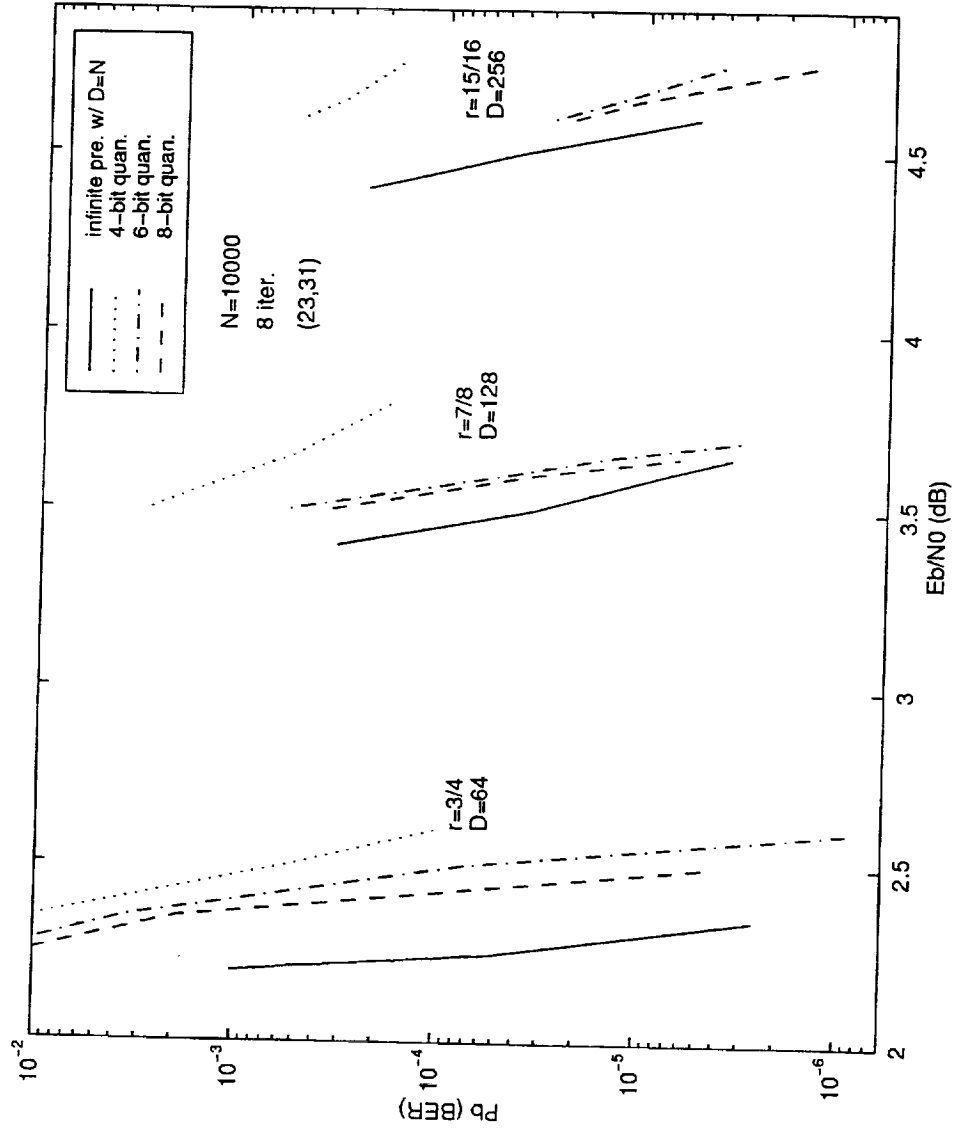
Performance of rate 7/8 TC



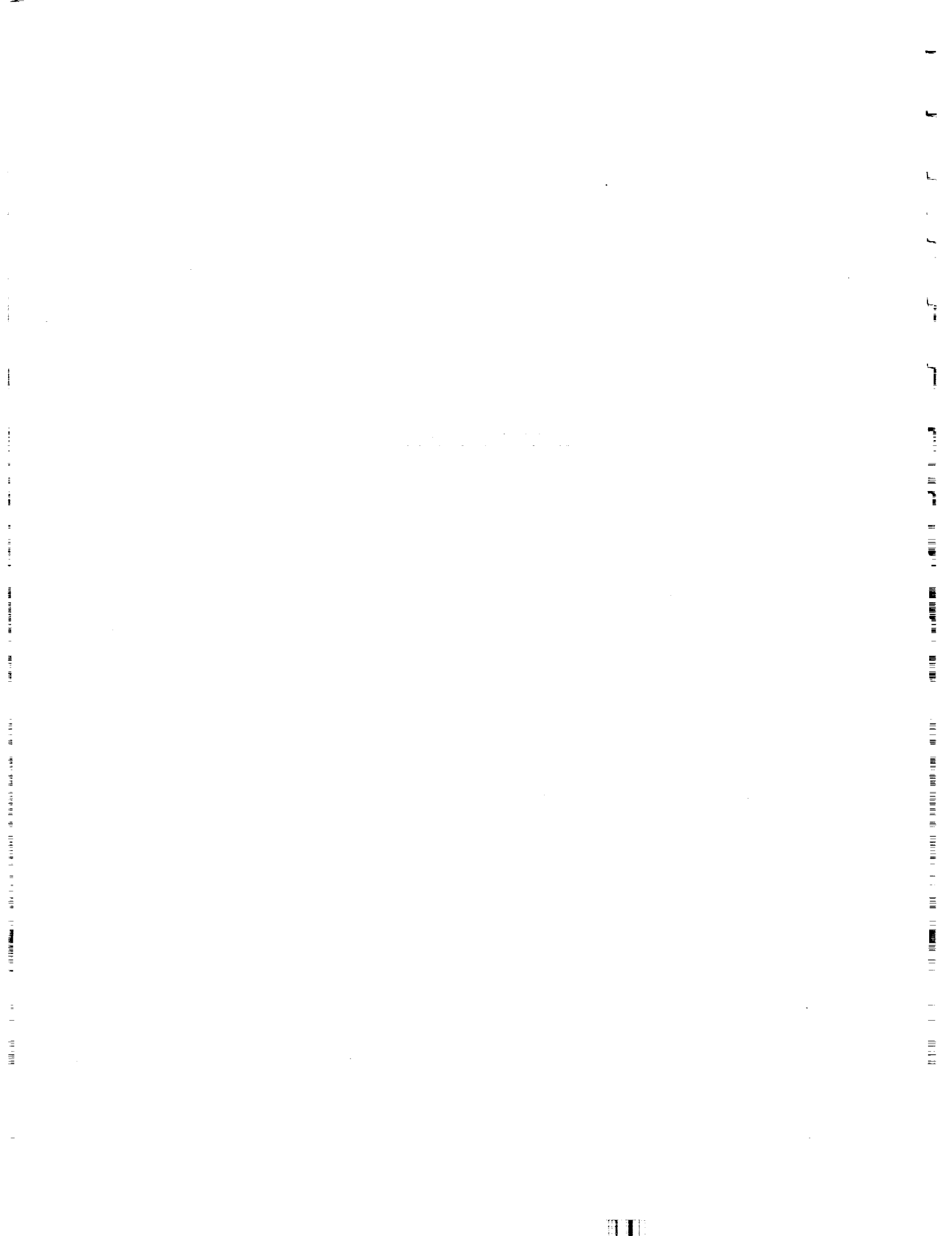
Rate 3/4, 7/8, and 15/16 TC Performances with Different Decoding Delays (D)



Quantized TC Performances for rate $3/4$, $7/8$, and $15/16$



FLIGHT SATELLITE



Flight Experiments

Stephen Horan
Klipsch School of Electrical and
Computer Engineering

February 23, 1999

Flight Experiments

Topics

- Hitchhiker Status
- Air Force Nanosatellite Program

February 23, 1999

Flight Experiments

Hitchhiker Status

- Experiment Goals:
 - Demonstrate fixed-antenna point and access of TDRS using small antenna configurations, e.g. patch arrays
 - Demonstrate real-time Doppler access of a signal transmitted through TDRS
 - Demonstrate low-power optical communications techniques

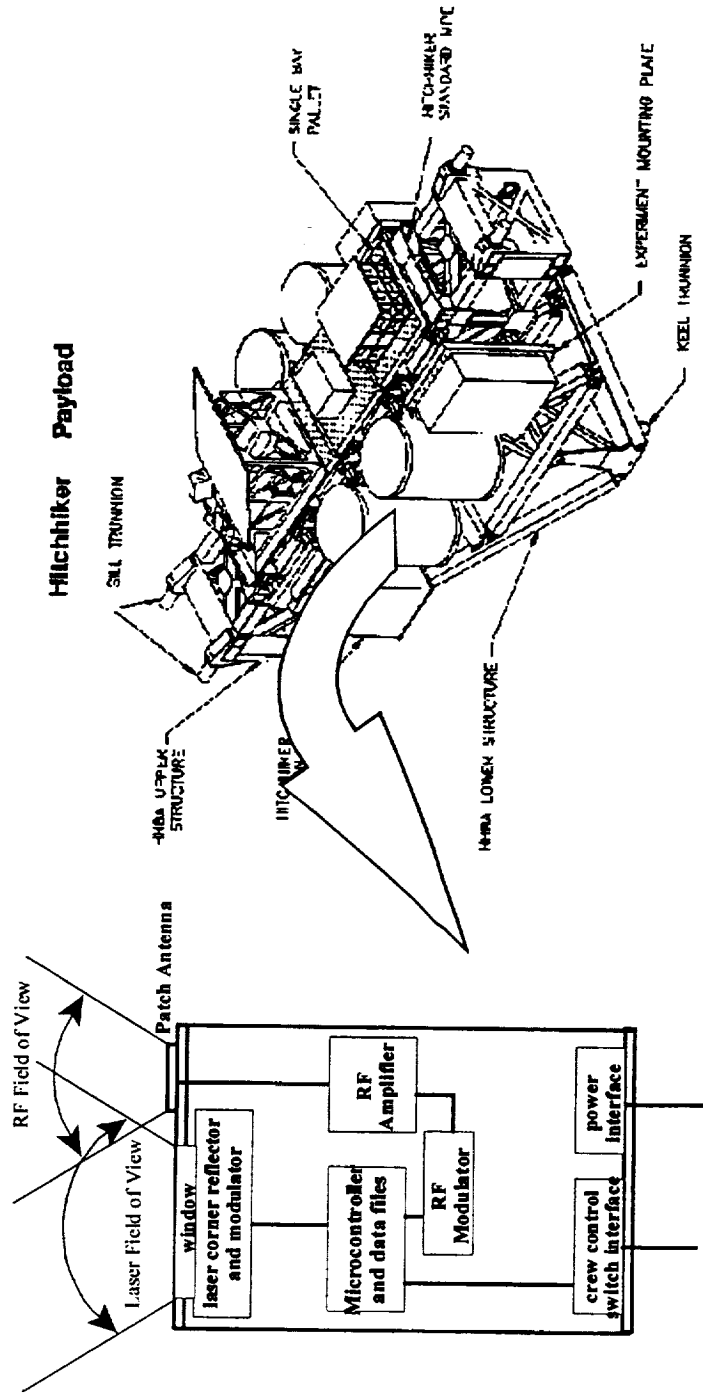
Hitchhiker Status

- Draft Customer Payload Requirements document developed and sent to GSFC
 - GSFC review showed no major concerns at this time
- Form 1628 to request a flight is in internal review
- Technical Interchange Meeting is being scheduled between GSFC and NMSU

February 23, 1999

Flight Experiments

Hitchhiker Status



Experiment Package

February 23, 1999

Flight Experiments

Hitchhiker Status

- Plans
 - Use the Hitchhiker mission as the basis for a senior-level capstone design class next academic year
 - Have a PDR and CDR as part of the class

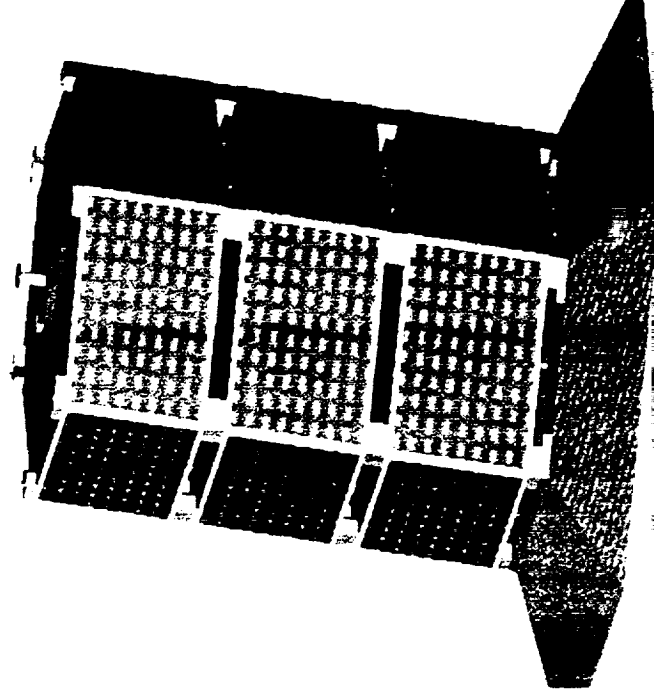
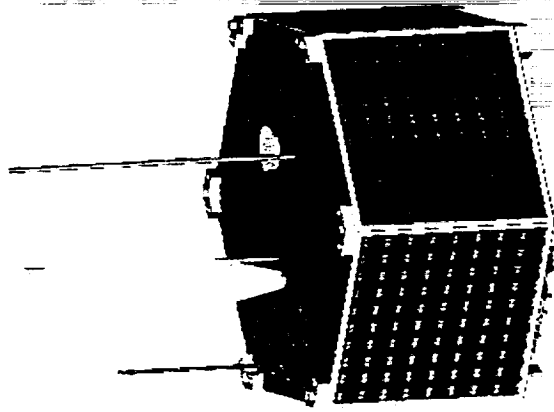
Nanosatellite Program

- NMSU teamed with University of Colorado and Arizona State University to bid on the Air Force University Nanosatellite Program
- Proposed a constellation of three satellites to be called the 3 Corner Satellite (3▲ Satellite) where each satellite would be controlled by their assigned school
- Our team won along with 7 other schools

Nanosatellite Program

Individual Satellite

Launch Configuration



February 23, 1999

Flight Experiments

Nanosatellite Program

- 3^A Satellite Program Goals:
 - Design and build satellites within 2 years
 - Use electronic cameras to image cloud formations
 - Operate the satellites in a cooperative manner
 - Provide a demonstration of formation flying
 - Provide a testbed for communications technology and related development

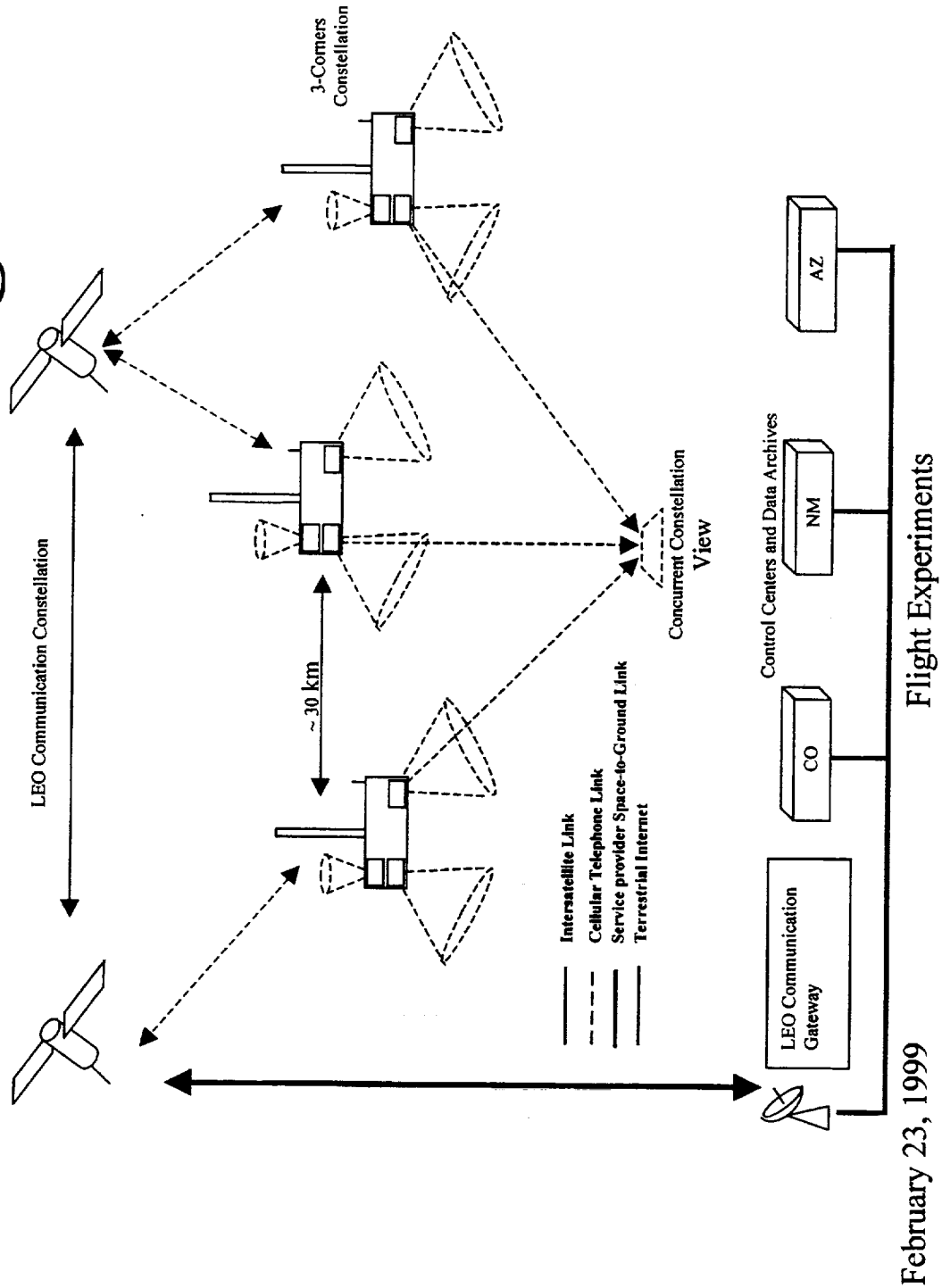
Nanosatellite Program

- 3A Satellite Test Concepts:
 - Formation flying and pointing of the sensors
 - Use cellular telephone LEO or MEO constellations for T&C support
 - Cross-link communications via cell phone, laser communications or RF (mode to be determined soon)
 - Provide space for NASA or Air Force technology demos, e.g. star tracker

February 23, 1999

Flight Experiments

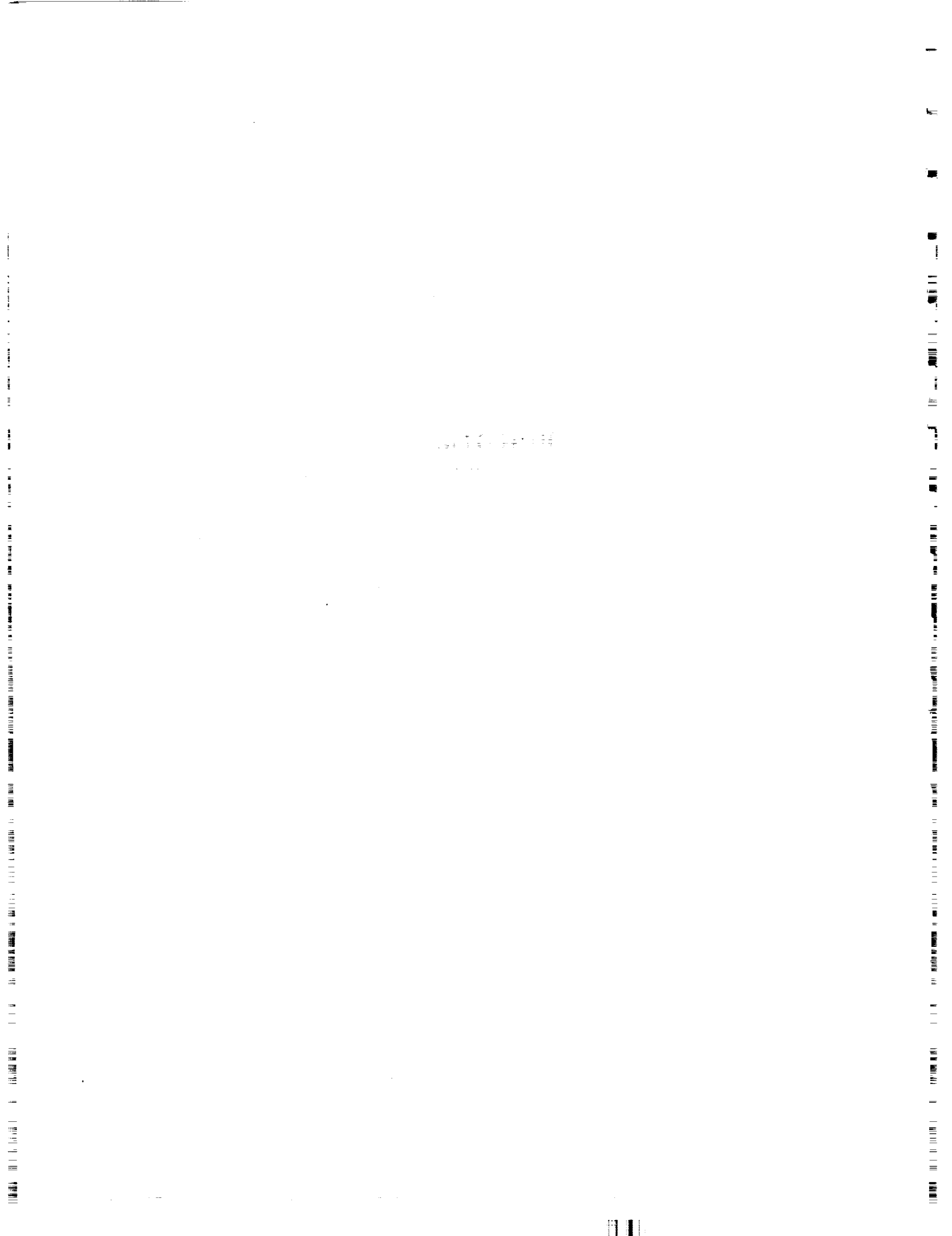
Nanosatellite Program



Nanosatellite Program

- GSFC Code 572 is interested in cooperating on the formation flying and cross link aspects of this program

**REAL-TIME
DOPPLER TRACKING**

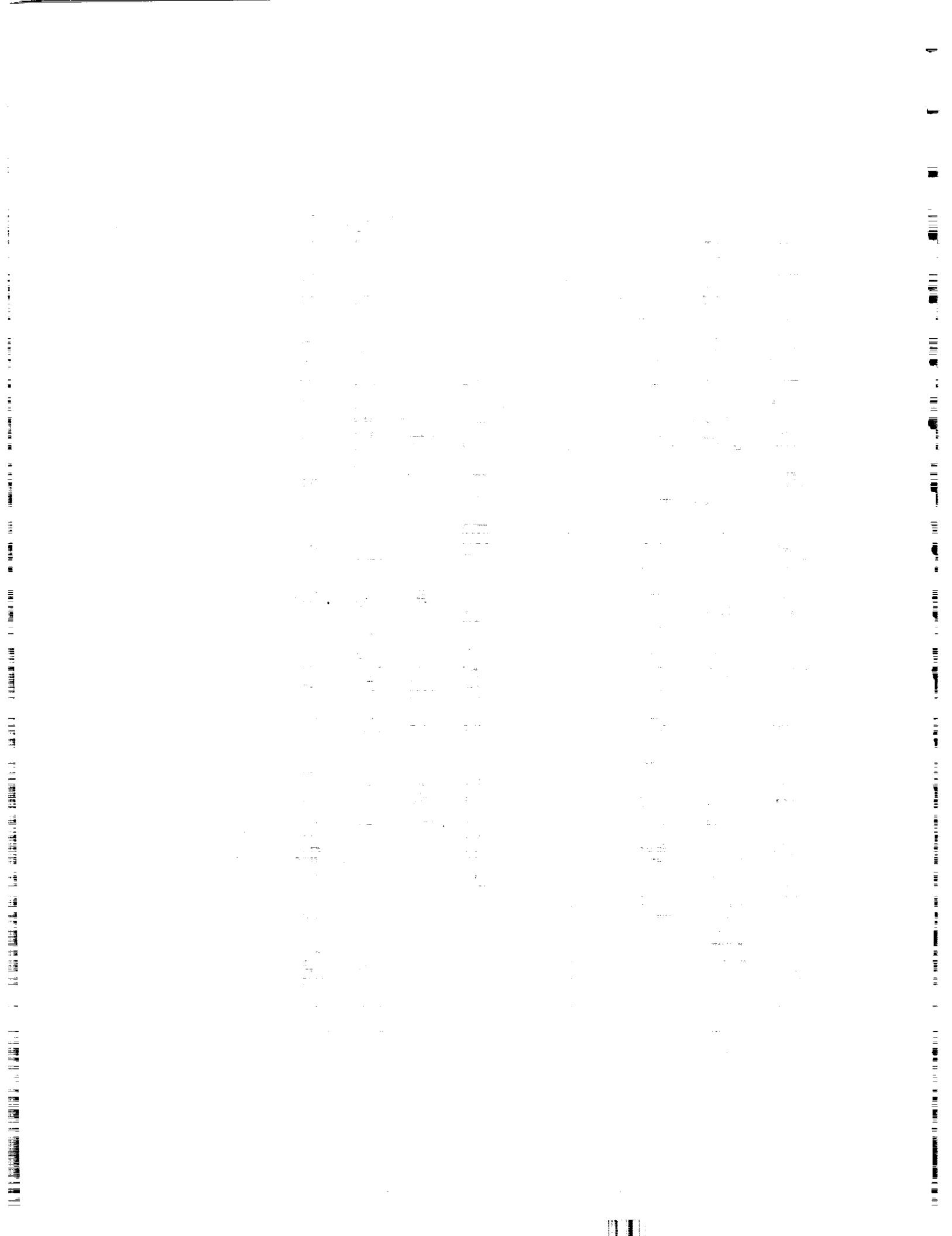


Investigation of an Architecture for Parallel Signal Processing Applicable to Communications Problems

Stephan Berner and Phillip De Leon

New Mexico State University

Klipsch School of Electrical and Computer Engineering
Center for Space Telemetry and Telecommunications



Fundamental Problems

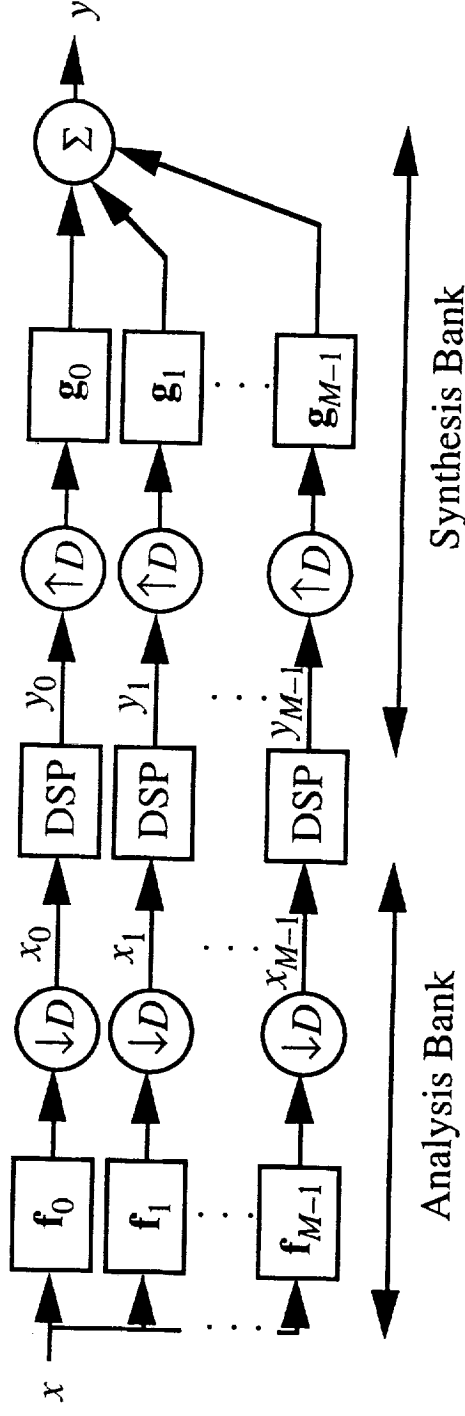
- Sequential nature of data (signal) combined with high-bandwidth, complex processing, i.e. high data rate, DSP-based receiver, yields a formidable challenge
- Algorithm partitioning is often difficult and/or ineffective with the above problem
- An alternate approach is to partition (decompose) the signal itself and assign a processor to each data partition
 - Data partitioning approach has been applied successfully in a number of problems such as search problems
 - Not all problems have data which can be partitioned

Preliminary Objectives

- Investigate low-order, oversampled, linear-phase filterbanks for use in signal decompositions
 - Require very good reconstruction properties with minimal subband aliasing
 - Filterbank should be linear phase for all-digital receiver applications (essential for tracking the phase and determining Doppler effects)
 - Require efficient filterbank architecture for high-bandwidth applications
- Investigate a FPGA implementation of a filterbank for use in a parallel processing architecture
 - Configurations of 4, 8, and 16 subbands and scalable
 - Serial distributed arithmetic in filtering
 - 2x oversampled subbands
 - Area efficient as well as high-speed implementation versions

Parallel Signal Processing in Subbands

- Sampled signal is decomposed through the analysis bank
- Subbands are independently processed on multiple DSPs
- Subband outputs are synthesized to form fullband output



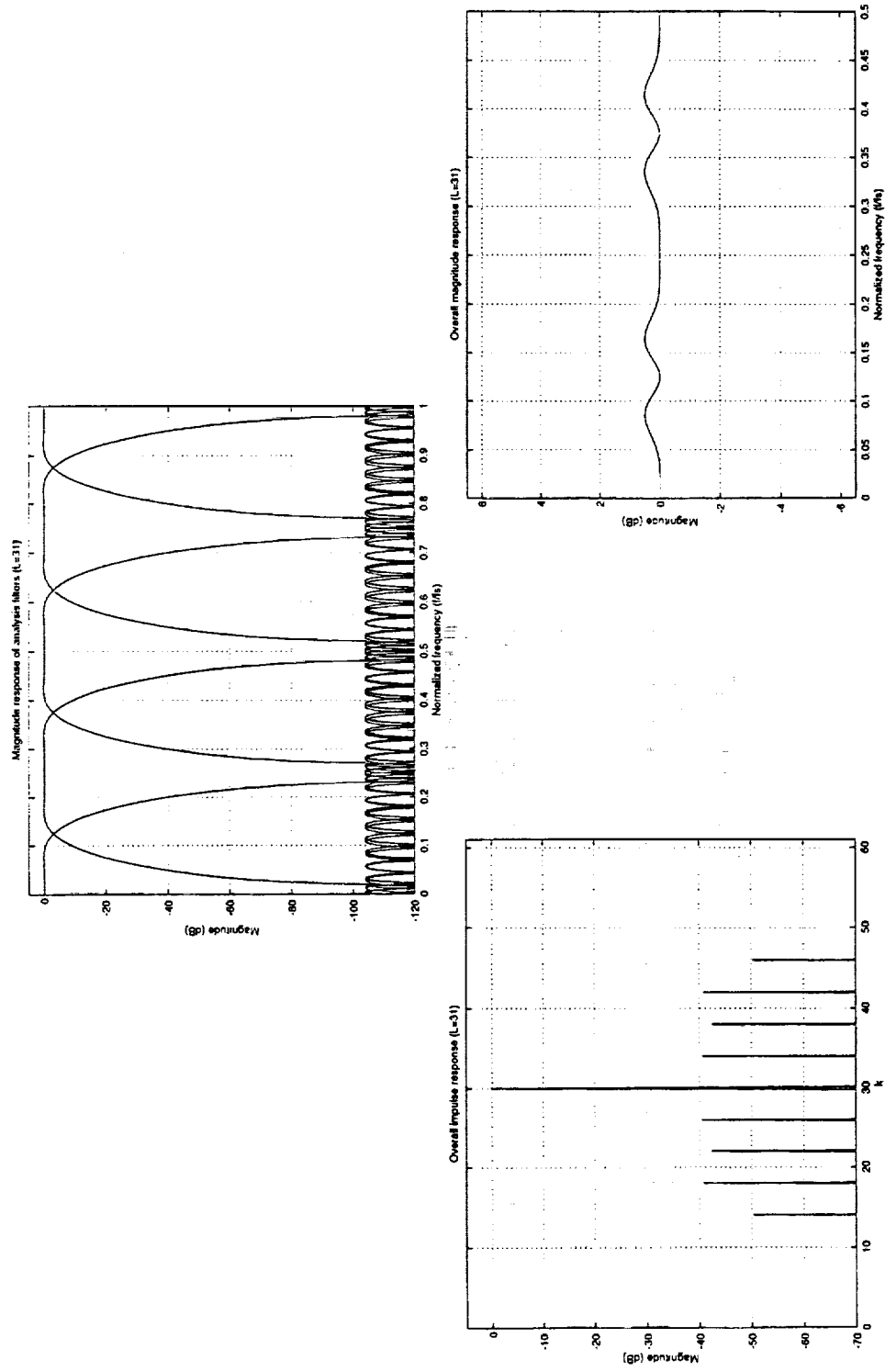
Potential Applications

- Many communication applications lend themselves to subband processing
- All-digital modem using filter banks
 - JPL Publication 94-20 (R. Sadr, P.P. Vaidyanathan, D. Raphaeli, S. Hinedi)
 - Lower processing rate in DSP hardware than input sample rate
 - Expansion to higher rates is easily accommodated due to parallel structure
 - Detected symbol stream is directly output from subbands with no increase in error rate
 - Suited for high data rate applications such as gigabit satellite channels
- Discrete Multitone Transceivers (DMT)
 - Employs a *set* of modulation functions (filters) which utilize unevenness of channel response in order to maximize total achievable bit rate
- Spread-spectrum codes based in subband transform bases

Filterbanks

- Filterbank decomposes or analyzes signal into M subbands using a bank of bandpass filters
- After filtering, signals are downsampled by a factor of D
 - Choose oversampled subbands ($D < M$) to avoid subband aliasing which will interfere with subband processing
- After subband processing, signals are upsampled to original rate and synthesis filtered to remove spectral images
- Fullband signal is constructed from the sum of synthesis filtered signals
- If analysis/synthesis filters are designed properly and no modifications are made to subbands, overall impulse response of filterbank will be equal to a pure delay

Example of Low-Order, Oversampled, Linear-Phase Filterbank Response



New Filterbank Design Result

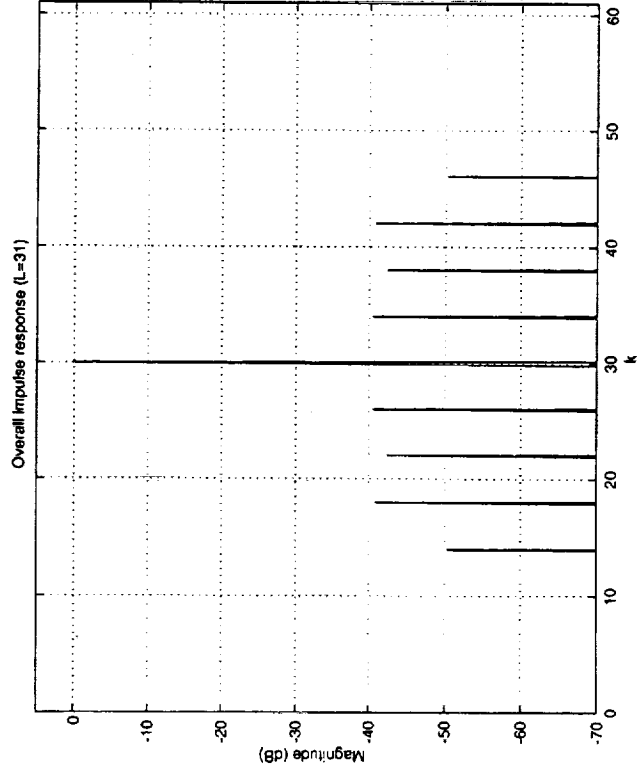
- Numerical methods are often employed for perfect or near-perfect reconstruction filterbanks (critical and oversampled) under linear-phase, uniform-DFT constraints
- We have shown that assuming a linear-phase prototype, i.e. window or Parks-McClellan design, with -3dB crossover magnitudes, virtually all phase distortion (primarily at crossover) can be eliminated by a simple filter length rule:

$$2(L - 1) / M \text{ is odd}$$

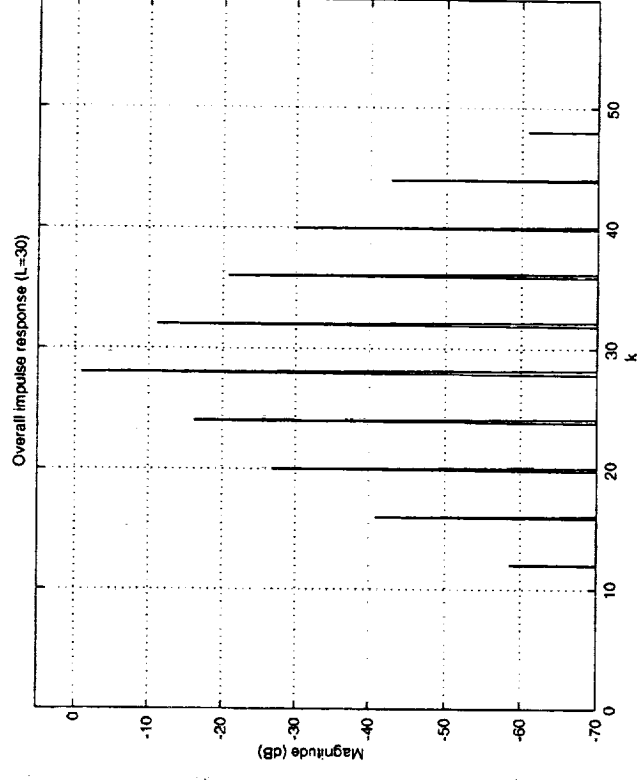
- Numerical methods can then be applied (if desired) to further enhance filterbank (even though above rule is usually “good enough”)

Filterbank Design Example

- Filterbank parameters $M = 4$, $D = 2$
- Parks-McClellan designs Case I: $L = 31$, Case II: $L = 30$



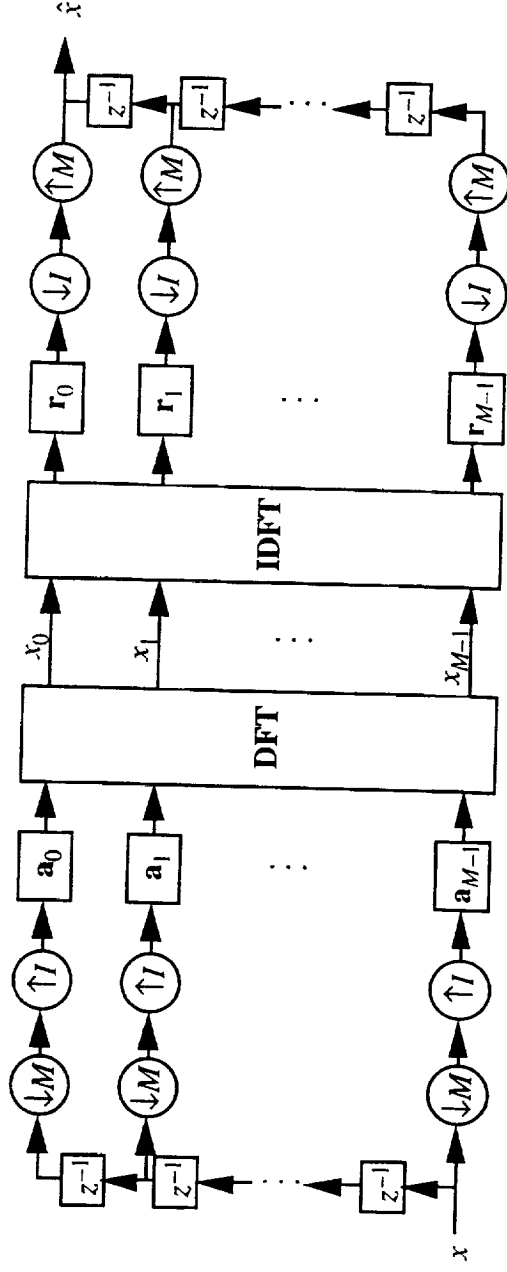
Simple rule satisfied



Simple rule not satisfied

Polyphase, Uniform-DFT Filter Bank

- Polyphase representation of filterbank (standard form) greatly reduces computations
- Filterbank constraints
 - equal bandwidth subbands (uniform)
 - analysis/synthesis filters derived from prototype via frequency shifting



High-Speed Filterbank Implementation

- High-speed filter bank implementation completed
 - Filterbank described in VHDL and scalable in subbands and wordlengths
 - COTS FPGA selected for reprogrammability and efficient implementation compared with with PALs or TTL-ICs
 - Analysis/synthesis filters realized with serial distributed arithmetic and lookup tables
 - 8MHz input/output sample rate, $8(2) / M$ MHz subband rate

	# Subbands, M		
	4	8	16
Analyzer ($L = 31$)	701 CLBs 18K Gates	1544 42K	3237 88K
Synthesizer ($L = 31$)	680 17K	1407 39K	2861 78K

Work in Progress

- Further investigation of low-order, linear-phase, uniform-DFT filterbanks with good reconstruction properties
- Refine VHDL codes for more area-efficient filterbank implementations especially at higher subbands levels
 - Use of arithmetic Fourier transform to reduce area
- Prototype end-to-end unit

Conclusions

- Subband decompositions appear to be a useful method for data (signal) decomposition in parallel signal processing
- Several communications applications have been simulated in subbands and results indicate better performance than the fullband counterpart and/or reduced processing rates
- Designs for low order, linear-phase, uniform-DFT filterbanks have been studied and successfully applied
- Filterbank has been described in VHDL which leads to an easily scalable design on FPGA

Spread-Spectrum Carrier Estimation under Unknown Doppler Shifts

WSC Data Collection / Hardware Description

Phillip De Leon and Brad Scaife

New Mexico State University

Klipsch School of Electrical and Computer Engineering

Center for Space Telemetry and Telecommunications

1



Topic Outline

- WSC Data Collection Experiment
 - Motivation
 - Data Collecting/Processing
 - Comparison to Simulation Results
- Real-Time DSP based Carrier Estimation Hardware
 - Hardware and Software Description

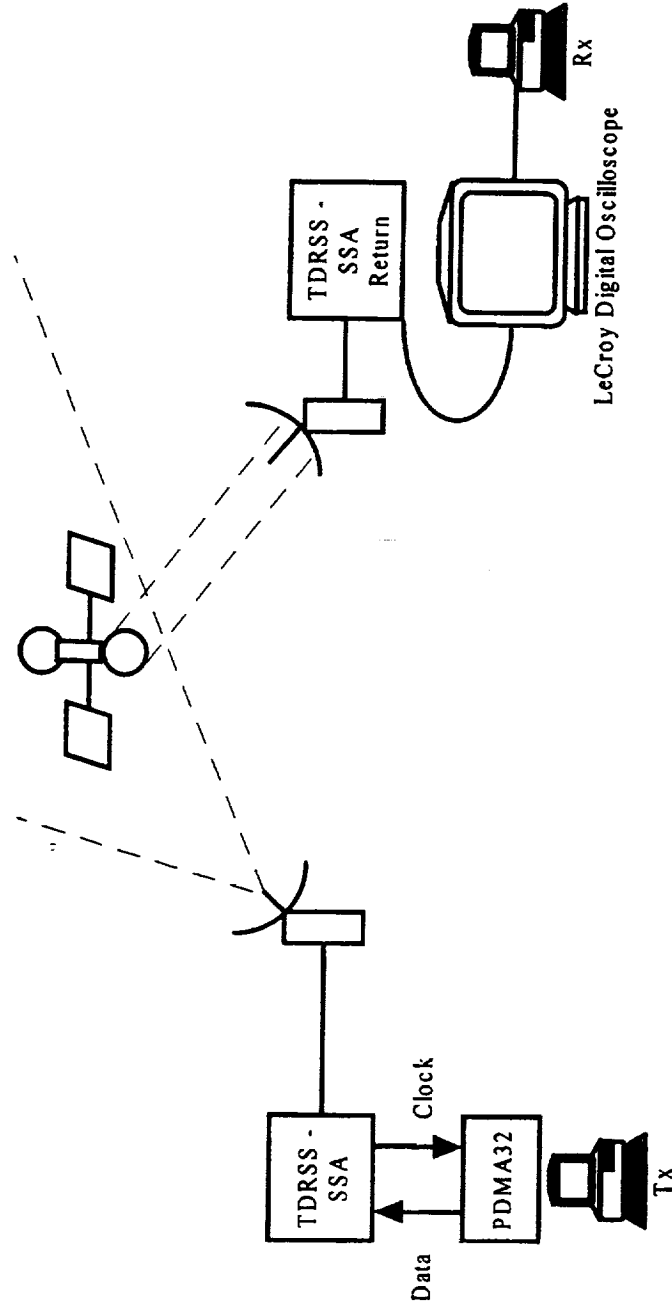


TDRSS Data Collection: Background

- Data Collected on July 13-15 and on July 20, 1998.
- Team included Cliff Baxtor and Frank Hartman, WSC staff.
- NMSU Data Collection Equipment used included: LeCroy DSO, PDMA-32, PCs.



TDRSS Data Collection: Setup



WSC Tests: Motivation

- Important to determine accuracy of simulation.
 - High correlation between WSC collected data and simulations verify simulation model.
 - Additional hardware tests may be run with computer generated signals to verify operation.
 - Insight into real (practical) bounds of operation.



WSC Experiment: Data Collection

- Test Set Description (Reduced)
 - Data Rate set to $R_b = 1$ kbps
 - Chip Rate set to $R_c = 10$ k chips/s
 - Sample Rate set at $f_s = 100$ MHz on DSO
 - Carrier frequency set to span DAMA range in 50 kHz increments (models Doppler shift).
 - Collected signal vectors of 50,000 samples and 100,000 samples.

5



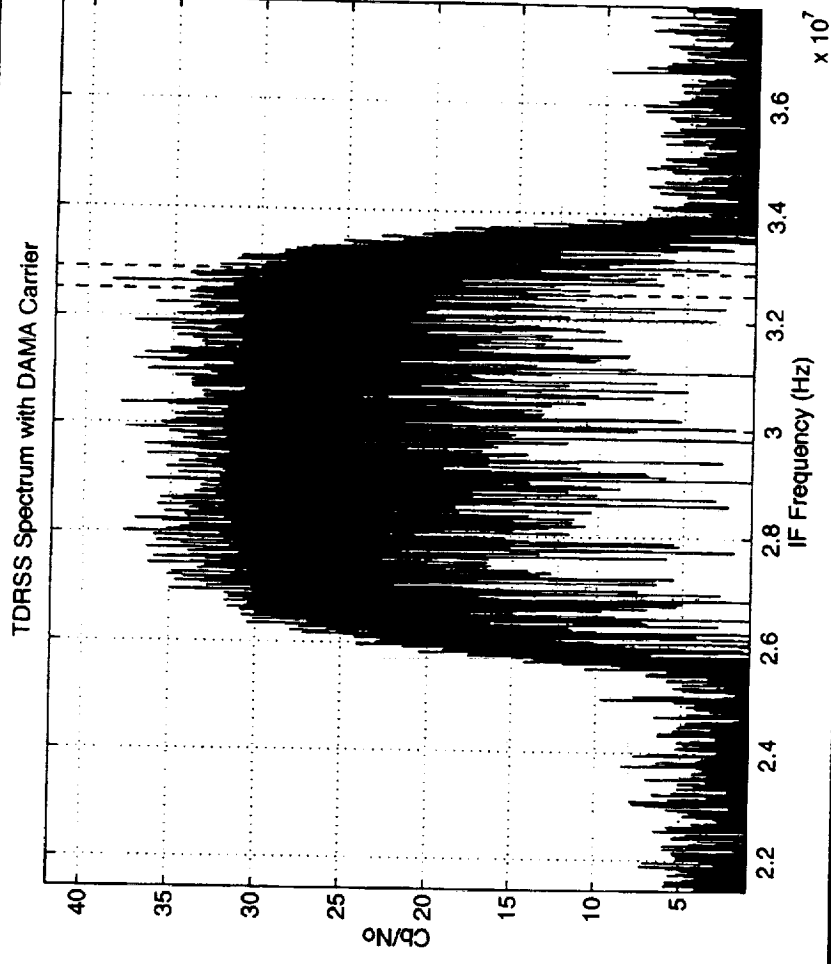
WSC Experiment: Data Collection

- DFT resolution is an important factor
 - Hardware Resolution is $1562.5 \text{ Hz} - f_s = 800\text{kHz}$
 - WSC Data Resolution is $1525.8 \text{ Hz} - f_s = 100\text{MHz}$
 - 50,000 sample vectors were zero padded to 65,536 achieve WSC resolution.
 - 100,000 sample vectors were split into two 65,536 length vectors with some overlap.
 - Avoid sample rate conversion problems.

6



TDRSS Response with DAMA Carrier

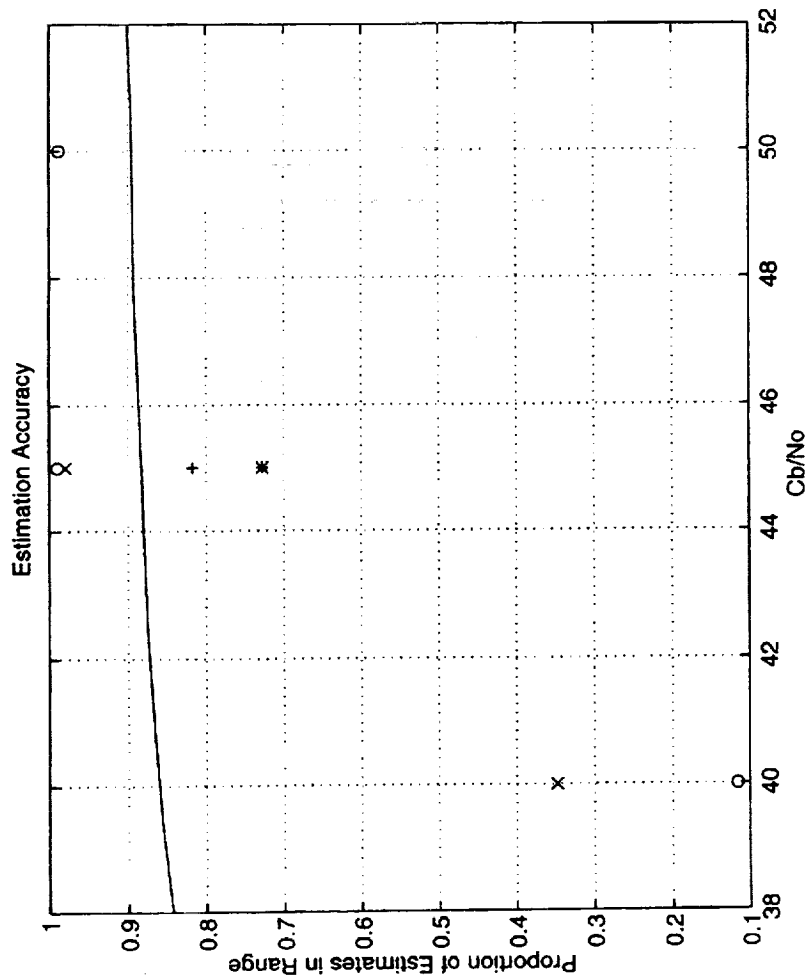


7



New Mexico State University, Klipsch School of Electrical and Computer Engineering

WSC Experiment: Results



$C_b/N_0 = 40$:
 x = 32.65 MHz
 o = 32.70 MHz
 $C_b/N_0 = 45$:
 x = 32.60 MHz
 o = 32.65 MHz
 + = 32.70 MHz
 * = 32.80 MHz
 $C_b/N_0 = 50$:
 x = 32.65 MHz

8



WSC Experiment: Results

- At $C_b/N_o = 40$, correlation between data and simulation poor. Lower power increases estimation error.
- At $C_b/N_o = 45$, good grouping of data to simulation. Error increases as f_c nears TDRSS null.
- Overall, estimation with actual data verifies simulation.

9

DAMA Hardware

- Algorithm implemented in DSP hardware:
 - Motorola DSP56303EVM
 - Burr Brown ADS7810/19C 12 bit 800kHz A/D
- Algorithm utilizes:
 - 682 bytes of program memory
 - 2048 bytes of L memory
 - 540 bytes of X, 512 bytes of Y memory



DAMA Hardware

- Additional analog hardware is required to frequency shift the DAMA frequency range to baseband.
- From end of sample collection (8 x 512 samples), carrier estimation is performed in 0.5 ms.

Conclusions

- Data Collection performed at WSC verified simulation model and estimation algorithm.
- Results justify use of synthesized signals to test hardware.
- DSP hardware implementation provides accurate estimation at efficient cost.



PROTOCOL TESTING

Space Protocol Testing

Stephen Horan & Ru-hai Wang
Klipsch School of Electrical and
Computer Engineering

February 23, 1999

Space Protocol Testing

Topics

- Background
- LabVIEW-based Channel Simulator
- SCPS and TCP/IP Test Configuration
- SCPS and TCP/IP Test Results
- Next Test Steps
- Summary & Conclusions

Background

- The Space-to-Ground Link Simulator (SGLS) is designed to provide a means to test data networking protocols at baseband
- This is needed to
 - test the performance of current networking protocols, e.g. TCP/IP, for space-to-ground links
 - test interfaces with the Internet and space links

Background

- Desirable attributes
 - allow user-selectable error rates (we allow E_b/N_0 from 0 dB to 11 dB)
 - allow time-variable error rates over several minutes as would be found in a satellite pass
 - allow different data rates on the forward and return links as would be found in satellite links, e.g. 2400 baud forward, 57600 baud return

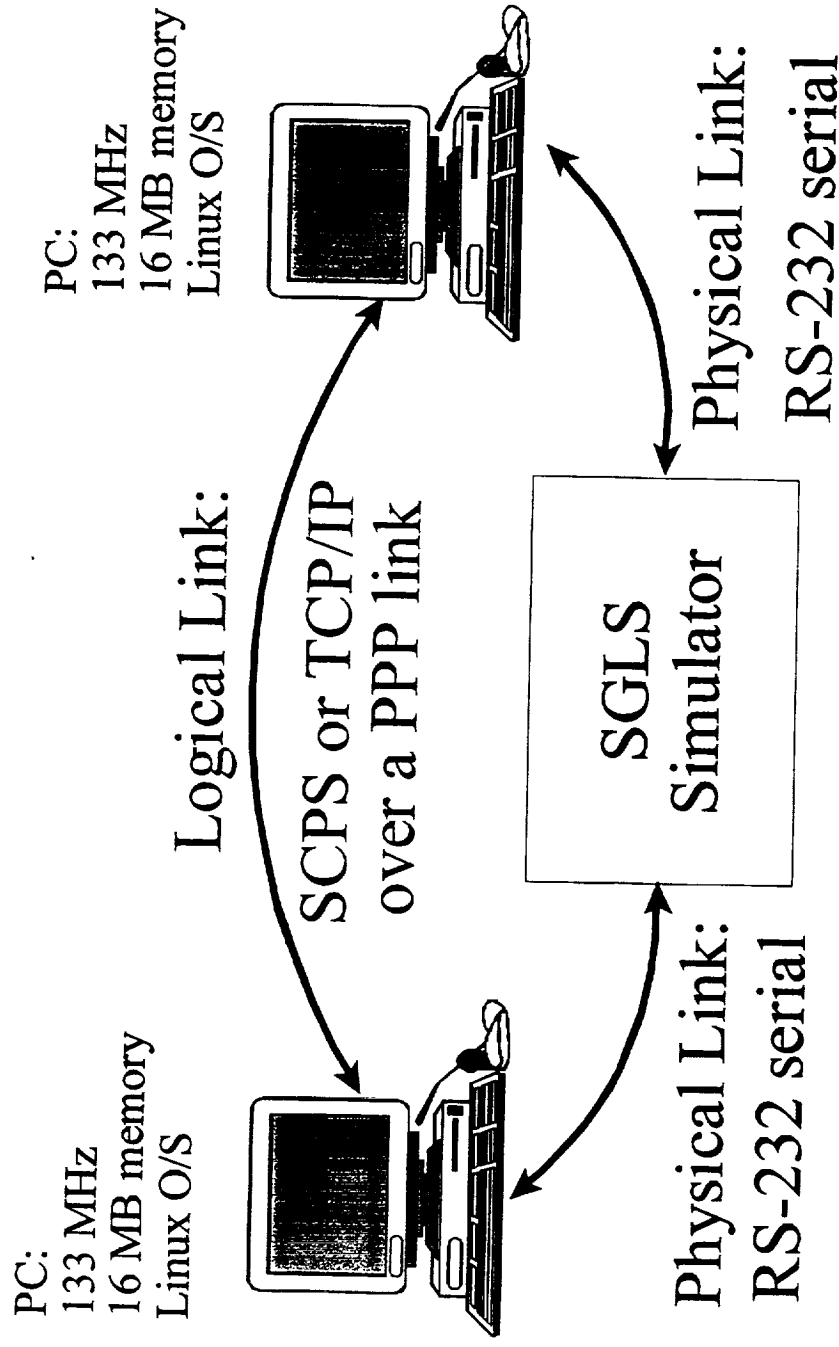
Background

- **Advantages:**
 - Allows test on actual data streams and not simulations of those data streams
 - Portable - basic technology can be placed in a lap-top PC, with appropriate interface cables
 - Can be configured to work with multiple networking technologies (RS-232, RS-422, Ethernet)

Background

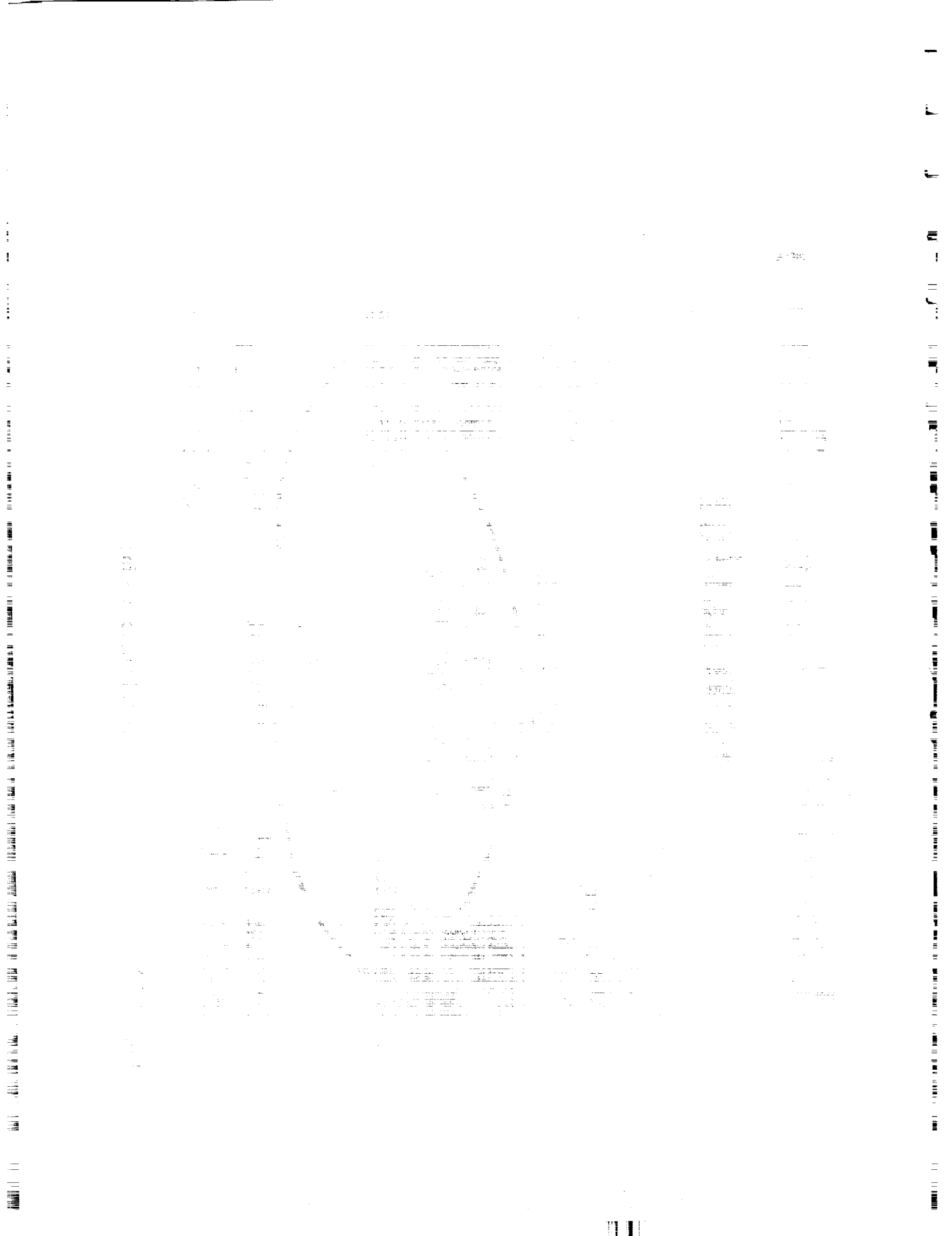
- Potential Other Users:
 - SBS Berg Telemetry
 - Avtec Systems
 - Both have expressed interest in this technology for testing their CCSDS board-level products
 - Papers on this work are expected to be presented at ITC '99

LabVIEW Based Channel Simulator



February 23, 1999

Space Protocol Testing



LabVIEW Approach

- LabVIEW also has built-in functions for numerical analysis, logical operations, control, and user interface
- The complete package forms a Virtual Instrument (VI) that acts like a dedicated piece of test equipment built into the computer (runs on PC, MAC, UNIX workstations, etc)

LabVIEW Approach

- **Development Stages:**
 - **Error Generator** to model actual generation of channel errors
 - **Rate Splitter** to provide different forward and return data link baud rates and provide a common interface to host computers
 - **Orbital Analysis** to provide time-variable BER
 - **Delay** to provide $\frac{1}{4}$ -second link delay

LabVIEW Approach

- **Development Status:**
 - **Error Generator:** complete and being used in tests
 - **Rate Splitter:** software complete and hardware verification needs to be finished
 - **Orbital Analysis:** software in validation test
 - **Delay:** needs to be developed

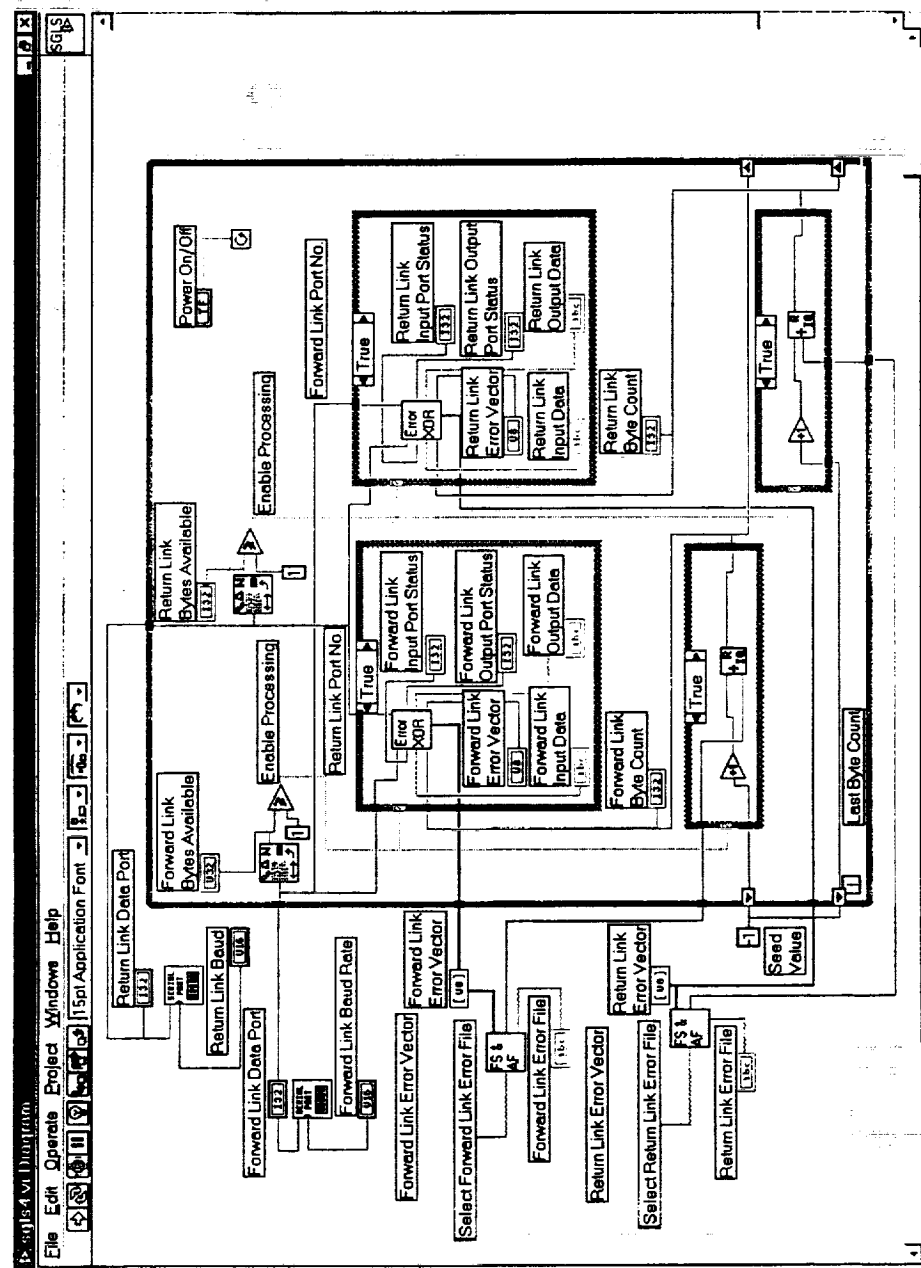
LabVIEW Approach

- Baseband error generator works on the principle that the error process can be taken to be the Exclusive-OR of the input data with a error vector having a 1 at locations where a bit flip occurs and a 0 where no data modification occurs
- Error vector is precomputed and based on the statistical properties of the channel

LabVIEW Approach

- **Process**
 - User initializes the VI and sets ports
 - VI reads each directional serial port
 - XOR the data with the error vector
 - VI writes the data to the appropriate directional data port
 - VI continuously loops as quickly as possible (no waits: if no data available at the input port, loop back an poll again)

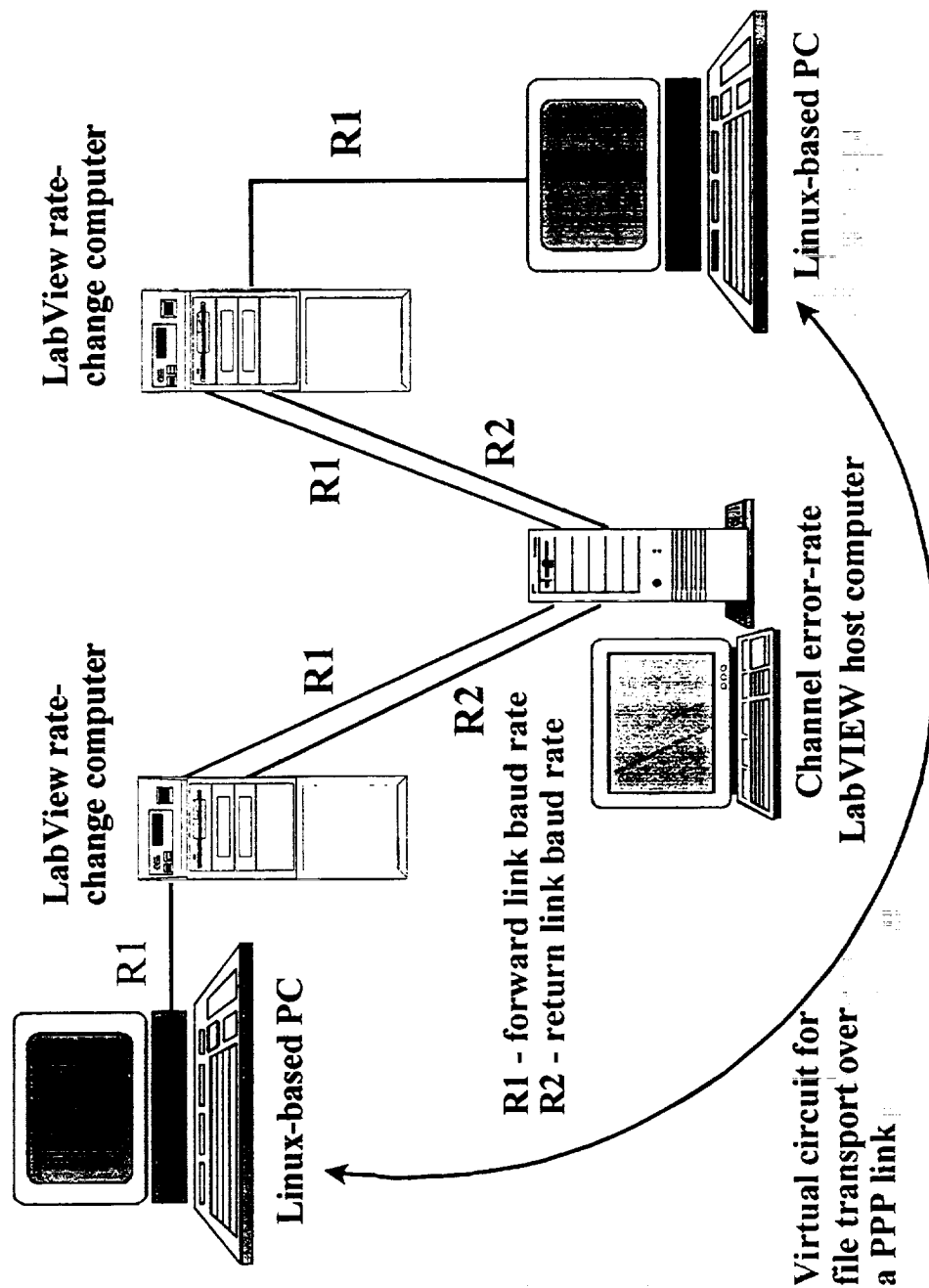
LabVIEW Approach



LabVIEW Approach

- **Rate Changer**
 - Most small satellite and science satellite communication links have unbalanced forward and return link rates. Forward link of a few 1000 bps and Return link up to several Mbps for large satellites to a few 100 kbp for small satellites
 - These links can be configured as serial bit stream of packet protocol links

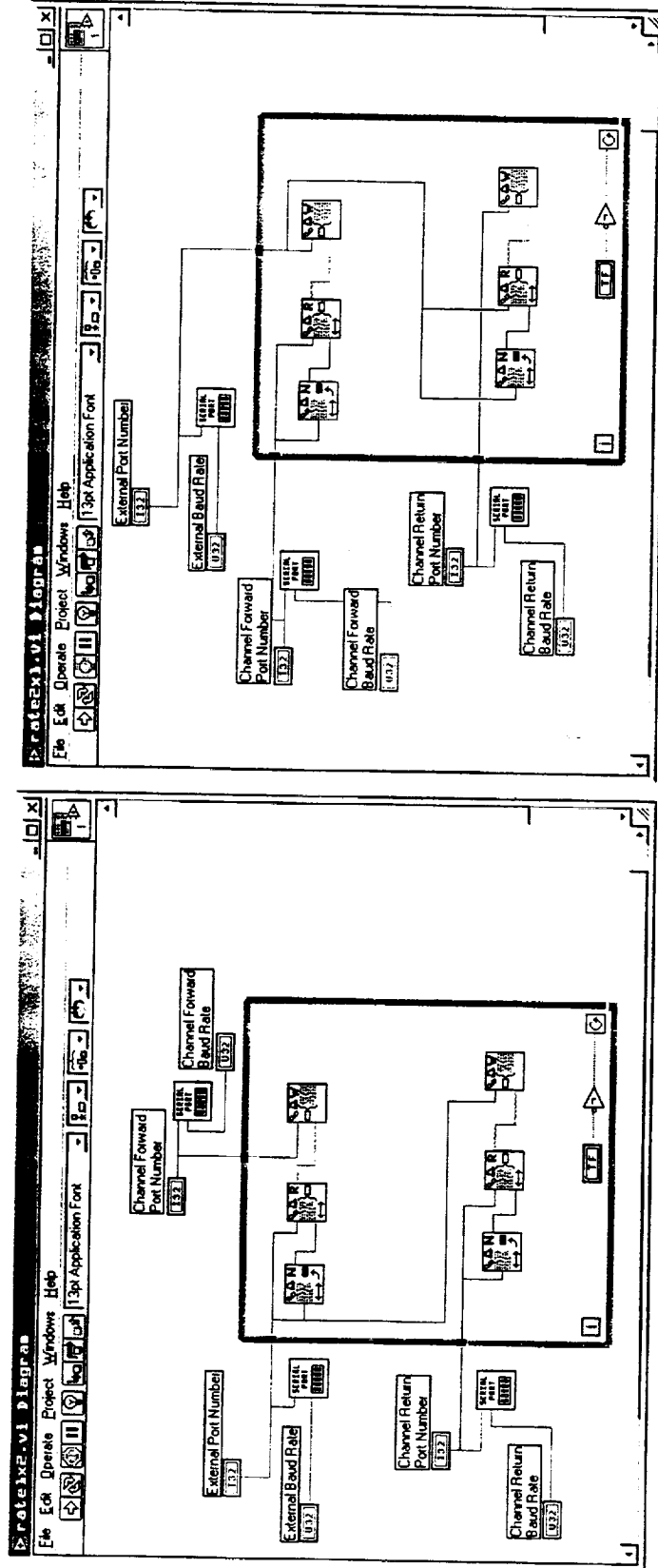
LabVIEW Approach



February 23, 1999

Space Protocol Testing

LabVIEW Approach



VIs to split and combine forward/return data channels with different baud rates

February 23, 1999

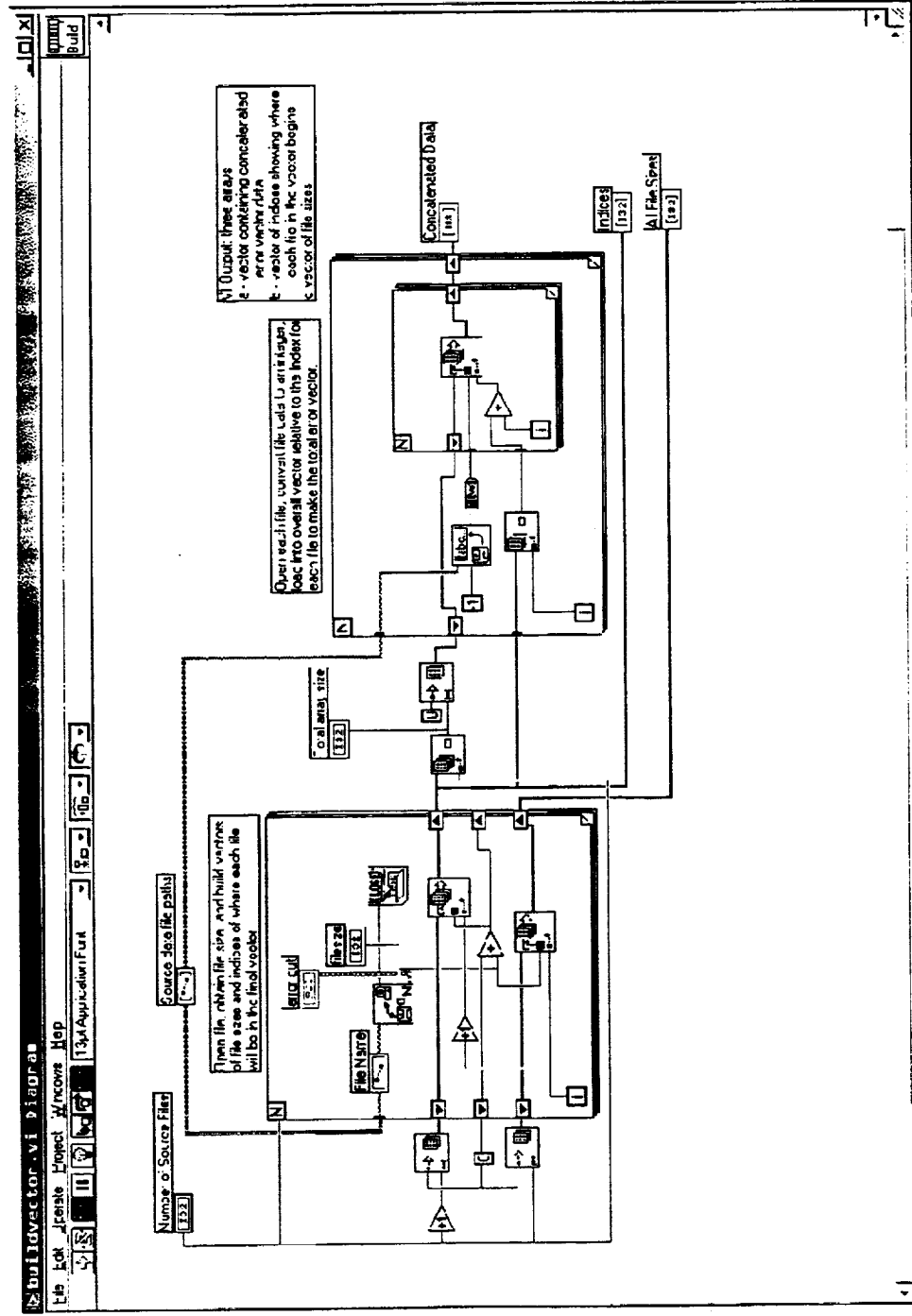
Space Protocol Testing

LabVIEW Approach

- **Orbital Operations:**
 - Take basic SGLS module and have LabVIEW sequence through the error files for the forward and return links based on a time schedule specified by the user
 - Time-variable BER can be determined using analysis like that provided by Satellite Tool Kit

Space Protocol Testing

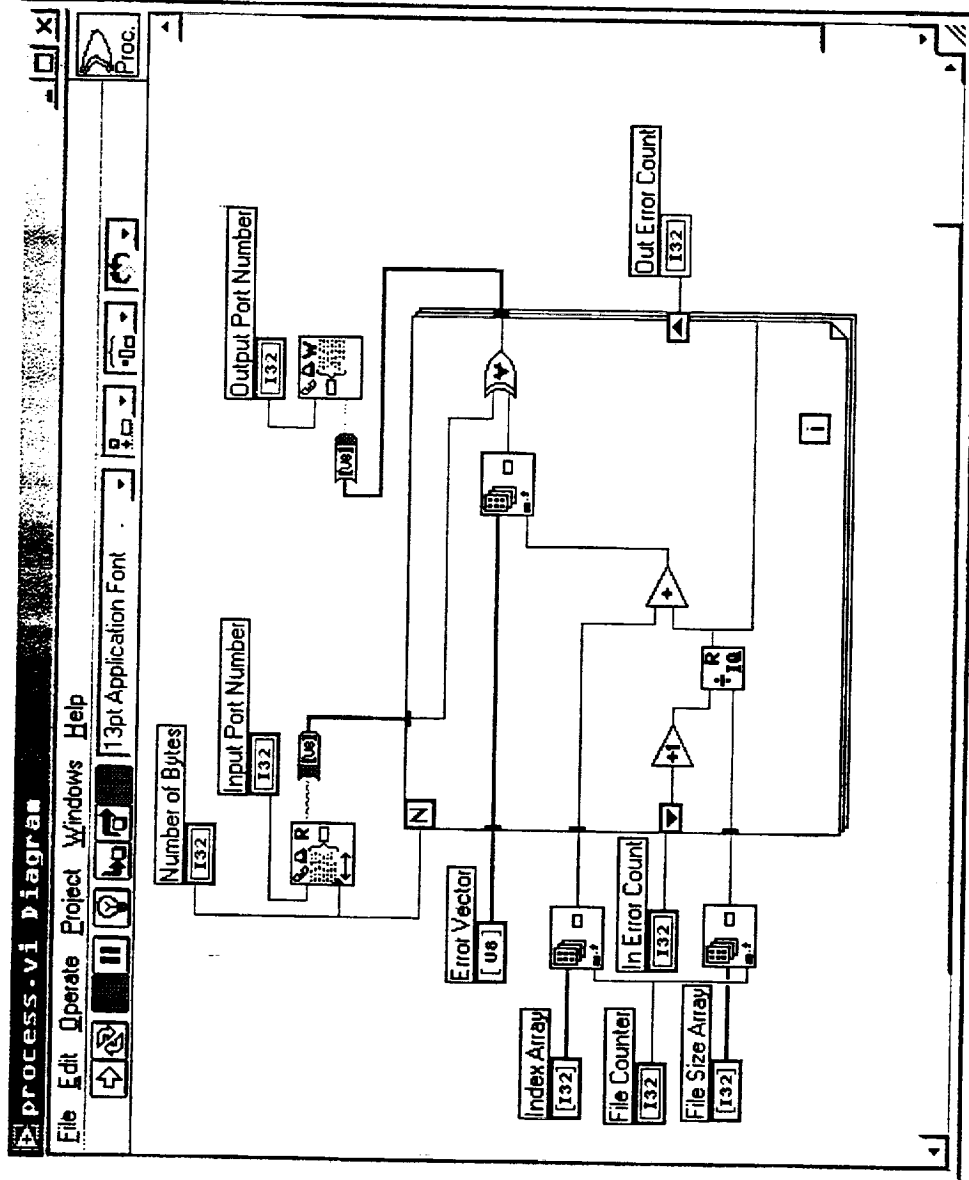
LabVIEW Approach



February 23, 1999

Space Protocol Testing

LabVIEW Approach



February 23, 1999

Space Protocol Testing

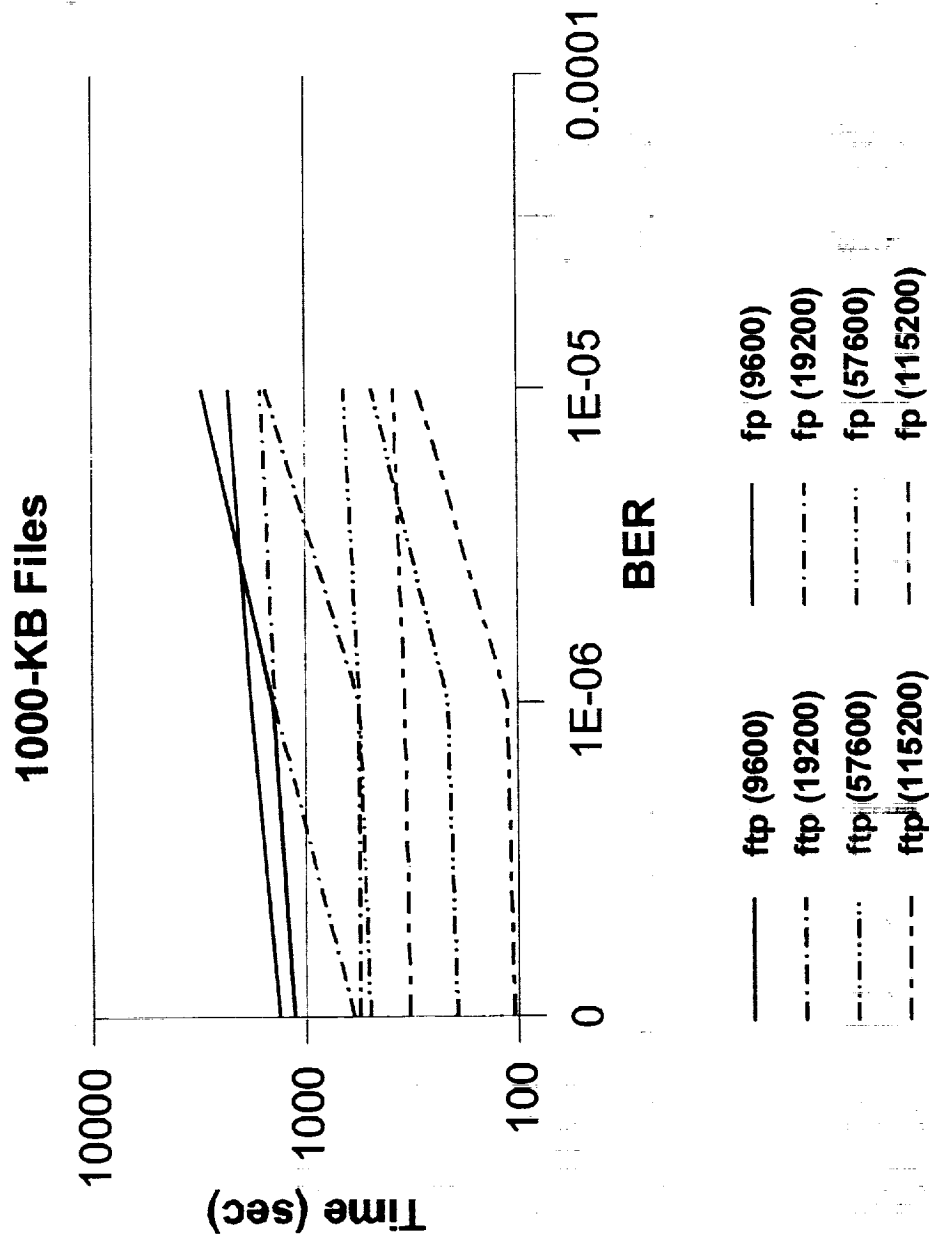
SCPS and TCP/IP Test Configuration

- TCP/IP ftp and SCPS ftp resident on two PCs
 - 133 MHz, 16 MB RAM
 - Linux Operating System
- Use PPP serial link-level packet structure
- Use RS-232 serial connection to exchange data at 9600 through 115200 baud transmission range

SCPS and TCP/IP Test Results

- Transferred random data files between the two PCs and measure transfer time
 - 1 KB, 10 KB, 100 KB, 1000 KB file sizes
- Includes interaction with the operating system
- ftp and fp used in “out of the box” mode without trying to optimize any parameters at initial test stages

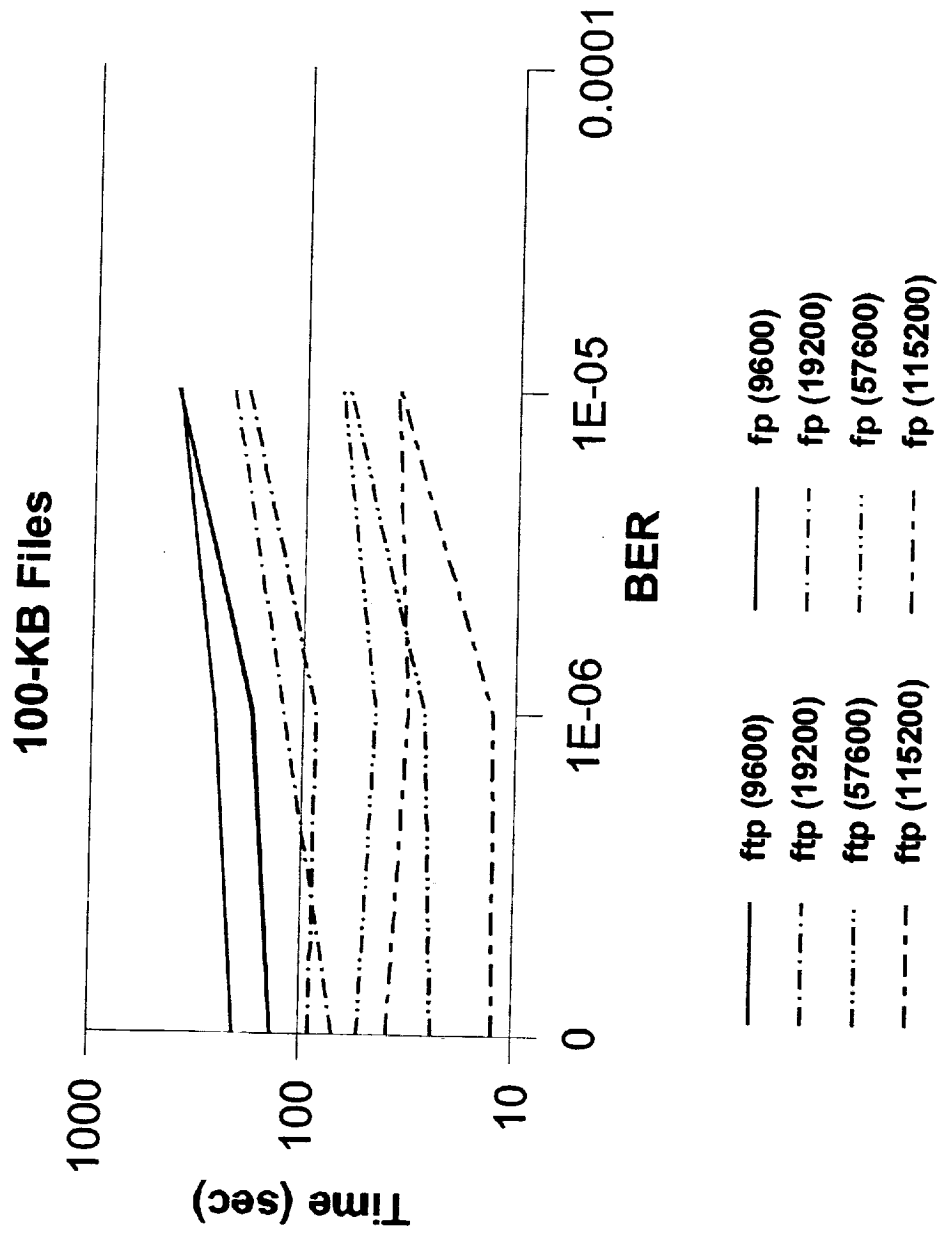
SCPS and TCP/IP Test Results



February 23, 1999

Space Protocol Testing

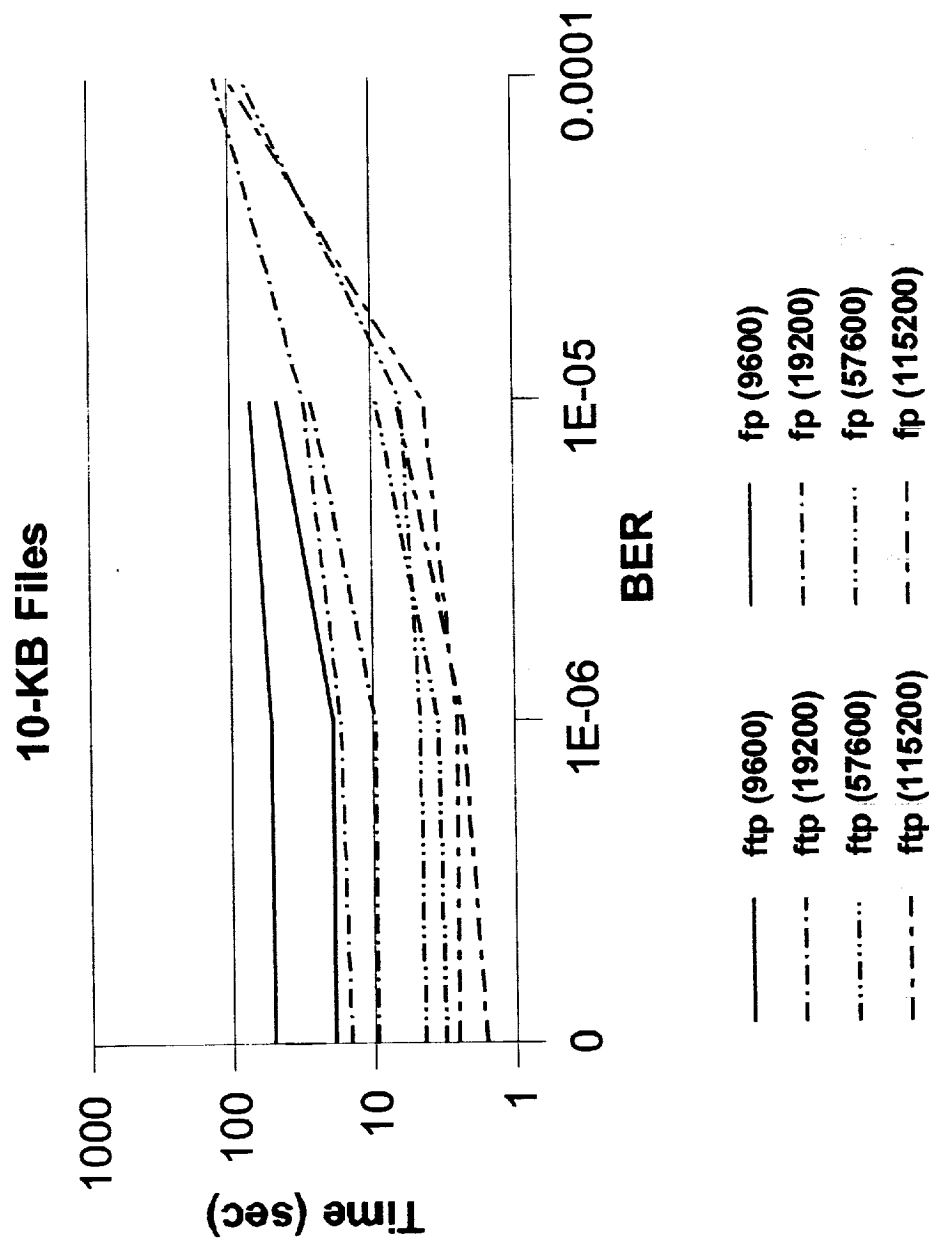
SCPS and TCP/IP Test Results



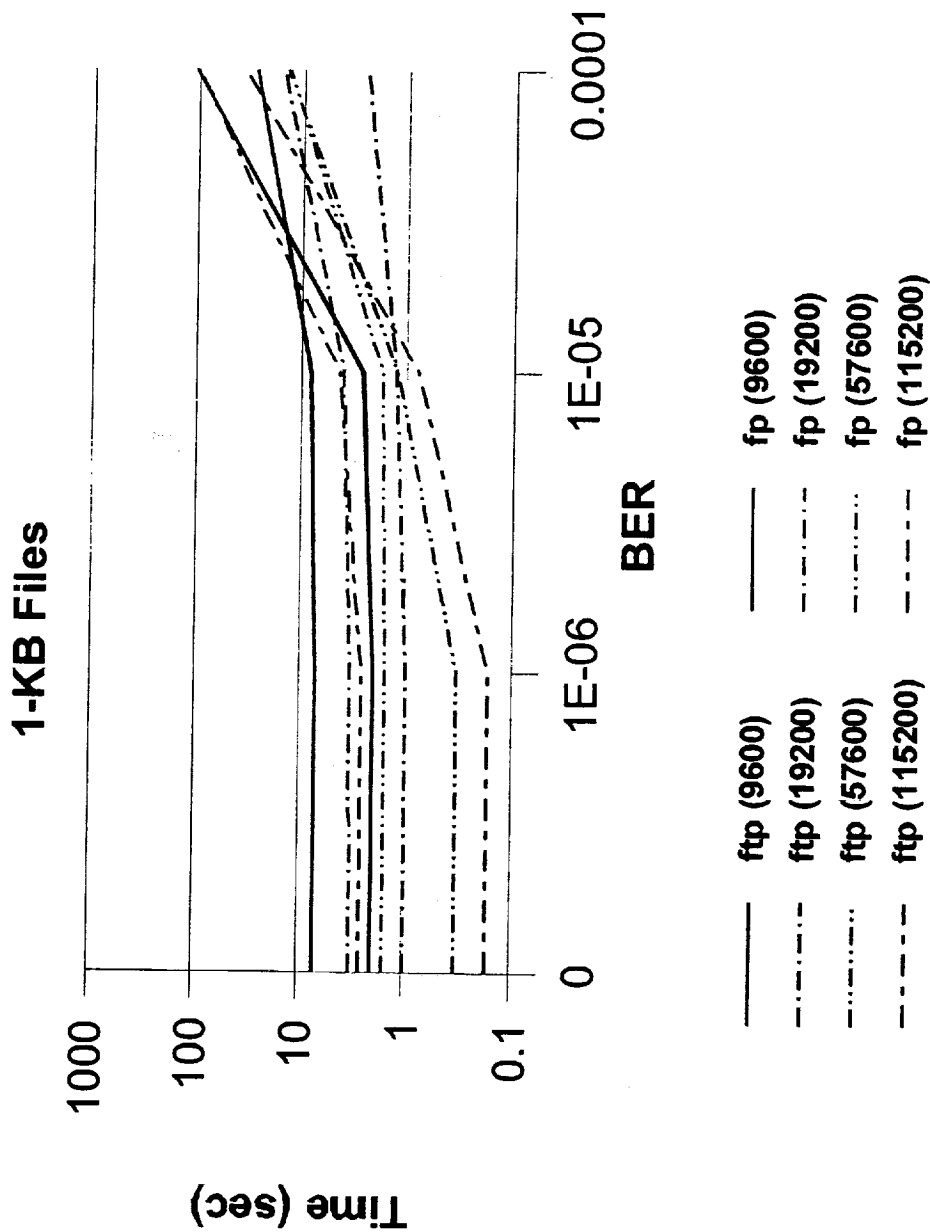
February 23, 1999

Space Protocol Testing

SCPS and TCP/IP Test Results



SCPS and TCP/IP Test Results



February 23, 1999

Space Protocol Testing

Next Test Steps

- Complete 1/4-second delay module
- Complete test set with different forward and return data rates; orbital pass simulations
- Share results with MITRE, JPL, SBS, Avtec, CU Boulder and ask for critique and further tests to run
- Finish ITC papers
- Obtain ESA's Protocol X and other protocols when available

Summary & Conclusion

- Used LabVIEW to make a software replica of a VME hardware module to generate errors for simulating channel error scenarios
- Using software rather than hardware gave added flexibility and ease of development
- LabVIEW allowed adding extra features quickly and validate the operation as development proceeded

Summary & Conclusion

- Tests show that in this configuration
 - SCPS fp is a bit better than ftp in high error rate channels (able to complete a connection)
 - TCP/IP ftp generally ran faster and had lower timing variance than SCPS fp on these slow-speed tests

OPTICAL COMMUNICATIONS

LOWCAL

Lightweight Optical Communications Without Carrying a Laser In Space

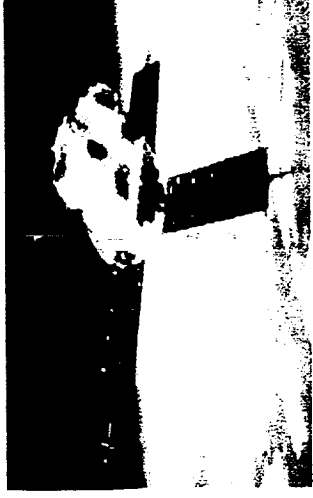
D. Hazzard, G. Lee, J. MacCannell, D. Moore, E. Selves,
J. Payne, Norman Dahlstrom and T.M. Shay

New Mexico State University

505-646-4817

tshay@nmsu.edu

LOWCAL vs. RF



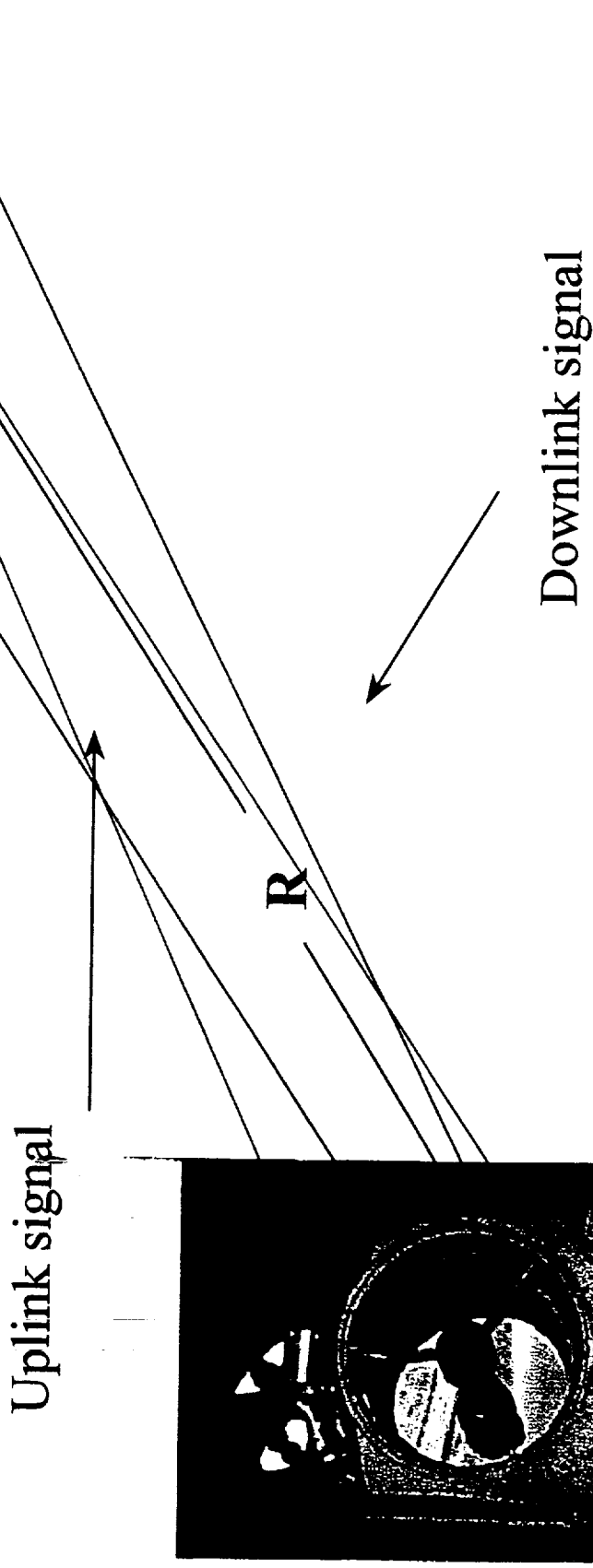
LOWCAL Goals

- Data Rate: 10 Kbps
- Lightweight: < 1 pound
- Ultra low power consumption: < 100mW
- Day / night operation
- Monostatic operation
- LEO communication without a laser in space

RF Communication

- Data Rate: 10 Kbps
- Weight: ~ 10 pounds (heat sink weight)
- Power consumption: ~ 10W

LIGHTWEIGHT OPTICAL COMMUNICATIONS WITHOUT A LASER IN SPACE (LOWCAL)



LOWCAL

COMPARISON WITH OTHER EXPERIMENTS

	NASA/NMSU	AF/PL/USU
PLATFORM	Space Shuttle	Balloon
RANGE	640 km	32 km
DATA RATE	10 kb/s	1.2 kb/s
RECEIVER DIAMETER	0.6 m	1.5 m
MODULATOR FOV	$+\pi/4$	$+\pi/4$
MODULATOR WT.	1-2 kgm	28 kgm
MODULATOR AREA	20 cm ²	1-10 cm ²
24 HOUR CAPABILITY	Yes	No
TRANSMITTER POWER	4 W	5 W
Full duplex	Yes	No

February 23 99

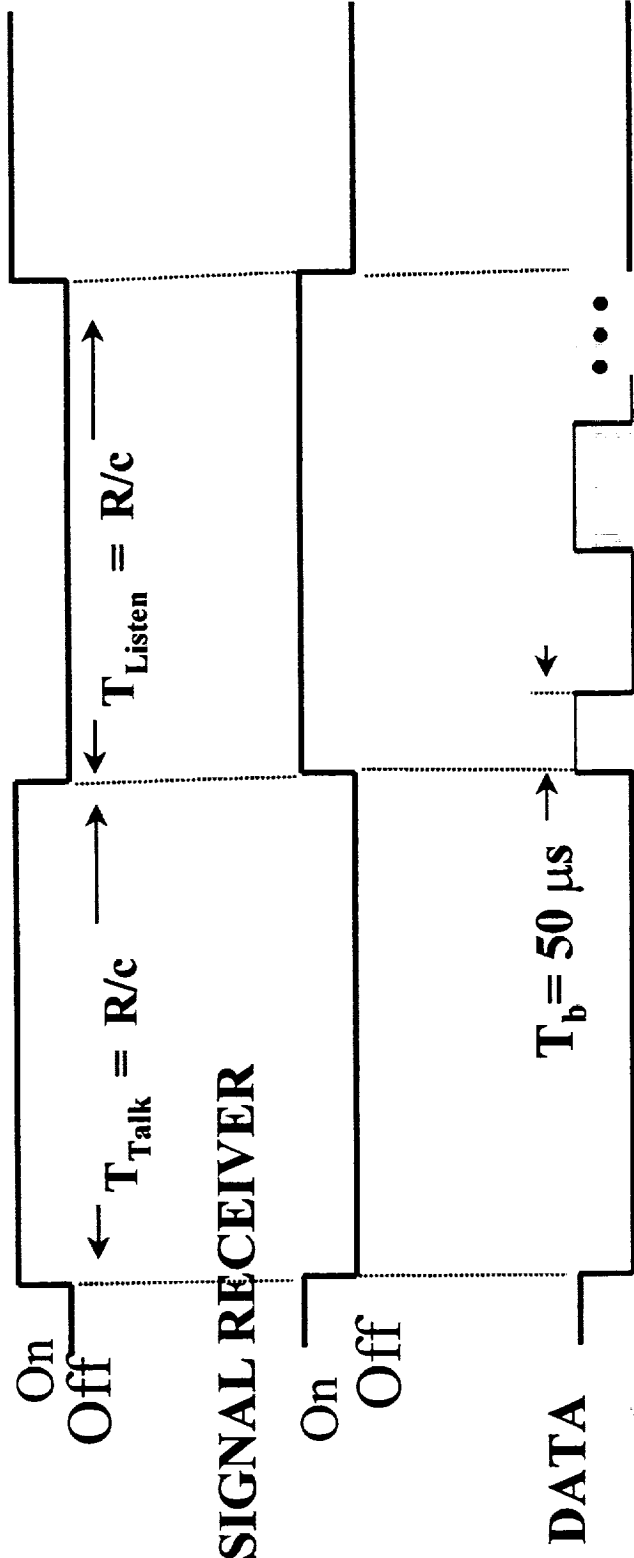
LOWCAL

PRESENTATION OUTLINE

- **DOWNLINK**
- **UPLINK**
- **SUMMARY**

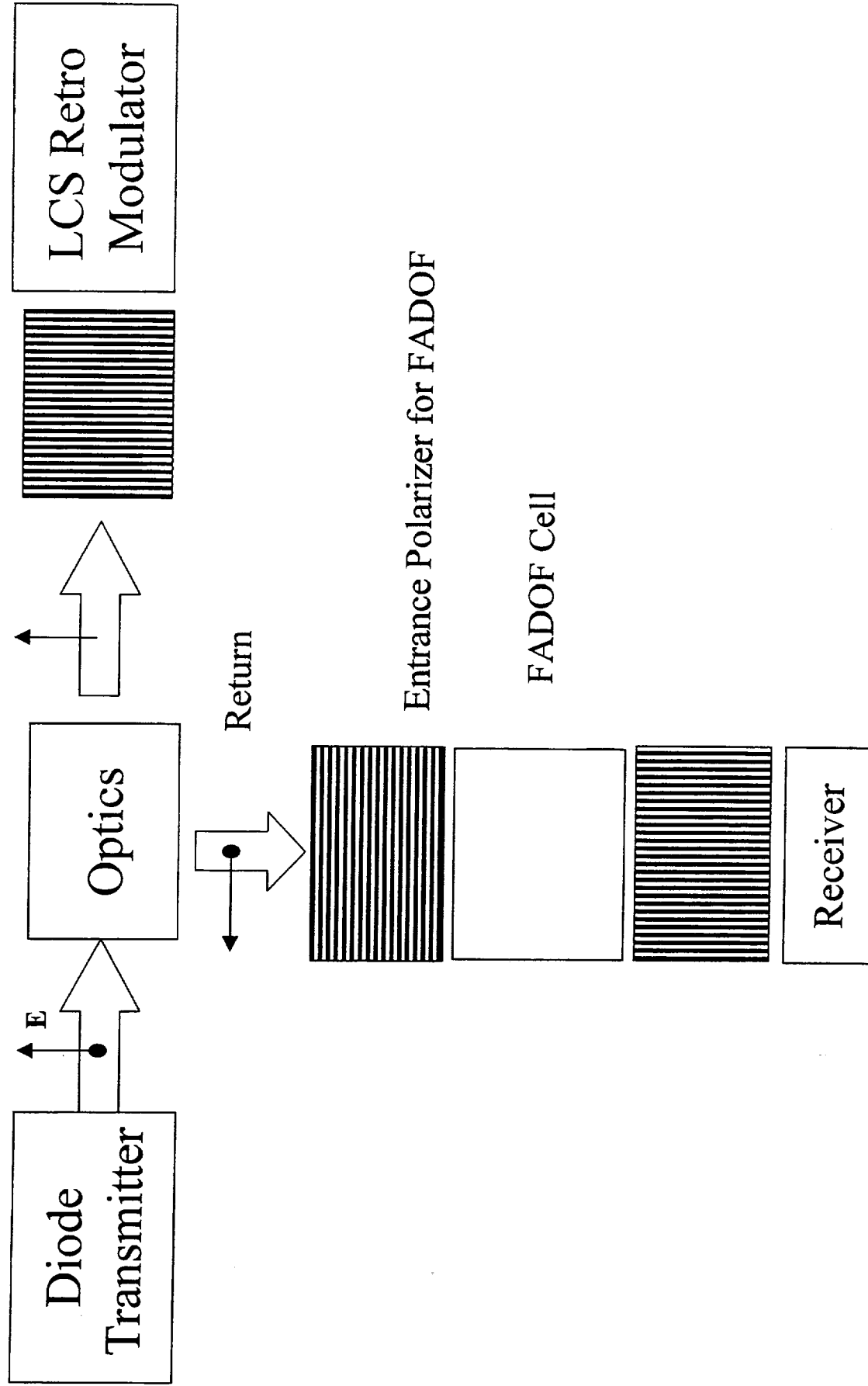
DOWNLINK COMMUNICATIONS FORMAT

CARRIER TRANSMISSION



where c represents the speed of light

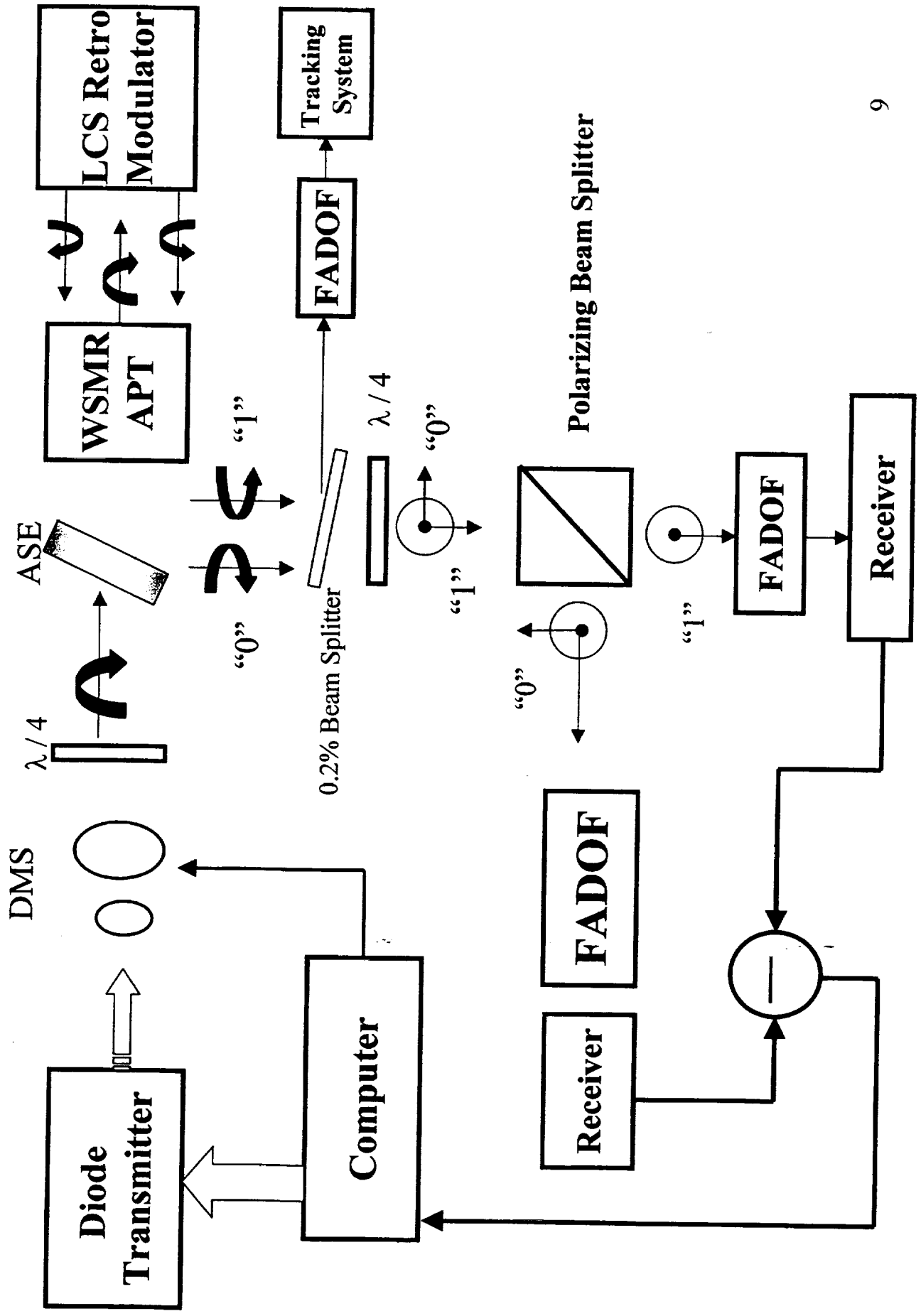
Original Concept



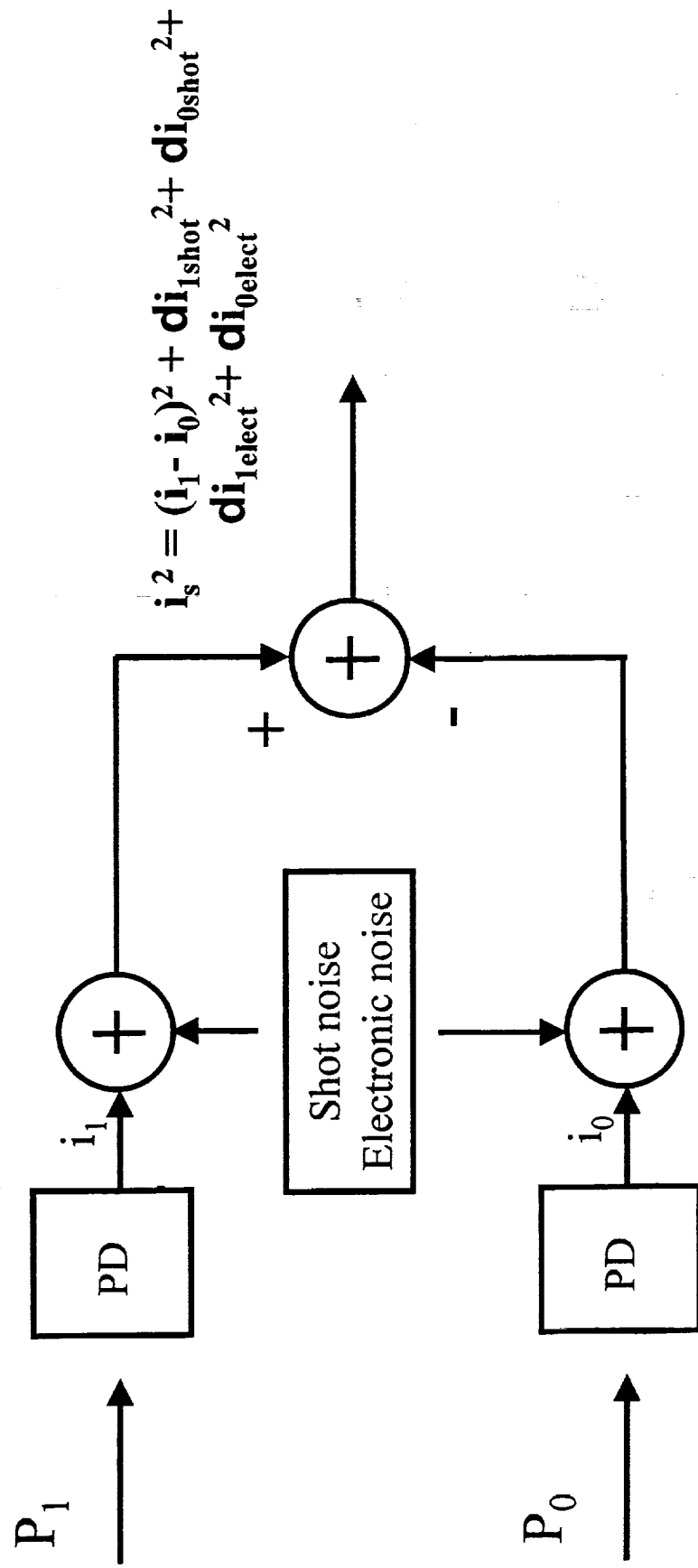
DIFFICULTIES WITH THIS APPROACH

- The transmitter and modulator polarizers must be aligned or significant losses occur.
- The spacecraft's retro-modulator and the FADOF's entrance polarizers must be aligned or significant losses can occur.
- The first two items would require a polarization tracking loop and thus, adding complexity.
- The power in the zeros is discarded.

LOWCAL with Differential Circular Polarization Keying



DCPK BLOCK DIAGRAM



DCPK SNR

$$SNR = \frac{(2 \cdot P_s \cdot R_{PD})^2}{\left[2 \cdot q \cdot B \cdot (P_s \cdot R_{PD} + I_D) + 2 \cdot \left(\frac{4 \cdot k \cdot T \cdot B \cdot F_t}{R_L} \right) \right]}$$

Where:

q represents the electron charge.

B represents the signal bandwidth.

R_{PD} represents the photodetector responsivity.

I_D represents the photodetectors dark current.

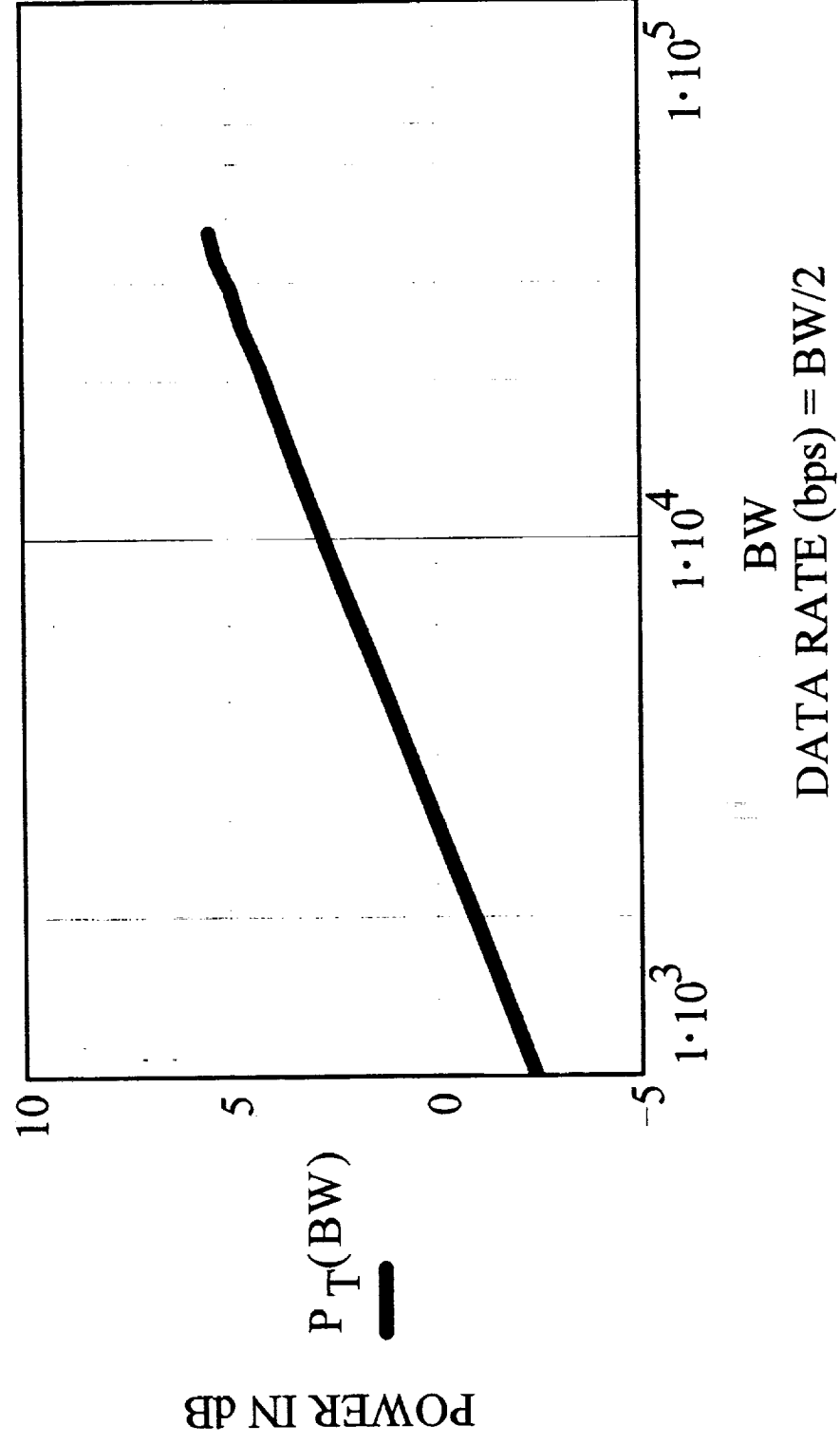
k represents Boltzmann's constant.

T represents the temperature in degrees Kelvin.

R_L represents the load resistor.

F_t represents the noise figure of the amplifier.

DATA RATE VERSUS POWER



DOWNLINK MODEL SUMMARY

COMMUNICATIONS MODE

D_{retro} (inches)	Margin (dB)	P_{min} (dBm)
2	10	-69

ACQUISITION MODE

D_{retro} (inches)	Margin (dB)	P_{min} (dBm)	
2	20	-112	Night
2	17	-109	Day

SYSTEM CHARACTERISTICS

Transmitter power	6 dB
Receiver diameter	60 cm
Maximum data rate	10 kb/s
Acquisition integration time	1 sec.
$M_{\text{scintillation}}$	5 dB

Modulator Aperture Independent Losses

Description	Loss (dB)
Modulator	1.4
Atmospheric	2*3
Telescope	2*0.5
FADOF	1
SUM	9.4

Beam Intercept Losses

D_{retro} (inches)	L_{SIE} (dB)	L_{CIE} (dB)	DW	Mode
2	27	78	$1.2 \cdot 10^{-6}$	Acquire
2	27	48	$4 \pi \cdot 10^{-10}$	Comm

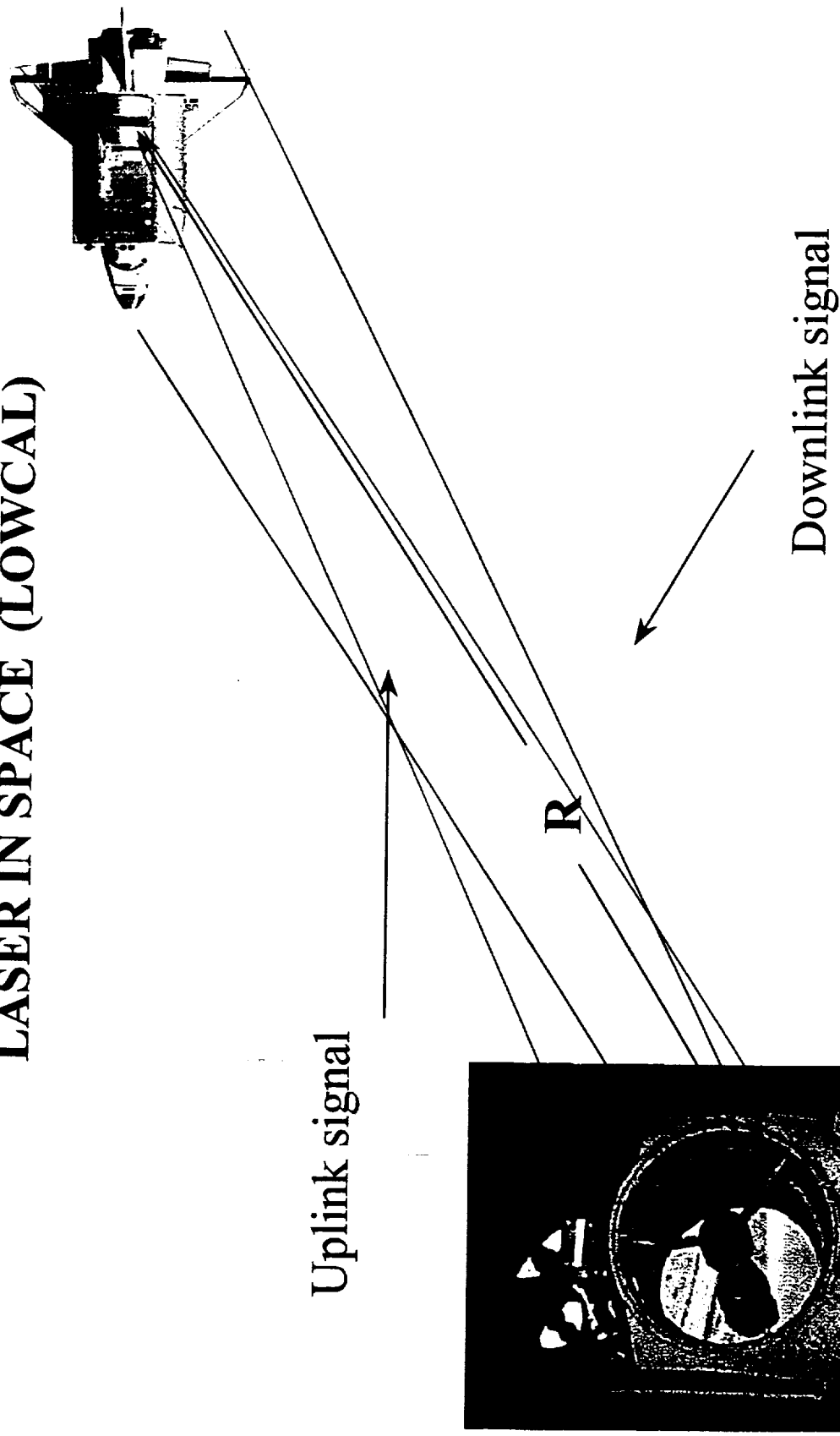
DW_{acquire} is determined by the shuttle orbit downtrack position accuracy expected (~ 0.2 km).

DOWNLINK SUMMARY

- A LOWCAL Link to LEO is feasible.
- The transmitter is located on the ground and only requires 4 Watts.
- First optical link to LEO without a laser in space.
- Data rate of 10 kbps should be possible.
- No mechanical scanning of the beam.
- First Differential Circular Polarization Keying concept.
 - DCPK provides 6 dB SNR increase
 - Some scintillation compensation
- Lightweight and low power consumption in space.
- WSMR/Army will provide the tracking telescope and manpower.

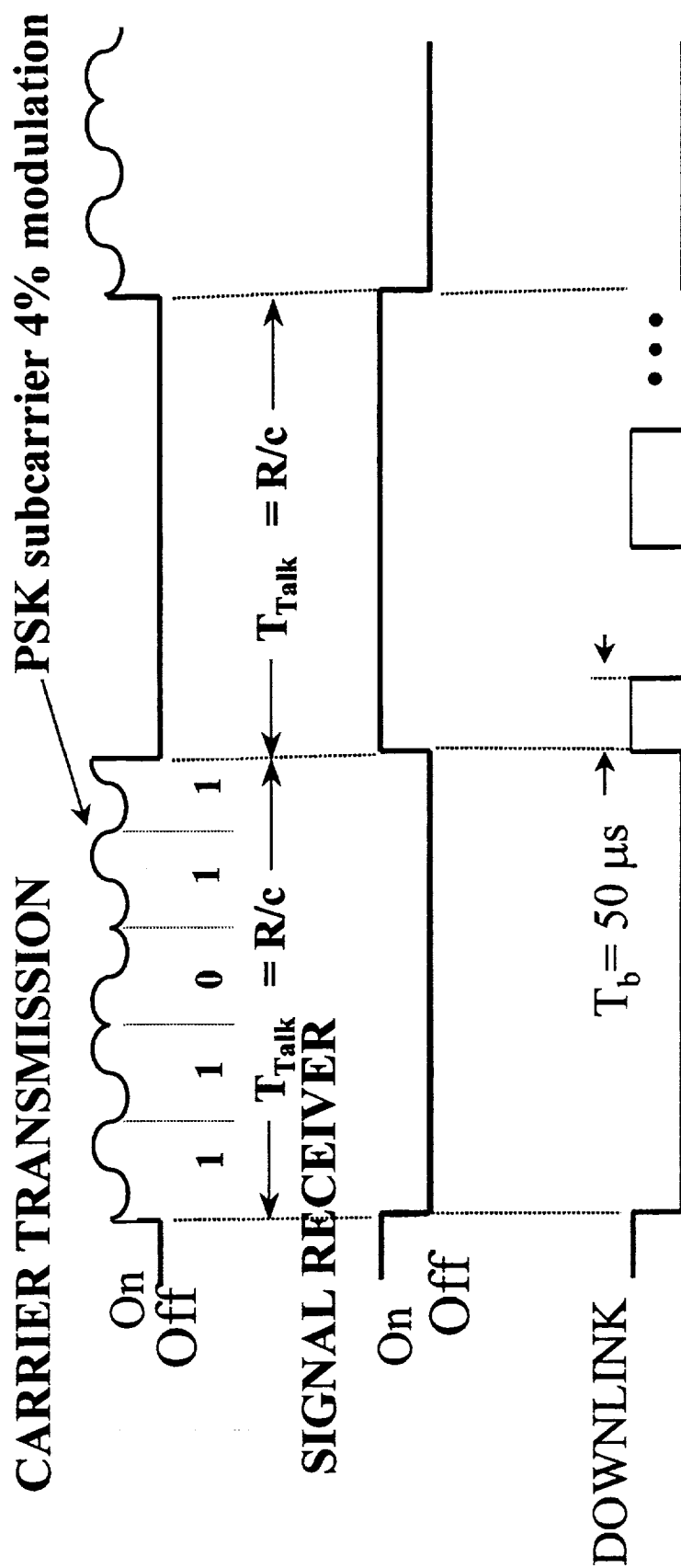
UPLINK SECTION

LIGHTWEIGHT OPTICAL COMMUNICATIONS WITHOUT A LASER IN SPACE (LOWCAL)



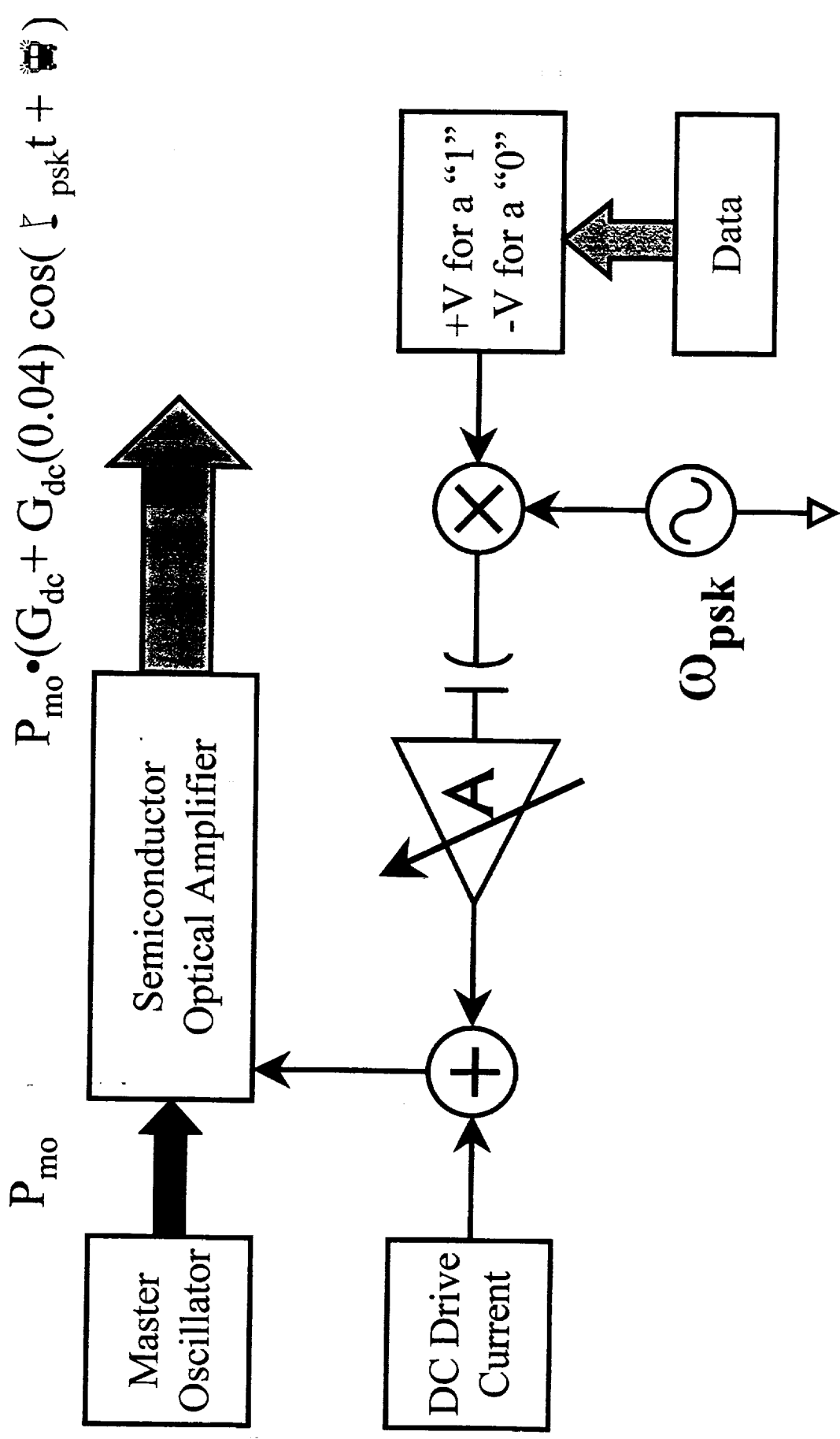
LOWCAL

LIGHTWIRE FORMAT

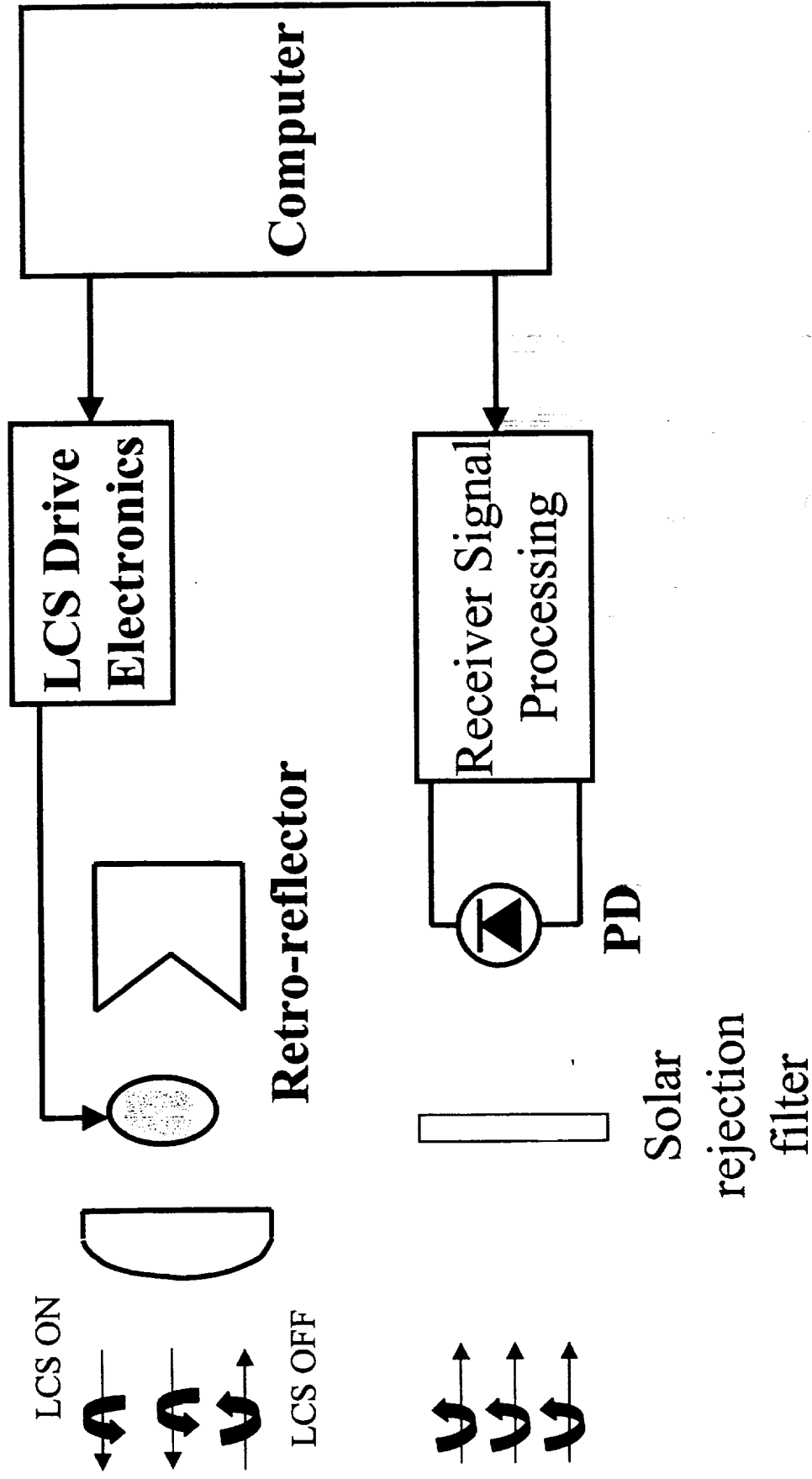


where c represents the speed of light

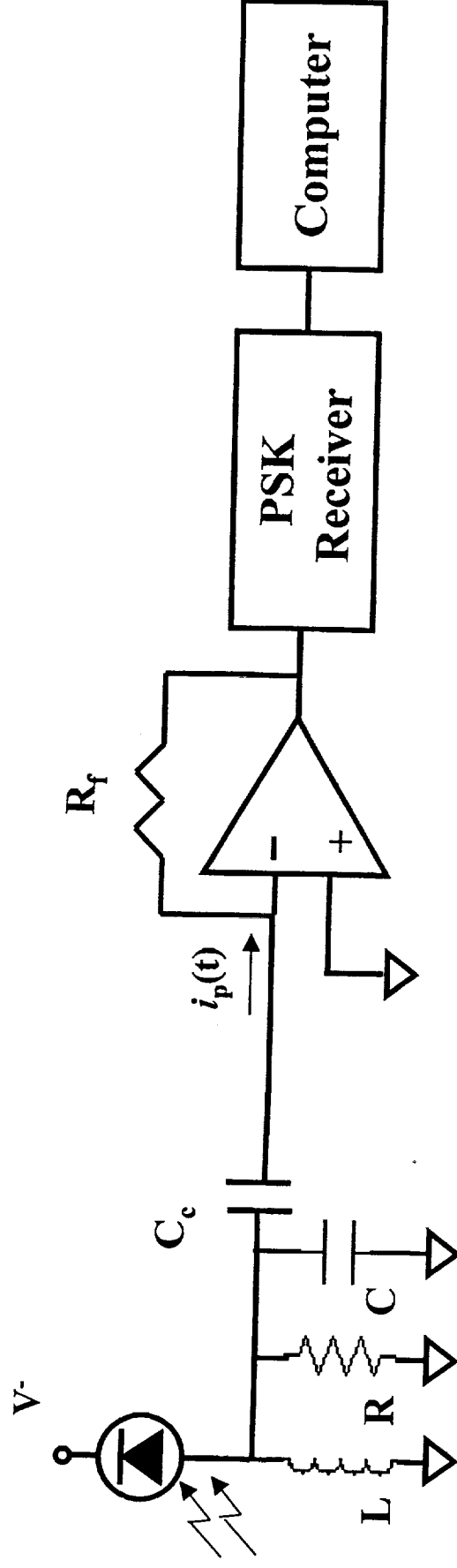
Conceptual Block Diagram for Uplink Modulation



LIGHTWIRE FLIGHT SUBSYSTEMS



Flight Receiver Electronics



Transimpedance amplifier
(photoconductive mode)

UPLINK SIGNAL

The optical power incident upon the spacecraft P_r is,

$$P_r = I_i A_{PD} [1 + m \cos(\omega_{PSK} t + f(t))]$$

where:

P_r represents the received optical power at the spacecraft.

I_i represents the intensity incident upon the spacecraft.

m represents the modulation index.

ω_{PSK} represents the subcarrier frequency.

$f(t)$ represents the phase of the subcarrier.

UPLINK SNR CALCULATIONS

$$SNR = \frac{\frac{1}{2} \cdot (m \cdot P_r \cdot R_{PD})^2}{\left(2 \cdot q \cdot B \cdot (P_r \cdot R_{PD} + I_D) + RIN \cdot B \cdot (R_{PD} \cdot P_r)^2 + \frac{4 \cdot k \cdot T \cdot B}{R_L} \cdot F_t \right)}$$

Where:

q represents the electron charge.

B represents the signal bandwidth.

R_{PD} represents the photodetector responsivity.

I_D represents the photodetectors dark current.

RIN represents the laser relative intensity noise.

k represents Boltzmann's constant.

T represents the temperature in degrees Kelvin.

R_L represents the load resistor.

F_t represents the noise figure of the amplifier.

PRELIMINARY UPLINK

MODEL RESULTS

Incident Intensity	1 mW/cm ²
Eye Safety limit	2 mW/cm ²
Photodetector diameter	1 in
Photodetector responsivity	0.6 amp/watt
modulation index	0.04
Data Rate	10 kHz.
Load resistance	1 Mohm
RIN	-130 dB/Hz
PSK Signal to Noise	54 dB
PSK signal current	0.4 mA

UNIQUE FEATURES OF LOWCAL

- First optical downlink without a laser in space
- The transmitter is located on the ground and only requires 4 Watts.
- First Differential Circular Polarization Keying concept
 - DCPK provides 6 dB SNR
 - Some scintillation compensation
- Lightweight and low power consumption in space.
- Full duplex using the lightwire concept.

PLANS FOR FY 99-00

- BUILD AND TEST LABORATORY SYSTEM FOR SHORT RANGE FIELD TEST
- PREFORM SHORT RANGE FIELD TEST
 - TEST HARDWARE
 - CIRCULAR POLARIZATION KEYING TEST
 - TEST SCINTILLATION RESISTANCE
 - With and without coding

February 23 99

LOWCAL

LOWCAL PROGRESS 98-99

- DCPK CONCEPT INVENTED AND MODEL DEVELOPED
 - GROUND PHOTORECEIVER ASSEMBLED AND TESTED
 - FULL DUPLEX CONCEPT “LIGHTWIRE” INVENTED
 - GROUND BASED RECEIVER OPTICAL TRAIN DESIGNED
-
- LIQUID CRYSTAL MODULATOR TESTED

LOWCAL DELIVERABLES FY 99-00

- | | |
|----------------------------|---------|
| •FIELD TEST DESIGN REPORT | JULY 99 |
| •LABORATORY TEST REPORT | NOV. 99 |
| •FINAL REPORT FOR FY 99-00 | MAY 00 |

LOWCAL SCHEDULE

FY 99-00

**DESIGN, BUILD AND TEST CRITICAL SUBSYSTEMS.
COMPLETE DESIGN OF GROUND BASED SYSTEM.
SHORT GROUND FIELD LINK TEST.**

FY 00-01

**ASSEMBLE AND TEST REMAINING SUBSYSTEMS.
INSTALL SYSTEM AT WSMR.
PERFORM 80 km FIELD TEST.
DESIGN FLIGHT EXPERIMENT.**

FY 01-02

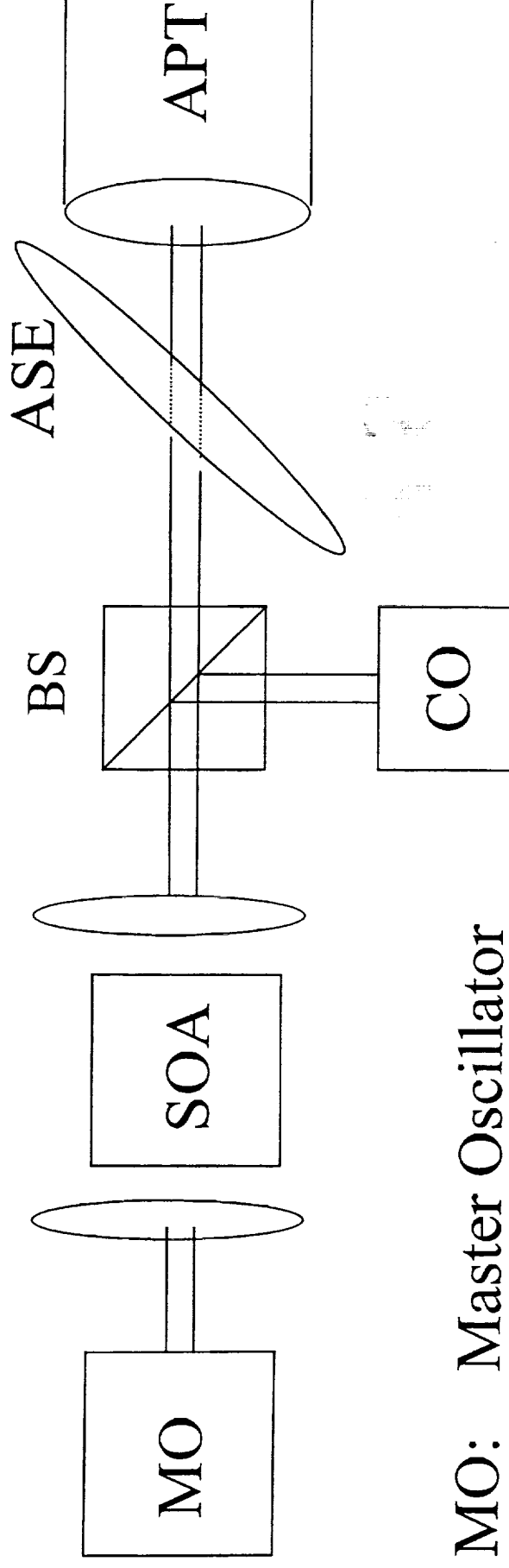
**BUILD FLIGHT HARDWARE
FLIGHT EXPERIMENT**

February 23 99

LOWCAL

BACKUP SLIDES

Transmitted Beam Train



MO: Master Oscillator

SOA: Semiconductor Optical Amplifier

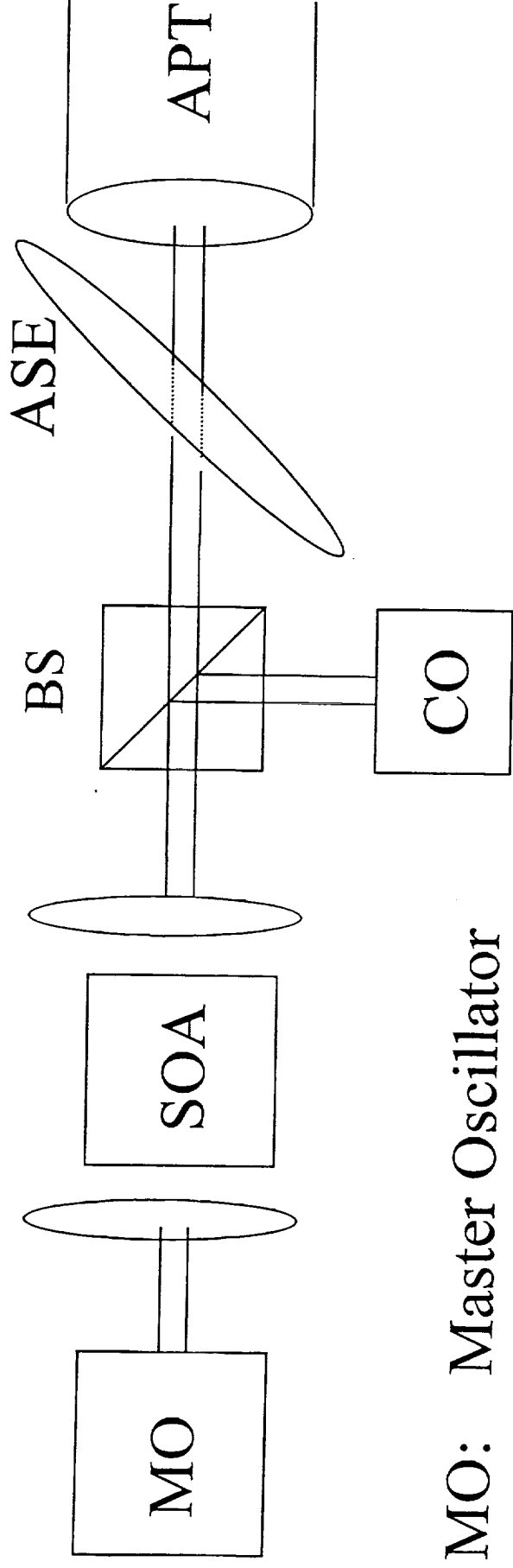
BS: Beam splitter

CO: Collimeter

ASE: Aperture Sharing Element

APT: Advanced Pointer and Tracker

Transmitted Beam Train



MO: Master Oscillator

SOA: Semiconductor Optical Amplifier

BS: Beam splitter

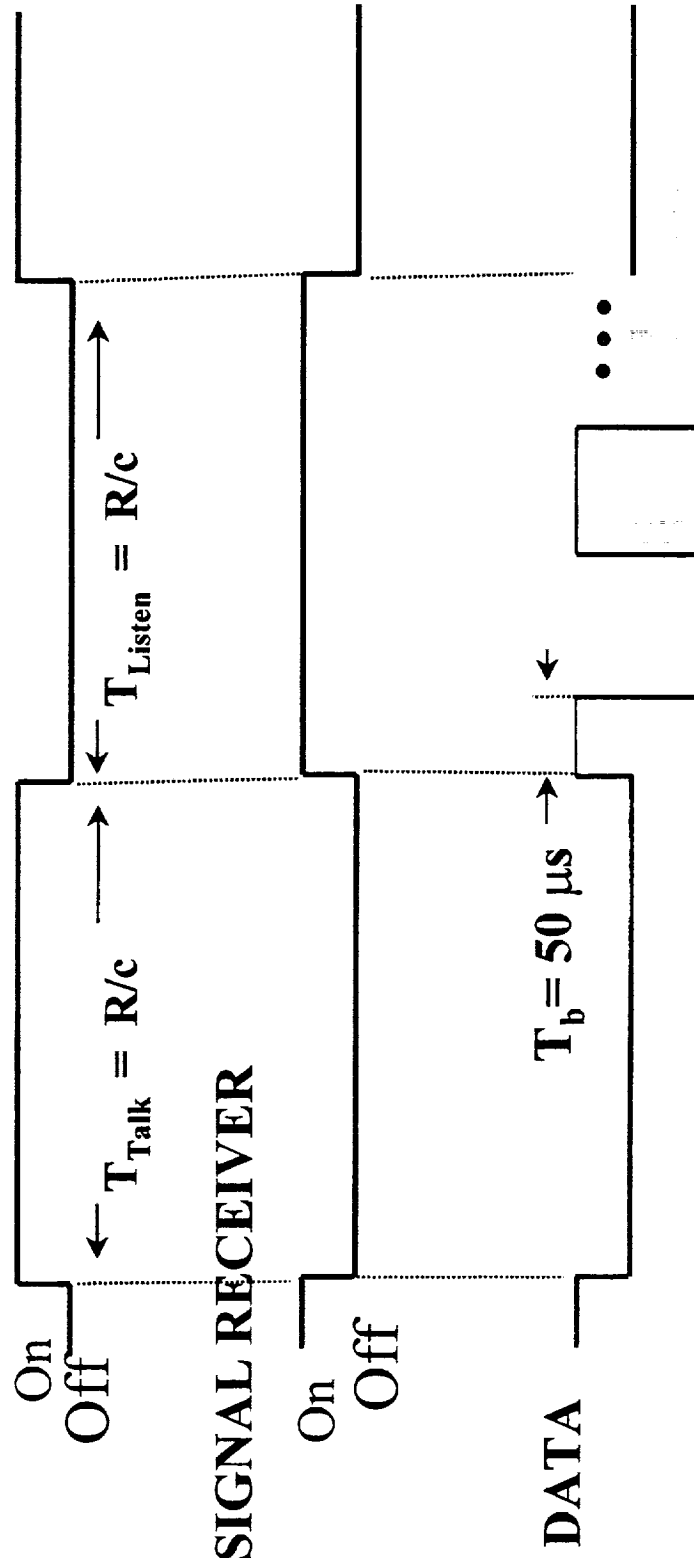
CO: Collimeter

ASE: Aperture Sharing Element

APT: Advanced Pointer and Tracker

DCPK COMMUNICATIONS FORMAT

CARRIER TRANSMISSION



where c represents the speed of light

DOWNLINK LOWCAL SIGNAL MODEL

The received signal, P_s , is,

$$P_s = P_T \cdot \eta_T \cdot T_{Atm} \cdot \frac{A_{retro}}{R^2 \cdot \Delta\Omega_{up}} \cdot \eta_{mod}^2 \cdot \eta_{retro} \cdot T_{Atm} \cdot \frac{A_r}{R^2 \cdot \Delta\Omega_{down}} \cdot \eta_T \cdot T_{FADOF}$$

Carrier Intercept Efficiency
"CIE"

Signal Intercept Efficiency
"SIE"

where:

P_T represents the transmitter laser power.

T_{mod} , and T_{retro} represent the telescope, the modulator, and the retro-reflector efficiencies, respectively.

T_{atm} and T_{FADOF} represent the atmospheric and the FADOF transmissions, respectively.

A_r and A_{retro} represent the receiver and retro-reflector areas respectively.

up and down represent the carrier and signal beam solid angles, respectively.

R represents the range to the satellite.

DOWNLINK LINK EQUATION

$$P_s(\text{dB}) = P_T(\text{dB}) + 2 L_T + 2 L_{\text{Atm}} + L_{\text{mod}} + L_{\text{CIE}} + L_{\text{SIE}}$$

where:

$$L_T = -10 \log(\eta_T)$$

$$L_{\text{Atm}} = -10 \log(T_{\text{Atm}})$$

$$L_{\text{FADOF}} = -10 \log(T_{\text{FADOF}})$$

$$L_{\text{mod}} = -10 \log(\eta_{\text{mod}}^2 \eta_{\text{retro}})$$

$$L_{\text{CIE}} = -10 \cdot \log \left(\frac{A_{\text{retro}}}{R^2 \cdot \Delta \Omega_{\text{up}}} \right)$$

$$L_{\text{SIE}} = -10 \cdot \log \left(\frac{A_{\text{retro}}}{R^2 \cdot \Delta \Omega_{\text{down}}} \right)$$

$$\text{Margin} = P_T + 2 L_T + 2 L_{\text{Atm}} + L_{\text{mod}} + L_{\text{CIE}} + L_{\text{SIE}} - P_{\text{min}} - M_{\text{scintillation}}$$

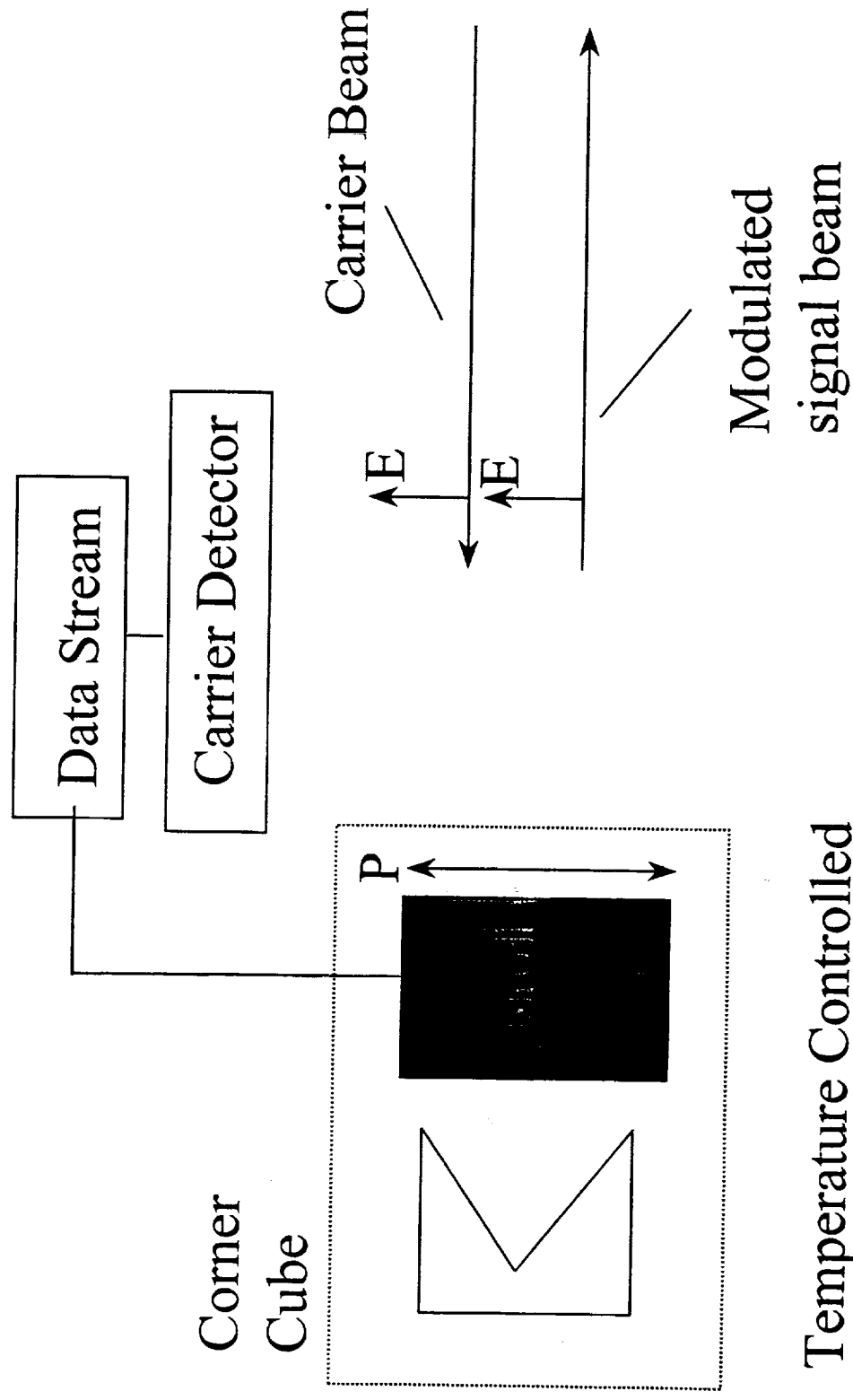
where:

$M_{\text{scintillation}}$ represents the margin required to compensate for beam scintillation.

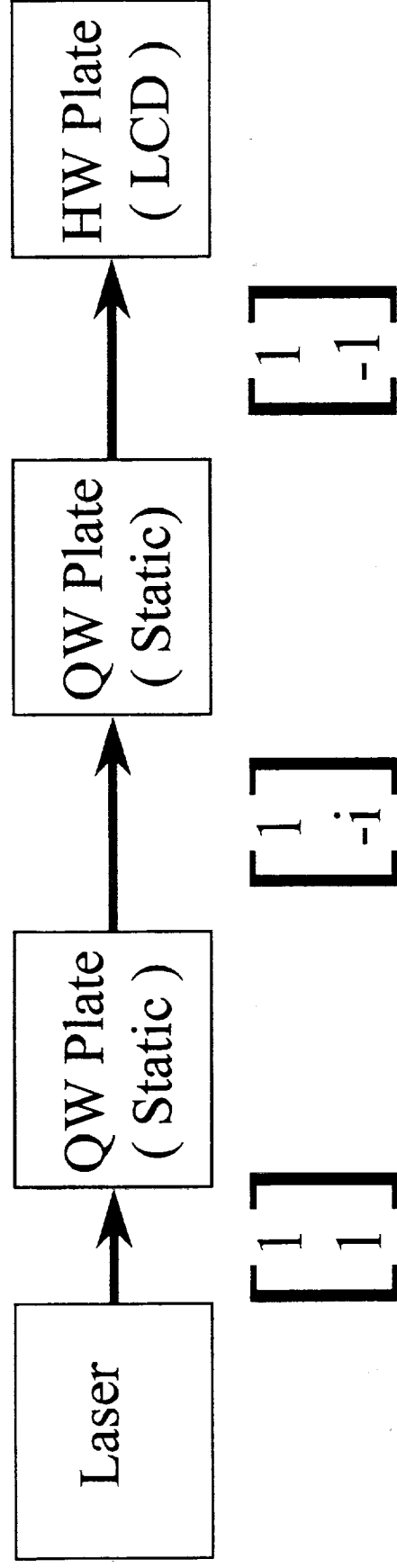
February 23 99

LOWCAL

LAST YEAR'S FLIGHT SYSTEM



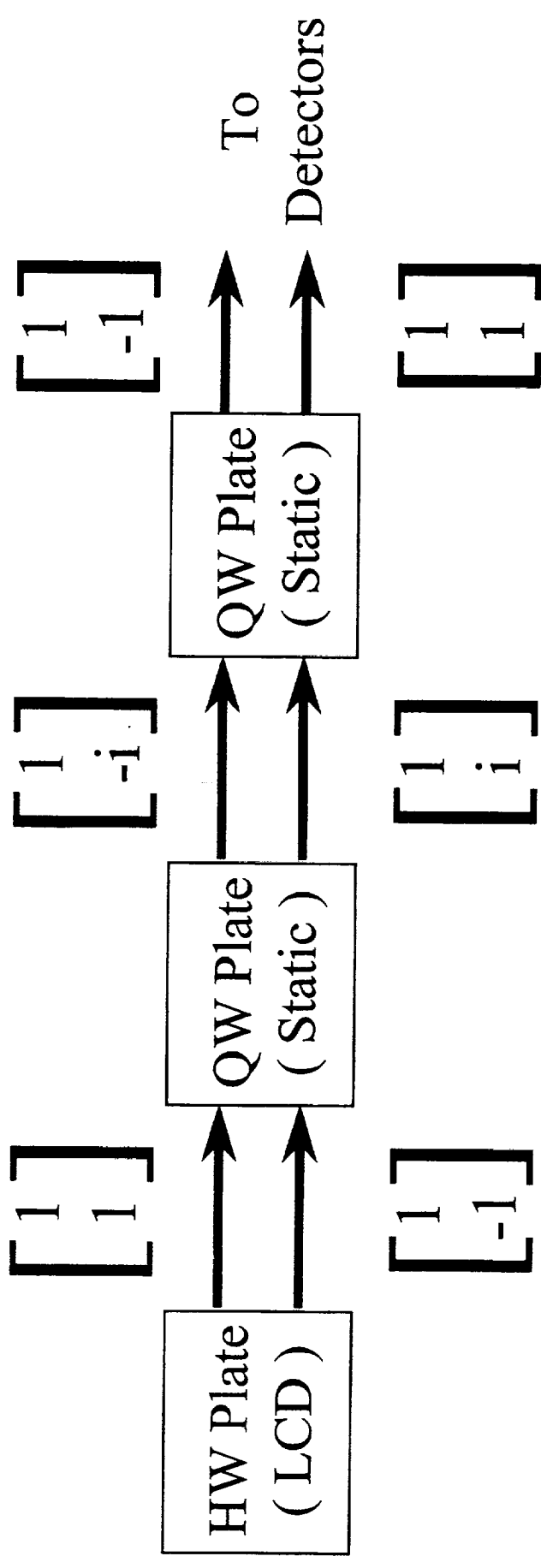
UPLINK POLARIZATION FLOW CHART



$$M_{QW} = \begin{bmatrix} e^{i\pi/4} & 1 \\ 1 & e^{-i\pi/4} \end{bmatrix}$$

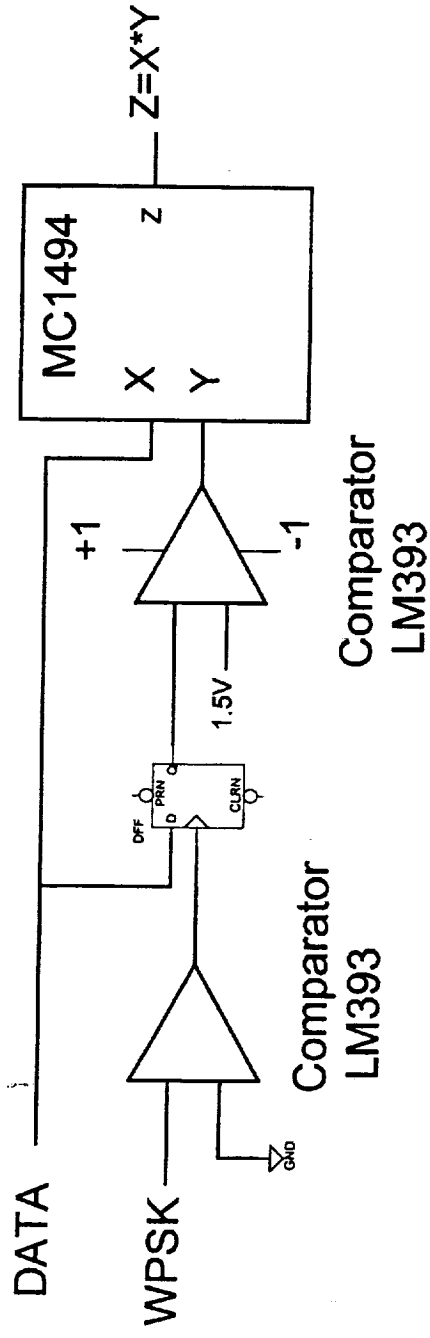
$$M_{HW} = \begin{bmatrix} e^{i\pi/2} & 1 \\ 1 & e^{-i\pi/2} \end{bmatrix}$$

DOWNLINK POLARIZATION FLOW CHART



Red: LCD ON
Black: LCD OFF

BPSK MODULATION CIRCUIT



Circuit allows sign bit to change the phase of the sinusoidal(WPSK) input. The use of comparators and D-flip flop reduce transients by allowing a sign change only at a zero crossing of the sinusoid.